UNIVERSITÀ DEGLI STUDI DI MILANO

Doctoral School of Pharmaceutical Sciences

Department of Pharmacological and Biomolecular Sciences

XXVIII course

Role of the long pentraxin 3 (PTX3) in cardiometabolic diseases

Bio/14

Student:

Fabrizia Bonacina

R10149

Supervisor:

Chiarissimo Prof. Giuseppe Danilo Norata

Coordinator of Doctoral School:

Chiarissimo Prof. Alberto Corsini

Academic Year

2015

"...Everything that drowns me makes me wanna fly...

...Everything that kills me makes me feel alive..."

Counting star, OneRepublic

Alle persone a me più care

Index

Introduction

The immuno-inflammatory response in cardiometabolic diseases

Cardiometabolic diseases, collectively represented by cardiovascular and metabolic diseases (obesity and diabetes), remain the leading cause of global mortality, accounting for about 1 in every 2 adult deaths worldwide.

Inflammation has been addressed as the key feature of cardiometabolic diseases; however, compared to the classical, short-term inflammatory response, described as the principal response of the body invoked to deal with injuries (the hallmarks of which include swelling, redness, pain and fever (tumor, rubor, dolor and calor) [1]), the inflammation in cardiometabolic diseases is a long term, often referred as low-grade, inflammation associated with detrimental consequences. This condition is principally triggered by nutrients and metabolic surplus, and engages a similar set of molecules and signaling pathways to those involved in classical inflammation [2]. Therefore, inflammation can be classified in distinct forms of injury responses or subclasses, as the case of the short-term or low-grade inflammation compared to the acute inflammation; otherwise, the low-grade immuno-inflammatory response, triggered by the metabolic surplus and closely associated with cardiometabolic diseases, can be described with new terms, as "metaflammation", defined as the metabolically triggered inflammation [2] (**Figure 1**), or "immunometabolism", referred as the ability of systemic and intracellular metabolism to drive innate and adaptive immune response [3].

Pentraxin superfamily

Pentraxins are a superfamily of essential components of the humoral arm of innate immunity and are evolutionarily conserved proteins characterized by a structural motif, in their carboxy-terminal, of a 200 amino acid with an 8 amino acid–long conserved pentraxin signature (HxCxS/TWxS, where x is any amino acid), referred as the pentraxin domain [4-6]. Their conservation is testimony to their role in complex organisms. Pentraxins recognize a wide range of exogenous pathogenic substances, altered self molecules and, in species-specific manner, behave as acute phase proteins. Based on the primary structure of the subunits, pentraxins are divided in short and long pentraxins [7-9] (**Figure 2**).

Short pentraxins

Short pentraxins are 25-kDa proteins characterized by a common structural organization generally in five or ten identical subunits arranged in a pentameric radial symmetry. Prototypic short pentraxins are CRP and SAP which share approximately 51% amino acid sequence identity and are thought to have originated from a single gene duplication [10]; however, CRP and SAP sequence and regulation have diverged between mouse and human, with CRP being an acute phase proteins in man and SAP in mouse [11]. In healthy adults plasma levels of CRP are barely detectable (≤3 mg/l), but they increase as much as 1000-fold following an acute-phase stimulus as a result of accelerated rates of transcription in the liver, mainly in response to the pro-inflammatory cytokine IL-6 [5]; for this reason, CRP plasma levels have been used clinically for 75 years as a nonspecific systemic marker of infection, inflammation, and tissue damage. Although CRP mRNA expression in other tissues has also been reported, apparently extra hepatic sources of CRP do not contribute to its plasma levels [11]. Similarly, SAP is produced exclusively by hepatocytes and is the main acute-phase protein in mice, whereas in human serum it is constitutively present at 30 to 50 mg/L [11].

The physiological functions attributed to short pentraxins involve the recognition and binding to different ligands, mostly in a Ca^{2+}-dependent manner: various microorganisms (including fungi, yeasts, bacteria, and parasites through

phosphorylcholine (PC) and carbohydrate structures, promoting phagocytosis and resistance to infections) [12]; damaged and apoptotic cells, favoring their clearance [5]; the first component of complement C1q, activating the classical complement pathway [13]. Furthermore, CRP binds to modified low-density lipoprotein (LDL) via the PC and cholesterol moieties present on LDL [14] and colocalizes with LDL in human atherosclerotic lesions, but studies in mouse models of human atherosclerosis failed to address a atheroprotective or proatherogenic role of CRP [15]. Instead, only SAP binds to matrix components such as laminin, type IV collagen, fibronectin, and proteoglycans, to the β-amyloid peptide in a Ca^{2+}-dependent manner and contributes to the pathogenesis of amyloidosis [16].

Long pentraxins: PTX3

The long pentraxin 3 (PTX3) is the prototype of the long pentraxin family. Members of this family were identified in the 1990s as cytokine-inducible genes or molecules expressed in specific tissues: guinea pig apexin in spermatozoa [17, 18], neuronal pentraxin (NP) 1 or NPTX1 [19, 20], NP2, also called Narp or NPTX2 [21, 22], and neuronal pentraxin receptor (NPR), a transmembrane molecule in neurons [23, 24]. The PTX3 protein is 381 amino acids long, with a molecular weight of 45 kDa and consists of a C-terminal 203 amino acids pentraxin-like domain coupled with an N-terminal portion of 178 amino acids unrelated to other known proteins [8]. A single N-glycosylation site has been identified in the C-terminal domain of PTX3 at Asn220, which is occupied by complex type oligosaccharides, mainly fucosylated and sialylated biantennary sugars with aminofraction of tri- and tetrantennary glycans; changes in the relative content of bi-, tri-, and tetrantennary oligosaccharides and the level of sialylation are highly variable amongst PTX3 isolates from different cellular sources, thus influencing biological activities where glycosylation pattern has functional implication [25]. Furthermore, human PTX3, beyond a typical multimeric organization, shows a complex quaternary structure with eight protomer subunits assembled into high order oligomers stabilized by disulfide bonds [25] and evidence has proved that the quaternary structure of this long pentraxin is fundamental in mediating its binding properties and, ultimately, its biological functions [26].

PTX3 differs from CRP and SAP also for gene organization, cellular source and ligand-binding properties. Unlike the classic short pentraxins CRP and SAP, whose sequence and regulation have diverged from mouse to man, PTX3 is highly conserved in evolution and share 82% of identical amino acids and 92% of conserved amino acids. Thus, results obtained using genetic approaches in the mouse are likely to be informative for the function of PTX3 in man [8].

A variety of cells, as endothelial cells (ECs), smooth muscle cells (SMCs), adipocytes, fibroblasts, mononuclear phagocytes, and dendritic cells (DCs) [27-35] can produce PTX3 *in vitro* upon exposure to primary inflammatory signals. PTX3 production is induced by primary inflammatory signals, such as IL-1, TNFα, and microbial moieties (e.g., LPS, lipoarabinomannans) [27, 36]; specifically, agonists for different members of the TLR family, microbial moieties (LPS, OmpA, and lipoarabinomannans), and intact microorganisms stimulate PTX3 production [37], while IL-6 is generally a poor inducer of PTX3 [31]. However, different signaling pathways can affect PTX3 production, depending on cell type and/or stimuli: oxidized and enzymatically modified low density lipoproteins (ox-LDL) promote PTX3 production in ECs and human primary vascular smooth muscle cells [38]; IFN-γ inhibits PTX3 production in DCs, monocytes, and macrophages, while IL-10 amplifies LPS-induced its expression [39, 40]; the NF-κB pathway controls PTX3 expression in an experimental acute myocardial ischemia [41], while high-density lipoproteins (HDL) requires the activation of the PI3K/Akt pathway through G-coupled lysosphingolipid receptors [42]; finally, glucocorticoid hormones (GCs) induce or enhance PTX3 production in non-hematopoietic cells (fibroblasts and ECs), but inhibit PTX3 production in hematopoietic cells (DCs and macrophages) [43]. Neutrophils constitutively store PTX3 in specific granules and release the protein, which partly localizes in neutrophil extracellular traps (NET), in response to TLR engagement by microorganisms or TLR agonists [40, 44, 45], where it can contribute to the generation of an antimicrobial microenvironment essential to trapping and killing microbes [46, 47].

PTX3 has been described to play a complex, non-redundant role *in vivo*, recognizing a diverse range of pathogens, modulating complement activity by binding C1q and

facilitating pathogen recognition by macrophages and DCs, thus proposing PTX3 as a multifunctional protein at the crossroads between immunity and inflammation, extracellular matrix construction and female fertility [8, 48].

PTX3 and the immuno-inflammatory response

Similar to the short pentraxins, PTX3 can bind a variety of ligands, one of the best described is the first component of the complement cascade C1q [49, 50]: activation of the classical complement cascade is observed *in vitro* when PTX3 interacts with surface-immobilized C1q; on the contrary, inhibition is observed when interaction occurs in the fluid-phase, thus addressing at a dual role of PTX3 which enhances the clearance of bound-material, such as microbes, while on the other hand it may protect against unwanted complement activation in the fluid phase [51]. PTX3 bind specific pathogens, such as fungi, bacteria and virus, promoting phagocytosis and consequent clearance of the pathogen (conidia of *Aspergillus fumigatus*, *Pseudomonas aeruginosa, Salmonella typhimurium, Paracoccidioides brasiliensis*, *zymosan;* selected Gram positive and Gram negative bacteria as *Staphylococcus aureus, Pseudomonas aeruginosa, Salmonella thyphimurium, Neisseria meningitides*) [52-54], but not LPS. Indeed, *in vivo* studies with PTX3 deficient mice showed that PTX3 plays non-redundant roles in innate resistance to infections caused by these microorganisms, and for some of them the protective role of PTX3 is mediated by complement [52], however, PTX3 deficiency does not cause a generalized impairment of host resistance to microbial pathogens but it seems to be involved in recognition and resistance against specific microorganisms [8].

PTX3 may also play a regulatory role in inflammation as an increased resistance to LPS toxicity and to cecal ligation and puncture has been observed in PTX3 transgenic mice [55]. Furthermore, PTX3 deficiency has been associated to more severe tissue damage in experimental models of kainate-induced seizures [56], cardiac ischemia and reperfusion [41], pleurisy and acute lung and kidney injury [57, 58]. The regulated expression of this molecule in macrophages and DCs suggests that PTX3, unlike the short pentraxins made in the liver, represents a mechanism of amplification of innate resistance against pathogens mainly acting locally at the site

of infection and inflammation [8]. However, PTX3 plasma levels are low (about 25 ng/mL in mice, <2 ng/mL in humans) in normal conditions but increase rapidly (peak at 6–8 h) and dramatically (200–800 ng/mL) during endotoxic shock, sepsis, and other inflammatory conditions [59, 60], possibly reflecting a role in the pathogenesis of damage, such as by amplifying the complement and coagulation cascades [50, 61].

PTX3 as a component of the extracellular matrix

The most robust observation that PTX3 is a component of the extracellular matrix came from the finding that PTX3 deficient mice displayed a severe defect in female fertility [52, 62], ascribed to an abnormal cumulus oophorus, characterized by an unstable extracellular matrix in which cumulus cells were uniformly dispersed instead of radiating out from a central oocyte [63]. During cumulus matrix assembly the heavy chains of serum inter α trypsin inhibitor (IαI) protein bind covalently to hyaluronic acid (HA) or to the HA-binding glycoprotein TSG-6 and indeed, mice deficient in the light chain of IαI, bikunin [64], or in TSG-6 [65] are infertile because of instability of the cumulus matrix and lack of oocyte fertilization, like PTX3 deficient mice. PTX3 and TSG-6, which are synthesized by cumulus cells [62], interact at a site distinct from TSG-6 HA-binding surface [63]. Therefore, PTX3/TSG-6 complexes might thus serve as anchoring sites for multiple HA molecules, thereby substantially strengthening and stabilizing the HA network. It has been shown that the interaction with HA is critical for the formation and stability of extracellular matrix in several tissues, both in physiological and pathological conditions [66, 67], thus suggesting a similar localization and function of PTX3 in certain HA-enriched inflammatory tissues [68, 69].

In a different experimental setting, PTX3 was shown to play a non-redundant role in the orchestration of tissue repair and remodeling: after tissue injury, PTX3 interacts with fibrinogen/fibrin and plasminogen at acidic pH promoting fibrin degradation, which is an essential step in tissue remodeling and scar formation [70].

PTX3 and cardiovascular diseases

Recently a role of PTX3 in cardiovascular diseases has been addressed as the protein was detected in the myocardium and in the vasculature under different pathological conditions which was paralleled by the observation of increased plasma PTX3 levels in patients with cardiovascular disorders [71]. So far a role for PTX3 was described in the context of angiogenesis, vascular restenosis, atherosclerosis, and myocardial infarction (**Figure 3**).

Angiogenesis and restenosis

PTX3 was shown to dampen fibroblast growth factor-2 (FGF2)-dependent ECs proliferation [72] *in vitro*, thus inhibiting angiogenesis [73, 74]. Transfection of PTX3 in normal microvascular endothelial cells (MVECs) blunts their angiogenic properties, while PTX3 silencing by small interfering RNA restores the ability of the cells to produce capillaries and promotes angiogenesis [75]. This effect depends on the ability of PTX3 to bind with high affinity and selectivity FGF2, which in turn results in the inhibition of the interaction of FGF2 with tyrosine-kinase receptors (FGFRs) and heparin sulphate proteoglycans (HSPGs) on the surface of ECs and SMCs, thus dampening the generation of the proangiogenic complex HSPG/FGF2/FGFR [74, 76].

The FGF/FGFR system plays also a crucial role in SMC proliferation, migration, and survival *in vitro* [77-80], and neointimal thickening after arterial injury *in vivo* [81, 82]. These processes are critically involved in restenosis, the process of blood vessel narrowing that frequently occurs after percutaneous transluminal coronary angioplasty of atherosclerotic arteries. Experimental data confirmed that the overexpression of PTX3 in vivo or exogenously added PTX3 in vitro resulted in the inhibition of FGF2-dependent SMCs proliferation. This effect was associated with the suppression of the mitogenic and chemotactic activities exerted by endogenous FGF2 on SMCs, sequestering the growth factor in an inactive form [76].

The FGF-binding domain was identified in the PTX3 N-terminus by monoclonal antibodies and surface plasmon resonance analysis [74], while TSG6, the secreted product of tumor necrosis factor-stimulated gene, was shown to revert the inhibitory

effects exerted by PTX3 on FGF2-dependent angiogenesis through the interaction with the N-terminal domain of PTX3 [83].

These observations suggest that PTX3 could act as an "FGF2 decoy" and may represent a potent inhibitor of the autocrine and paracrine stimulations exerted by FGF2 on ECs and SMCs and point to a novel therapeutic role of PTX3 in the treatment of restenosis after angioplasty [84].

Atherosclerosis

PTX3 was detected in advanced atherosclerotic lesions on lumen surface as well as within the atherosclerotic plaque, in both animal models and in humans [85, 86]. Cholesterol accumulation in the intima of the vessels, the major pathological feature of atherosclerosis, is associated with the induction of an immune-inflammatory response resulting in the recruitment of monocyte/macrophages, PMNs (polymorph nuclear cells) and in the activation of ECs, which produce PTX3 in response to inflammatory stimuli normally associated with atherogenesis, as IL-1 and TNFα [87-89]. Furthermore, neutrophils and monocytes/macrophages contribute to the large amount of PTX3 observed in arterial thrombi and aortic tissue in patients with different degrees of atherosclerosis with acute myocardial infarction [90]. PTX3 expression, similar to that of CRP, is increased also in coronary plaques of patients with unstable angina pectoris (UAP) compared to those with stable angina (SAP). Nevertheless, PTX3 and CRP distribution is different; PTX3 expression is increased in complicated plaque compared to fibroatheroma, while the opposite is true for CRP; moreover abundant PTX3 was detected in intraplaque hemorrhage, while CRP staining was more intense in lipid rich plaque. Finally PTX3 is highly expressed in CD163-positive areas which normally marks anti-inflammatory M2 macrophages [91].

A causal role of PTX3 during atherogenesis was addressed in PTX3/apolipoprotein E (apoE) double knockout mice [85]. Normally mice are poorly susceptible to atherosclerosis [92]; therefore, the effects of the deficiency or the overexpression of a protein have to be tested in mice with a background susceptible to atherosclerosis. For this reason, specific transgenic mice were generated and among them, mice

lacking apoE or LDL-receptor are widely used [92-94]. PTX3 KO/apoE KO mice developed larger atherosclerotic lesions compared to apoE KO, an observation that was coupled to increased macrophage accumulation, increased bone marrow monocytosis, and, interestingly, increased expression of adhesion molecules, cytokines, and chemokines in the vascular wall. These findings suggested an increased immune-inflammatory response in PTX3 KO/apoE KO mice compared to apoE KO animals, demonstrating an athero-protective role of the protein [85]. The atheroprotective role of PTX3 was further confirmed by the observation that HDL induce PTX3 expression in ECs, an effect mainly dependent on apolipoprotein AI (apoAI) [42, 95]; furthermore, PTX3 could favor the clearance of lipid-loaded macrophages and VSMCs apoptotic cells mediating their removal by mature DCs, but, at the same time, oxidized LDL (but not native LDL) increases PTX3 mRNA expression in vascular SMCs (VSMCs), an effect dependent on NF-κB activation [35].

Ischemic Diseases

Plasma concentration of PTX3 rapidly rises in the early phase after ischemic heart disorders in humans and animal models [41, 60, 86, 96] suggesting the possibility that PTX3 could also play a role in myocardial infarction. In experimental models of myocardial infarction (coronary artery ligation and reperfusion) an increased PTX3 mRNA and protein expression was observed in the ischemic area of the heart; however, PTX3 KO mice had greater myocardial lesions, an increased tissue damage with a greater no-reflow area, increased neutrophils and macrophage infiltration, decreased number of capillaries, and increased number of apoptotic cardiomyocytes, a phenotype reversed by the use of exogenous PTX3 [41]. The protective effect of PTX3 was referred to a dampening of an excessive complement system activation: indeed, C3 deposition was increased in infarct areas of PTX3 KO mice compared to WT [41]. In agreement with the latter findings, a recent study revealed a crucial role for PTX3 in cardiomyocyte ischemia reperfusion (I/R) injury: PTX3 ameliorated cardiomyocyte apoptosis and infiltration of neutrophils and macrophages and then improved hemodynamic performance; this was associated with restricted expansion of γδ T cell and decreased expression of IL-6 and IL-23/IL-17A [97]. Of note, the protective role of PTX3 during I/R injury was depended on the protein produced by

bone marrow (BM)-derived cells, which inhibited infiltration of neutrophils and ROS generation at the ischemic myocardium, thereby resulting in the reduction of infarct size [98]. After 6 days from an ischemic brain injury, PTX3 KO mice presented a higher blood–brain barrier (BBB) damage and an impaired edema resolution compared to WT, while at early time point (48 h) no differences were observed in infarct volume, brain edema and blood–brain barrier (BBB) damage [99].

However, other works highlighted different roles played by PTX3: in an intestinal ischemia/reperfusion model, obtained by the total occlusion of the superior mesenteric artery, PTX3 overexpression was associated with increased cytokines production, tissue inflammation, and a reduced survival [100], a finding later confirmed in PTX3 KO mice which showed an opposite profile [101]. Instead, a reversible effect was reported in ischemic acute kidney injury (AKI): PTX3 KO mice was shown to have a reduced early expression of endothelial adhesion molecules and chemokines, and an ameliorated acute kidney injury [102]; however, other reports showed that the post-ischemic renal injury was aggravated in PTX3 KO mice [103], and PTX3 administration was able to prevent renal leukocyte recruitment and post-ischemic kidney injury.

These works clearly reveal that the molecule may have different functions in different settings or temporal windows of pathophysiological conditions.

Neutrophils recruitment: PTX3/P-selectin interaction

Neutrophils recruitment and infiltration into tissues is a common hallmark observed during the inflammatory/infectious response, where they can act as a double-edged sword, participating in tissue repair and defense but also further promoting tissue damage, as observed in ischemia-reperfusion injury.

During inflammation, flowing neutrophils tether to and roll on vascular surfaces by reversible binding of P-, L- and E-selectin to glycosylated ligands [104, 105]; P-selectin is rapidly mobilizes from secretory granules to the surfaces of endothelial cells and platelets after activation by thrombin, complement and other mediators and initiates rolling by interacting with the transmembrane mucin PSGL-1 on neutrophils [106]. Mantovani and colleagues demonstrated that PTX3, either derived from

activated leukocytes or administered exogenously, through the interaction with P-selectin, could attenuate neutrophils recruitment at sites of inflammation in a model of pleurisy or acute lung injury, thus dampening inflammatory response [57]. The inhibition of neutrophils rolling on P-selectin arose the possibility that this mechanism could have also been relevant in disorders where an excessive neutrophil recruitment to activated endothelium and collateral damages associated to leukocyte activation, such as acute coronary syndromes, could play a role [107].

PTX3, stored in neutrophils' secondary granules, was identified as the source of circulating protein, whose plasma levels dramatically increased after early acute myocardial infarction (AMI): the depletion of neutrophils intracellular PTX3 was associated with decreased platelets-neutrophils aggregates and with the binding between PTX3 and activated platelets, which dampens their inflammatory potential and pro-thrombotic effect [108].

PTX3 and cancer

Inflammation is a constant feature of tumors. The tumor microenvironment (TME) is rich in inflammatory cells and inflammatory mediators that strongly affect tumor growth and progression as well as metastatic spreading. Therefore the involvement of PTX3 in the pathogenesis of cancer has been widely investigated.

Increased levels of PTX3 have been associated with cancer: PTX3 was identified by proteomic approaches as an important candidate biomarker for prostate cancer [109], lung cancer [110], liposarcomas [111] and more recently pancreatic carcinoma [112]. However, the role of PTX3 in cancer progression remains unknown. Molecular studies indicated that PTX3 exerts an anti-tumoral activity in prostate cancer by inhibiting FGF2/FGF8b-dependent angiogenesis [73, 113], and through autocrine and paracrine activities on cancer cells that may contribute to tumor progression [114]. The overexpression of the PTX3 N-terminal domain, which binds to FGF2 [74], strongly inhibits the tumorigenic activity of TRAMP (Transgenic Adenocarcinoma Mouse Prostate)-C2 transfectants, whereas overexpression of the C-terminus has only a minor effect on tumor growth [113]. Although, PTX3 expression appears to be significantly down-regulated in various human prostate

cancer datasets [115], more recently a strong correlation between the expression of pentraxin family members and prognosis of pancreatic carcinoma was found [112], thus proposing pentraxins, especially PTX3, as promising biomarkers in the prognosis of pancreatic carcinoma patients, whose plasma levels positively correlated with other pro-inflammatory markers as CRP, interleukin-6 and macrophage-inhibitory factor. Furthermore, it was shown that PTX3 is secreted by several pancreatic carcinoma cell lines [112].

However, contrasting results were obtained in experimental models: PTX3 was both associated with tumor progression, by preventing the phagocytosis of tumor cells induced by tumor associated macrophages (TAM) in nasopharyngeal carcinoma [116], but also with a pivotal role in controlling tumor growth, related to its ability to modulate the inflammatory response [117]: PTX3 deficiency was indeed associated with increased susceptibility to mesenchymal and epithelial carcinogenesis. Increased susceptibility of PTX3 KO mice was associated with enhanced tumor-promoting macrophage infiltration, CCL2 production and angiogenesis. Furthermore, in the same paper, PTX3 expression was found to be epigenetically regulated in selected human tumors (leiomyosarcomas and colorectal cancer) by methylation of the promoter region and of a putative enhancer, concluding that PTX3, an effector molecule belonging to the humoral arm of innate immunity, acts as an extrinsic oncosuppressor gene in mouse and man by regulating complement-dependent, macrophage-sustained, tumor-promoting inflammation [117].

PTX3 and metabolic diseases

The role of PTX3 in metabolic diseases has been investigated so far with associational studies in obese subjects; however, a protective or detrimental effect in these pathological conditions has not been clearly identify.

PTX3 production by adipocytes was first proved by the transient expression of the protein in the early 3T3-F442A preadipocytes [34], a finding linked to the macrophage-like functions of preadipocytes, consistent with the involvement of adipose tissue in immune response during inflammation [118]. Despite the fact that PTX3 expression and secretion becomes low, if any, in mature adipocytes, its

expression and secretion were dramatically induced *in vitro* during TNFα exposure [118]. Furthermore, genetically obese and diabetic obese mice (*ob/ob* and *db/db*) presented an increased mRNA PTX3 expression in epididymal fat pads compared to lean mice [118] and some evidence reported an increased levels of PTX3 plasma levels in obese mice. Similarly, in humans PTX3 is expressed by preadipocytes and mature adipocytes in visceral (VAT) and subcutaneous adipose tissue (SCAT) and is directly related to TNFα expression in the VAT only; furthermore PTX3 expression has been associated with obesity and with several cardiovascular risk factors [119]. However, over all data from human studies are contradictory suggesting that plasma PTX3 protein levels are both elevated in obese individuals [120], associated with increased visceral adipose tissue expression and a cardiovascular risk profile [119], and in individuals with a metabolic syndrome phenotype [121]; but also inversely related with body mass index [122-126]. In detail, Zanetti and colleagues showed a novel association between PTX3 and atherogenic lipid profile: PTX3 levels were higher in subjects with low HDL, a strong predictor of cardiovascular disease both in the general and metabolic syndrome population [127, 128] which it is implicated in the progression of carotid artery intima-media thickening in the syndrome [129], and directly correlated with elevated triglycerides and intimal media thickness (IMT) [121]. However, in another study, a negative correlation was found between plasma PTX3 and insulin secretion after both intravenous and oral glucose administration and with obesity indexes, specifically body weight and waist circumference [122].

These contrasting findings might be in line with different functions of PTX3 during obesity, as reported in other pathological contexts, at the paracrine/autocrine levels in adipose tissue or at the systemic level: PTX3 is indeed expressed in different tissues and cell types, therefore, further work will be necessary to ascertain the contribution of each of the tissues/cells characterized by an high-expression of PTX3 to plasma protein levels and a possible differential regulation.

PTX3 as a biomarker of human cardiometabolic diseases

The observation that PTX3, in contrast to the liver-produced CRP, is produced by different cell types suggests that it may represent a rapid marker reflecting the local

activation of innate immunity and inflammation. Indeed, the general characteristics emerging from studies on PTX3 blood levels in human pathologies are the rapidity of its increase as compared with CRP, consistent with the identification of PTX3 as an early induced gene, the correlation with the severity of the disease, and the lack of correlation between levels of CRP and PTX3 [71]. Increased levels of PTX3 have been associated with different pathological conditions, from cardiometabolic to autoimmune diseases. In a restricted set of autoimmune disorders, as the small-vessel vasculitis, PTX3 levels, derived from ECs [130], correlate with clinical activity of the disease and represent a candidate marker for monitoring the disease [131]. Pregnancy itself, a condition associated with relevant involvement of inflammatory molecules at the implantation site [132], is associated with slight increase in maternal circulating PTX3 levels compared with the non-pregnant condition. Higher maternal PTX3 levels were observed in pregnancies complicated by preeclampsia [133, 134], which represents the clinical manifestation of an endothelial dysfunction as part of an excessive maternal inflammatory response to pregnancy [133, 135, 136].

Because of the homology between PTX3 and CRP, the relevance of PTX3 measurement as diagnostic tool has been investigated in cardiovascular pathology: following myocardial infarction (MI), PTX3 plasma levels peak within 7.5 hours as compared to CRP which peaks around 50 hours [60]. In MI patients, PTX3 but not CRP, after adjustment for major risk factors and other acute phase proteins, independently predicted 3-month mortality [96], thus suggesting PTX3 as a strong prognostic marker of CVD death, independently of other acute phase proteins.

In the Bruneck study, PTX3 plasma levels, although not correlated with carotid artery IMT, were higher in individuals with atherosclerotic plaques and prevalent vascular diseases [137].

PTX3 is present in the intact myocardium, increases in the blood of patients with acute myocardial infarction, and represent an early indicator of myocytes irreversible injury in ischemic cardiomyopathy [60]. In a large cohort of patients with myocardial infarction, with ST elevation, PTX3 but not the liver-derived short pentraxin CRP or other cardiac biomarkers (NT-proBNP, TnT, CK) predicted 3-month mortality after adjustment for major risk factors and other acute-phase prognostic markers [96]. A

similar observation was confirmed in the Cardiovascular Health Study where PTX3 was showed to be independently associated with increased risk of all-cause death and cardiovascular-disease-(CVD) related mortality (also after adjusting for all major cardio-metabolic risk factors) [138]. Further studies confirmed that PTX3 represents a more specific marker for acute coronary syndrome (ACS) compared to neutrophils activating peptide-2 (NAP-2) and cardiac troponin I (cTnI) in patients with unstable angina pectoris, NSTEMI, and STEMI within the first six hours of the onset of chest pain [139]. These findings support the concept of PTX3 as a very sensitive marker of plaque inflammation and vulnerability and of the prognosis of the coronary disease. Patients with unstable angina pectoris and those who undergo percutaneous coronary intervention generally present PTX3 levels three times higher than the reference range [140]. Coronary stenting enhances circulating PTX3 levels in association with an inflammatory response and the levels are positively correlated with the increase in activated Mac-1 on the surface of neutrophils at 48 h in the coronary sinus [141]. These data suggest that PTX3 may be a useful marker for evaluation of inflammatory reaction and neointimal thickening after coronary vascular injury and also myocardial infarction.

Among the different markers of inflammation tested, PTX3 was consistently associated with outcomes in heart failure (HF) patients [142]. In two large independent clinical trials (CORONA and GISSI-HF), baseline elevated PTX3 was associated with a higher risk of all-cause mortality, cardiovascular mortality or hospitalization for worsening HF [142]. PTX3 levels were positively associated with the severity of dilatative cardiomyopathy and increased risk of HF [143]. Furthermore high PTX3 plasma levels (but not CRP, interleukin-6, or TNF-α) were associated with an echocardiographic measure of left ventricular dysfunction (E/e′ ratio) in controls without HF and in patients with HF and normal or reduced ejection fraction [144]. These findings would suggest that in humans PTX3 could be either a bystander resulting from the action of pro-inflammatory cytokines in damaged tissues or a molecule directly involved in the extent and outcome of the inflammatory response.

PTX3 and genetic variants

More informative data of the role of PTX3 in humans came from the analysis of single-nucleotide polymorphisms (SNPs) in the PTX3 gene: PTX3 SNPs have been shown to modify the risk of pulmonary tuberculosis [145] and colonization by *Pseudomonas aeruginosa* in patients with cystic fibrosis [146]. Furthermore, these SNPs were found to alter blood levels of the PTX3 protein in Ghanaian women [147] and in lung-transplant recipients with primary graft dysfunction [148]. In another study, three common PTX3 polymorphisms (rs2305619, rs3816527 and rs1840680) were found not to significantly influence the risk of acute myocardial infarction (AMI) in an European population, even if these SNPs, and the corresponding haplotypes, are associated with different levels of PTX3 in the blood; the most frequent haplotype, GAG, associated with lower plasma PTX3 levels than ACA and AAA. Conceivably haplotypes affecting PTX3 levels are not relevant for the risk of AMI, although the authors confirmed the prognostic value of PTX3 plasma levels in AMI patients [149]. The G-A/G-A haplotype was consistently associated with a defect in PTX3 expression in bronchoalveolar-lavage fluid, lung-biopsy specimens, and innate immune cells; the decreased expression of PTX3 transcript in neutrophil precursors was consistent with the predicted alterations in the mRNA secondary structure, which likely affects regulation of PTX3 expression. Clinically, genetic deficiency of PTX3 affects the antifungal function of neutrophils, increasing the susceptibility to invasive aspergillosis in patients undergoing hematopoietic stem cell transplantation [150].

Another PTX3 polymorphism (rs2305619, A/A genotype) was associated with high levels of PTX3 and with hepatocellular carcinoma (HCC) in individuals chronically infected by hepatitis C virus (HCV); in a multivariate analysis, adjusting potential confounding factors, patients carrying the A/A genotype had almost two times more chance to have HCC [151].

Physiopathology of arterial thrombosis

Clinical manifestation of arterial thrombosis

Arterial thrombosis is usually defined as the formation of a thrombus in an arterial vessel. In most cases, arterial thrombosis follows rupture of atheroma, and is therefore referred as atherothrombosis, the leading cause of mortality in the industrialized world (**Figure 4**). Atherosclerosis is a diffuse process that starts early in childhood and progresses asymptomatically through adult life. Later in life, it is clinically manifested as coronary artery disease (CAD), stroke, transient ischemic attack (TIA), and peripheral arterial disease (PAD) [152].

The earliest pathologic process of atherothrombosis is endothelial dysfunction, a systemic, reversible disorder [153], which results in the recruitment of inflammatory cells into the vessel wall and in the initiation of atherosclerosis [154]. Endothelial cells produce cytokines, express adhesion molecules such as ICAM-1, VCAM, and selectins, and assist leukocytes and other blood-derived cells in "homing" and atheroma infiltration. Although fatty streaks have been found to be present already in the intima of infants [155], in advanced disease stages, secondary changes may occur in the underlying media and adventitia, leading to the progression of lesions to fibroatheroma by developing a cap of smooth muscle cells and collagen. Atherosclerotic lesions can progress without compromising the lumen because of compensatory vascular enlargement (positive remodelling) [156], which characterizes lipid-rich lesions; plaque disruption and subsequent thrombus formation is responsible for the onset of most acute coronary syndromes (ACSs) and strokes. The magnitude of the thrombotic process triggered upon plaque disruption is modulated by different elements that determine plaque and blood thrombogenicity: local shear rate, tissue factor (TF), apoptotic microparticles, circulating monocytes, and others [152].

The major risk factors for the development of atherothrombotic diseases include smoking, diabetes, hypertension, obesity, physical inactivity, advancing age, positive family history, low high-density lipoprotein cholesterol level, and high low-density lipoprotein cholesterol level, while emerging risk factors comprise elevated levels of

triglycerides, small low-density lipoprotein particles, lipoprotein(a) and coagulation factors (plasminogen activating factor inhibitor 1 and fibrinogen) [157]. Treatment of atherothrombotic patients must include the management of modifiable risk factors through lifestyle changes, and antiplatelet treatment for the prevention of thrombotic complications. The aims of antiplatelet therapy are, firstly, to prevent the occurrence of acute ischemic events through inhibition of platelet thrombus formation and, secondly, to protect distal tissues by inhibiting microembolisation [152]. Despite the important beneficial effect of antiplatelet therapy in atherothrombotic disease, the mortality of this pathology is still high, therefore novel antithrombotic agents have been developed, as agents inhibiting the tissue factor metabolic pathway [152]; however, innovative therapies are warranted.

Hemostasis and blood coagulation

Thrombus formation at sites of vascular injury is crucial for normal hemostasis, but it also leads to arterial thrombosis in pathological conditions. The blood coagulation system comprises platelet adhesion, activation and aggregation, fibrin formation, and fibrinolysis. Activation of blood coagulation occurs primary through interaction between platelets, vessel wall and plasma proteins (primary haemostasis). When the endothelial layer is damaged and possibly disrupted as a consequence of the injury to blood vessel wall, the underlying extracellular matrix is exposed and triggers sudden platelet activation and adhesion [158]. Initial platelet adhesion to the damaged vessel wall is mainly mediated through interaction of the platelet GPIb–V–IX receptor complex with Von Willebrand factor (vWF) bound to exposed collagen [159]. After adhesion of the platelets, they become deformed due to cytoskeletal changes, thereby exposing activated integrins and releasing dense granule contents (ADP and ATP) and serotonin. Later, platelets secrete fibrinogen, fibronectin and vWF, stored in the alpha granules, expose fibrinogen and fibronectin receptors and P-selectin on their surface, and finally release lipid products [160], as the arachidonic acid, which is converted to thromboxane A2, a powerful mediator of platelet aggregating response. These phenomena lead to the “final common pathway” of platelet activation, the functional upregulation of integrin adhesion receptors, stable adhesion on the ECM and platelet aggregation. Among the integrins expressed by platelets, αIIbβIII is

considered the most important as it mediates adhesion to the subendothelium [161] and platelet aggregation by binding of fibrinogen [158]. Activated platelets also contribute to coagulation by exposing phosphatidylserine (PS) which enhances the assembly and activity of two major coagulation factor complexes on the platelet surface. Indeed, to insure stability of the initially platelet aggregate (platelet plug), a fibrin mesh (also called the clot) forms and entraps the plug by the activation of the coagulation cascade. If the clot contains only platelets it is called a white thrombus; if red blood cells are present it is called a red thrombus. The coagulation cascade, also known as secondary hemostasis, consists of the stepwise activation of inactive precursors (zymogens) leading to the formation of the ultimate product of fibrin. The coagulation cascade includes the intrinsic pathway (dependent on contact activation by a negatively-charged surface, and involving coagulation factors XII, XI, IX, VIII and V), and the extrinsic pathway (dependent on tissue-factor being exposed to the circulation, and involving tissue factor and factor VII), converging on a common pathway to activate factor X, leading to conversion of prothrombin (factor II) to thrombin (factor IIa) and culminating in the conversion of fibrinogen to fibrin [162].

In the extrinsic pathway, circulating factor VII is activated to VIIa (FVIIa) and form a complex with exposed tissue factor (TF-FVIIA); FVIIa directly activates factor IX and X. In the intrinsic pathway, high-molecular-weight kininogen (HMWK), prekallikrein, and factor XII (Hageman factor) generates a complex with exposed collagen. Prekallikrein is converted to kallikrein and factor XII becomes factor XIIa. Both the intrinsic and extrinsic use the common pathway which start with the activation of FXa. FXa generates the “pro-thrombin complex” with FV, platelet factors and Ca^{2+}, to activate FII to thrombin; thrombin cleaves fibrinogen in soluble fibrin, which thanks to FXIII becomes insoluble and bridges the initial platelet aggregate to form a stable clot. Finally, physiologically, the clot must be dissolved to resume normal blood flow following tissue repair, a process known as fibrinolysis. The dissolution of the clot occurs through the action of plasmin, a protease which is generated from circulating plasminogen by FXIIa [162].

P-selectin

P-selectin is an integral membrane protein, belonging to the selectins, a family of adhesion molecules, expressed on the surface of both platelet and endothelial cells. It is stored in platelet α granules and in Weibel-Palade bodies of endothelial cells [163]. P-selectin is involved in a number of processes, including platelet aggregation, platelet-endothelium and platelet-leukocyte interactions [164].

After degranulation, P-selectin rapidly translocates on plasma membrane where it mediates the stabilization of platelet aggregates and leukocyte rolling, the first step of cellular adhesion [163, 165, 166], which is crucial during inflammation and leukocyte recruitment at the injured site [164].

Furthermore, P-selectin is a key player for platelet and leukocyte interactions as platelet P-selectin binds PSGL-1 (P-selectin glycoprotein ligand 1), expressed on leukocyte surface, leading to aggregates formation which induce the release of chemokines as CCL2 and CCL5, cytokines as IL-1β responsible of the propagation of the inflammatory response [167, 168]. The relevance of this interaction has been proved in P-selectin KO [169] and PSGL1 KO mice [170], which show a dramatically reduced leukocyte rolling. Platelet-leukocyte rolling is a typical feature of inflammatory states as well as cardiovascular diseases [171-177] and the adhesion and following rolling of platelet-leukocyte aggregates is significantly stronger than those of single leukocytes [178]. Indeed, P-selectin KO mice exhibited a significant prolongation of time to thrombotic occlusion after arterial injury and decreased platelet-leukocyte aggregates [179]. Therefore, platelet-derived P-selectin has a key role during arterial thrombosis, enhancing stable interactions between platelets and leukocytes [179], and inducing the release of endothelial-derived P-selectin, thus resulting in leukocyte rolling on activated endothelium [167]. Furthermore, platelet-derived P-selectin contributes to atherogenesis promoting platelet-leukocyte and monocytes aggregates [180], increasing leukocyte adhesion on ECs and macrophage recruitment in the arterial wall [181]. Indeed, in mouse models of atherosclerosis (apoE KO mice), P-selectin deficiency is associated with a significantly reduction of atherosclerotic lesion and leukocyte recruitment [182].

Role of extracellular matrix proteins in the thrombotic event

The interactions between platelets and extracellular matrix (ECM) proteins, derived from the vessel wall, plasma, platelets themselves, are central to both the initial adhesion and the subsequent activation and aggregation of platelets, which, together with coagulation, generate the fibrin clot [158]. ECM proteins are actively synthesize by endothelial cells, which deposit them basally or retain them in the Weibel-Palade bodies; under the endothelial cell layer, the basement membrane contains type IV collagen, laminins, nidogens, and perlecan [183]. Below ECs, smooth muscle cells, in larger vessels, form a separate medial layer with its own extracellular matrix components including elastin and collagens [184]. Therefore, the ECM proteins to which platelets and leukocytes become exposed depend on the degree of injury to the vessels: mild injuries, as the damage to the endothelial layer, will expose type IV collagen, laminins, and VWF, whereas more extensive injuries exposing the smooth muscle layer or interstitial ECM will expose them in addition to fibrillar collagens, elastin and other ECM proteins [185].

Platelet adhesion under arterial high shear conditions (as in arteries) is a multistep process that requires interaction of various receptors, some generic and some platelet-specific, with their ligands in the ECM [158]. One of the best characterize ECM receptor is the integrin, αIIbβIII, which exhibits a tightly regulated switch between inactive and active states. Once activated, αIIbβIII binds many different ECM proteins, particularly fibrinogen, its major ligand, leading to platelet aggregation and formation of an occlusive thrombus [185]. Fibrillar collagens are potent activators of GPVI and are thus considered strong triggers of thrombosis. However, while fibrillar collagens type I, III, and V are found in the deeper layers of the ECM and are thus not accessible after superficial injury, collagens type IV, VIII, and XVIII are expressed in the basement membrane and studies on experimental models of thrombosis have demonstrated that even type IV collagen can trigger GPVI-dependent thrombosis induced by superficial injury to the vessel wall [186].

Collagen receptors: GPVI and α2β1

Collagen consists of GXY sequences (G glycine, X and Y are often proline and hydroxyproline). Barnes and Farndale showed that 10% of collagen type I and III is

constituted by GPO sequence (where O is hydroxyproline), which is the strongest stimulus of platelet activation through its interaction with GPVI [187]; they also demonstrated that another specialized sequence, the GFOGER, is recognized and bound by integrin α2β1 [188, 189]. The role of these receptors in platelet adhesion to collagen is highly debated: GPVI is essential for platelet activation and aggregation to collagen, while integrin α2β1 contributes to the firmly adhesion of platelets on exposed collagen [190].

GPVI is a component of immunoglobulin superfamily and its activity depends on the interaction with Fcγ (Fc receptor γ subunit). GPVI presents a ITAM sequence (immunoreceptor tyrosine-based activation motif), which, together with the adaptor proteins LAT e LCP2 and the tirosyn kinase SYK, activates PLCγ2 (phospholipase Cγ2), leading to the production of the second messengers DAG (1,2-diacylglycerol) and IP3 (inositol 1,4,5-trisphosphate). DAG activates PKC (protein kinase C), while IP3 promotes Ca^{2+} release from intracellular storage, increasing its cytosolic concentration. GPVI-mediated activation induces integrin exposure, release of intracellular mediators, thus playing a key role in thrombus formation [190, 191].

Integrins are heterodimeric receptors, with a big subunit α and a small one β, which controls the interaction with ECM proteins and between cells, contributing to a variety of biological processes [192]. Integrins are usually expressed in a low affinity state, which switches to an high affinity state after platelet activation, a process known as "inside-out" signaling. On the other way, integrin ligands can trigger other cellular processes, as the spreading on the exposed ECM proteins, with the "outside-in" signaling [193]. Integrin α2β1 has been shown to bind collagen type I, II, III, IV and XI, however its role in the haemostasis and thrombosis is still debated: α2β1 has an important, but not essential role in platelet adhesion together with other integrins, as αIIbβIII [194, 195]. Furthermore, the "inside-out" signaling, triggered by GPVI, regulates α2β1 expression and, at the same time, the interaction between collagen and α2β1 induces an intracellular activation, similar to that of GPVI (activation of PLCγ2) [190].

Experimental models of arterial thrombosis

The study of blood coagulation has been experimentally achieved by the knocking-out or over-expression of its components; in addition, numerous genes encoding platelet, vascular endothelial cell, and vascular smooth muscle cell proteins have been targeted in animal models, especially mice. These genetically modified animals have provided tremendous opportunities to examine the functions of specific genes *in vivo* and their roles in disease processes, to test the effect of different compounds affecting blood coagulation. Beyond these approaches, a variety of murine thrombosis models, which mimic human vascular diseases, have been developed to investigate blood coagulation, and directly visualize platelet-platelet and platelet-endothelium interactions [186, 196, 197]. The most used models, which generally induce lesions in different vascular beds usually by chemical injury, include the external application of ferric chloride ($FeCl_3$) [198, 199], injection of Rose Bengal followed by light excitation [200], or mechanical injury through arterial compression, ligation or introduction of a guide wire [201, 202].

Ferric chloride ($FeCl_3$) injury

$FeCl_3$ injury consists in the direct application of a filter paper saturated with a solution of ferric chloride (usually from 5% to 50%) to the adventitial surface of an artery which rapidly induces formation of a platelet-rich thrombus that typically progresses to complete vascular occlusion within 20 - 40 minutes [199]. A microvascular probe is used to monitor blood flow within the artery. The degree of arterial thrombosis depends on the concentration of $FeCl_3$ solution, the size of filter paper and the time of application (generally from 1 to 3 minutes); however, thrombi that form in mice after $FeCl_3$ injury are platelet-rich and exhibit a microscopic appearance that is very similar to that of arterial thrombi that form in humans [203]. The exact mechanism by which thrombus formation is triggered in this model has not been clear for many years. The $FeCl_3$ injury, which has been described as “outside-inside”, produces transmural cell necrosis and disrupts the integrity of the vascular endothelium. However, the precise mechanism by which ferric chloride triggers thrombosis is still debated: initially, clot initiation has been attributed to free iron-induced denudation of endothelial cells and the subsequent exposure of the

subendothelium that triggers platelet adhesion/aggregation and activation of the coagulation cascade [201], but later, studies using mice deficient in collagen receptor GPVI have produced contradictory results, reporting both normal and altered thrombus formation [204, 205]. However, more recent works showed that after $FeCl_3$ application platelet adhesion occurs both on a denudated endothelial layer with a limited collagen exposure in the vessel [206], and on a intact endothelium mediated by erythrocytes as revealed with scanning electron microscope (SEM) analysis [207]. Indeed, another recent work showed that $FeCl_3$ has multiple dose-dependent effects on blood, leading to a 2-phase mechanism of action: in the first phase, the charge-based complexation of positively charged iron species and negatively charged proteins (cell surface bound and in solution) initiates $FeCl_3$-induced thrombosis independent of biological ligand-receptor interactions. Erythrocytes are the first adherent blood component, and form the bulk of the initial aggregate. In the second phase, endothelial cell death and iron-bound, adherent blood components initiate the conventional biological clotting cascade [208].

Photochemical injury

The photochemical injury involves intravenous administration of a photoreactive substance, usually Rose Bengal, followed by illumination of an exposed arterial segment with green light (540 nm) delivered from a xenon lamp equipped with a heat-absorbing filter [200, 209]. Rose Bengal accumulates in the membranes of endothelial and other cells [210], and the exposure to green light triggers locally a photochemical reaction that produces singlet oxygen and promotes the formation of other reactive oxygen species that damage the vascular endothelium and induce the formation of occlusive thrombi within 30 - 40 minutes [200, 209].

More recently, lasers have been used to induce endothelial injury in the microcirculation [211], which typically triggers the formation of non-occluding thrombi within a few minutes; therefore, different type and severity of lesions can be achieved depending on the intensity and exposure time of the laser beam which may be useful to identify potentially different mechanisms of thrombus formation triggered by the exposure of different layers of the vessel wall [197].

Mechanic injury

Endothelial denudation can be induced mechanically in large arteries (aorta, carotid artery, femoral artery) either by direct damage of the luminal side of the vessel using a guide-wire [205, 212] or indirectly by compression or ligation of the vessel using a forceps or a filament [213, 214]. All these procedures result in the exposure of the native ECM thereby triggering thrombus formation by collagen- and thrombin-dependent mechanisms which may perhaps best reflect naturally occurring vascular lesions [197].

Obesity and metabolic diseases

Obesity and its metabolic complications (generally referred as metabolic syndrome, MetS) are a complex disease with high socio-economic cost and are considered a worldwide epidemic. MetS is associated with an increased risk of cardiovascular diseases [215], insulin resistance and type 2 diabetes [216], chronic kidney disease [217], risk of cancer [218] and pulmonary diseases [219].

Clinically, metabolic syndrome is defined as the presence of at least three of the following criteria: central obesity (waist circumference in men >102 cm and in women >88 cm), hypertriglyceridemia (≥150 mg/dL), low HDL cholesterol (men <40 mg/dL, women <50 mg/dL), elevated fasting glucose (>110 mg/dL), and hypertension (≥130/85 mmHg) [220]. A central feature is central obesity which predisposes to insulin resistance, resulting in hyperglycemia and hyperinsulinemia, and eventually leading to the development of diabetes [221]. Chronic inflammation is another feature of the metabolic syndrome, which, together with insulin resistance, results in complex metabolic derangements that contribute to the pathogenesis of hypertension, atherogenic lipoprotein profile, atherosclerosis, coronary artery disease, and other organ dysfunction [222, 223].

The pathogenesis of obesity-associated diseases has revealed a close relationship between nutrient excess and derangements in the cellular and molecular mediators of immunity and inflammation, a phenomenon known as “metainflammation” [2] which describes the chronic low-grade inflammatory response to obesity. The inflammatory response triggered during obesity is attributed to the excess consumption of nutrients and therefore referred as metabolic. Furthermore, specialized metabolic cells (such as adipocytes) are the cells that sustain the insult and begin the inflammatory response, contributing to an unbalanced metabolic homeostasis [224]. Indeed, the finding in the 1990s that tumor necrosis factor-alpha (TNFα) is overexpressed in the adipose tissue of obese mice provided the first clear link between obesity, diabetes and chronic inflammation [225]. This link between inflammation and metabolic dysfunction has also been proved in humans, as some pro-inflammatory markers have been positively correlated with the metabolic syndrome and insulin resistance [226-229]: obese subjects, indeed, present elevated white blood cell counts, plasma levels of

coagulation factors (fibrinogen and plasminogen activator inhibitor 1 (PAI-1)), acute-phase proteins such as C-reactive protein (CRP) and serum amyloid A (SAA), pro-inflammatory cytokines (TNFα, IL-1β and IL-6), and chemokines.

Tissue inflammation in obesity

Data from experimental and clinical studies have demonstrated that adipose tissue, liver, muscle and pancreas are sites of inflammation during obesity and insulin resistance. Particularly, macrophage infiltration into these tissue has been described as a key feature of obese-related inflammation in both humans and animal models of MetS. They act in an autocrine and paracrine manner releasing pro-inflammatory cytokines [230], including TNFα, IL-6 and IL-1β and by interfering with insulin signaling in peripheral tissues through activation of the c-JUN N-terminal kinase (JNK) and NF-κB pathways [231] (**Figure 5**).

Adipose tissue

The inflammatory response that emerges in the presence of obesity seems to be triggered by and to reside predominantly in adipose tissue, characterized by specific up-regulation of genes encoding inflammatory factors and an over-production of many cytokines and chemokines [232]. Adipose tissue has been associated with a marked accumulation in its stromovascular fraction of immune cells [230], particularly represented by macrophages, whose recruitment correlates with the degree of obesity and is crucial for the production of adipose tissue-derived pro-inflammatory cytokines [233, 234]. However, enlarged adipocytes themselves are directly involved in the production of pro-inflammatory cytokines and chemokines [235]. In the adipose tissue of lean individuals, macrophages are usually polarized toward an M2, “alternatively activated” or “anti-inflammatory” subset, characterized by low pro-inflammatory but high anti-inflammatory cytokines (as IL-10 and IL-1 decoy receptor) and arginase expression, which sustain the blockade of inflammatory responses and the promotion of tissue repair [236]. Therefore in adipose tissue, M2 macrophages, derived from CCR2– monocytes, have a potential beneficial role, maintaining normal adipocyte function and perhaps by promoting tissue repair and angiogenesis in adipose tissue [237]. However, nutrient excess leading to adipocyte

expansion, is characterized by increased secretion of monocyte chemoattractants that recruit inflammatory type CCR2+ monocytes to fat, causing a phenotypic switch from M2 to M1, "classically activated" or "pro-inflammatory" macrophages. M1 infiltration is directly correlated with adiposity, insulin resistance and adipose tissue inflammation. This tight relationship between obesity and inflammatory macrophages is confirmed by the observation that weight loss induced by surgery [238] or diet and exercise [239] results in a reduction in the number of adipose tissue macrophages in parallel to the decreased expression of pro-inflammatory markers in both adipose tissue and plasma of obese individuals. Although macrophages are the most abundant leukocyte population in expanding adipose tissue, other cells participate to the inflammatory response as neutrophils [240], mast cells [241], and natural killer T (NKT) [242]. Furthermore, the adaptive immune system may also contribute to obesity-induced inflammation: obesity is indeed associated with changes in the adipose tissue T cell populations, with an increased ratio of CD8+ and CD4+ T cells, especially of the effector phenotype, and decreased of the immunosuppressive T regulatory cells (Tregs), creating an environment favorable to immune activation [243-245] (**Figure 6**).

Among the different fat depots, the intra-abdominal visceral fat is the key component of metabolic syndrome and is indirectly measured by waist circumference in clinical practice. Therefore, besides total adiposity, the pathogenic role of adipose tissue seems to be determined by its specific anatomic location: although both subcutaneous and visceral adipose tissues are associated with metabolic risk profile, visceral adiposity is the most important predisposing factor to metabolic syndrome [246], positively associated with ectopic lipid accumulation in liver and skeletal muscle, further sustaining insulin resistance and metabolic complications [247]. This different clinical significance is determined by different phenotypic, physiological and functional characteristics of visceral adipose tissue [247]: obese subjects have an evident pro-inflammatory profile more in the visceral compared to subcutaneous adipose tissue.

Liver

The liver represents one of the major metabolic organ as it is involved in the control of gluconeogenesis, represent a glycogen storage, and it also contributes to lipogenesis, cholesterol synthesis and secretion [224]. Visceral obesity is often associated with nonalcoholic fatty liver disease (NAFLD), and its prevalence increases in parallel to that of type 2 diabetes (T2DM). NAFLD is one of the causes of fatty liver and includes a large spectrum of lesions, from simple steatosis to steatohepatitis (nonalcoholic steatohepatitis or NASH), which can lead to cirrhosis and hepatocarcinoma [248]. Similar to adipose tissue, inflammatory response has a pivotal role in the progression of the disease: NAFLD and subsequent hepatic insulin resistance in obesity are associated with increased expression and overproduction of inflammatory mediators, including TNFα, IL-6 and IL-1β [249]; however, unlike adipose tissue, the number of resident macrophages, which in the liver are known as Kupffer cells and represent the 10% of total liver cells, does not change but their activation status increased [249, 250]. Kupffer cells directly contribute to the production of pro-inflammatory mediators, sustaining insulin resistance in the liver [249, 250], which is associated with an increased level of circulating cytokines and acute-phase proteins as CRP, PAI-1, serum amyloid A, and IL-6 observed in obese animals and humans compared to lean controls [231, 251].

Muscle

The muscle is a key site of glucose uptake and energy consumption in the body, contributing to glucose homeostasis [224], and is another major site of insulin resistance during both obesity and type 2 diabetes. An infiltration of M1 macrophages has been described in the skeletal muscle [252] and in the inter-muscular adipose depots [233], associated with increased expression of inflammatory mediators, which contributes to locally insulin resistance and, indeed, gene expression of phenotype markers of pro- and anti-inflammatory macrophages in human skeletal muscle seems to correlate with insulin sensitivity [253]. However, muscle cells does not modulate inflammatory response during obesity or regulate metabolism through inflammatory kinase action; on the other hand, the influence of peripheral inflammation on muscle function is well established, as inflammatory cytokines are able to induce insulin resistance in muscle cells in culture [254, 255]

and *in vivo* by infusion into humans, resulting in decreased glucose uptake and glycogen synthesis [256].

Pancreas

The pancreas is directly involved in the maintenance of glucose homeostasis, as the source of insulin and glucagon. Failure of this organ to produce sufficient insulin in response to rising systemic glucose levels is at the center of diabetic disease [224]. Type 1 diabetes is an established autoimmune disease where auto-reactive immune cells destroy the insulin-producing β cells, however, accumulating evidence suggest a central role of inflammatory response in the dysfunction of pancreas during type 2 diabetes [224]. The insulin resistance, which is a key feature of obesity, is mainly related to a failure of pancreatic β cells to produce enough insulin to remove glucose from the circulation at normal concentration, leading to chronic hyperglycaemia. Therefore, an increased production of insulin, to compensate for its peripheral resistance, takes place, which is however associated with increased β cell stress and apoptosis. Indeed, an inflammatory response was demonstrated in the pancreatic islets of patients with type 2 diabetes as shown by the presence of amyloid deposits, fibrosis, increased β cell death and infiltration of macrophages along with increased levels of pro-inflammatory cytokines and chemokines [257], leading to immune cell recruitment in islets [258].

Animal models of obesity and MetS

Animal models have been extensively used to study the mechanisms by which obesity induces pathological dysfunctions; among the types of animal models, rodents represent the most used model of obesity and its metabolic complications. However, before choosing an animal model is important to understand the basics of the controls of food intake and how they might relate to obesity. Factors that influence food intake and consequently body fat can be classified in those that have an influence when individuals start eating, those that influence when eating and at the end of eating: in detail, satiation factors interact in the brain with signals generating mainly from adipose tissue and pancreas, therefore representing a mirror of how lean or fat the individual is. These signals, such as leptin and insulin, interact

with receptors in the hypothalamus and have potent effects on food intake, energy expenditure and the level of stored fat. Most of the animal models commonly used to investigate causes and treatments for obesity have therefore altered activity in brain circuits integrating satiation and adiposity signals [259]. Based on these findings, animal models of obesity can be distinguished into different categories, depending on whether obesity derived from mutations or manipulations of genes involved in the energetic homeostasis (satiation and adiposity signals) or triggered by the consumption of high-fat diets in genetically intact animals.

Genetically-induced obesity

Animals with a defect in the leptin-signaling pathway in the hypothalamus of the brain develop an obese phenotype. Leptin is known as the "satiety hormone" [260], which is made by adipose cells and helps to regulate energy balance by inhibiting hunger. Leptin is opposed by the actions of the hormone ghrelin, the "hunger hormone". Both hormones act on receptors in the arcuate nucleus of the hypothalamus to regulate appetite and achieve energy homeostasis [261]. Obesity is usually characterized by a decreased sensitivity to leptin, resulting in an inability to detect satiety despite high energy stores [262]. The models with a defect in the leptin-signaling pathway include animals that lack leptin production and/or are insensitive to leptin due to leptin receptor mutations or extreme leptin resistance. Mutations are spontaneous (Lep^{ob}/Lep^{ob} and Lep^{db}/Lep^{db} mice) or genetically engineered. Lep^{ob}/Lep^{ob} mice exhibit early-onset obesity characterized by hyperphagia, reduced energy expenditure and hypothermia; further defects are hypercorticosteronemia, insulin resistance associated with hyperglycemia and hyperinsulinemia, hypothyroidism and growth hormone deficiency leading to a decrease in linear growth [263-268]. The Lep^{db}/Lep^{db} is phenotypically similar to the Lep^{ob}/Lep^{ob}, but their leptin levels are markedly elevated as a consequence of leptin receptor mutation; they are insulin resistant and develop diabetes [269].

Another monogenic spontaneous mutation affects the expression of *aguti* protein. Agouti is a pigment control gene transiently expressed in follicular melanocytes to induce the production of red/yellow pheomelanin pigment and inhibit black/brown pigment [270-272]. The lethal yellow mutant mouse (A^y) is characterized by the

ubiquitous protein expression due to loss of the tissue-specific control promoter element [273, 274]. A^y mice exhibit several phenotypes such as a yellow coat color, mature-onset obesity, type-II diabetes, hyperleptinemia, increased linear growth, higher tumor susceptibility, and infertility [275].

Another monogenic mutation to mention is the melanocortin receptor 4 (MCR4) knock-out mice which is the model of the most frequent genetic cause of obesity in humans. MCR4 KO mice do not respond to leptin mice and are hyperinsulinemic, hyperglycemic and hyperleptinemic [276].

Beyond monogenic forms, other models of obesity include polygenic models which could be much more relevant to human obesity.

Diet-induced obesity

The diet-induced obese (DIO) rat and mouse offers more human-like models, where the obesity is based on several factors, including an excess intake of calories. However, diet-induced obesity in rodents can be obtained by different means; there is a large variation both with respect to the content of the diet used, as well as the strain used [277]. Among the various strains, C57BL/6J mice are the most widely used for high fat diet (HFD)-induced obesity because they exhibit abnormalities similar to human metabolic syndrome when fed the HFD [278]. The HFD usually used are composed by 45% or 60% of calories from fat as they are intended to mimic the western type diet. C57BL/6J exhibit an increase in body weight just after 2 weeks, but the increase is gradual and becomes apparent after 4 weeks. After 16–20 weeks of high-fat diet feeding, mouse will typically exhibit 20–30% increase in body weight when compared to chow-fed mouse [279]. The effects of HFD on blood glucose are more discrepant and depend on the type of dietary regimen. Hyperglycemia usually develops within 4 weeks of a high-fat diet [280]. The elevation of fasting glucose is usually accompanied by increases in fasting insulin levels and the hyperinsulinemic-euglycemic clamp experiments demonstrated whole-body insulin resistance. Nevertheless, the full manifested picture of obesity develops after 16 weeks of high-fat diet with adipocyte hyperplasia, fat deposition in mesentery, increased fat mass, diabetes, and hypertension [281].

Aim of the project

Pentraxin 3 (PTX3) belongs to the pentraxin superfamily, soluble, multifunctional, pattern recognition proteins, and is an essential component of the humoral arm of innate immunity. More recently, it's role in cardiometabolic diseases has gained attention thanks to the observation that, in humans, its plasma levels peak during cardiovascular diseases, while in mice PTX3 was shown to protect toward myocardial infarction, restenosis and atherosclerosis.

Aim of this PhD project was to investigate the role of PTX3 in two common morbidities that affect particularly Western countries: arterial thrombosis, a critical complication of atherosclerotic plaque rupture correlated with clinical manifestations as myocardial infarction or stroke, obesity and its related metabolic complications, a worldwide epidemic with increasing socioeconomic cost.

In vivo arterial thrombosis was characterized with the $FeCl_3$-induced thrombosis in PTX3 KO and WT mice and in PTX3 KO chimera mice generated by bone marrow transplantation to reveal the source of the protein responsible for the phenotype observed. To study the relevance of the interaction between PTX3 and P-selectin, arterial thrombosis was characterized in PTX3/P-selectin double KO mice. Later the molecular mechanisms of the phenotype observed were investigated with *in vivo* and *in vitro* studies to selectively evaluate the contribution of platelets, leukocytes and vascular wall in $FeCl_3$-induced arterial thrombosis.

Metabolic syndrome and obesity was investigated feeding for 20 weeks PTX3 KO and WT mice to a high fat diet (HFD), characterized by 45% of calories from fat, which is a commonly used model of diet-induced obesity. Weight gain was measured weekly, while adipose tissue deposition in the visceral, subcutaneous and intrascapular area was checked after 10 and 20 weeks of diet. A characterization of gluco-metabolism was performed at 10 and 20 weeks of diet through test of gluco- and insulin tolerance. Finally, to evaluate possible molecular mechanisms, a characterization of the immune-inflammatory response of the visceral adipose tissue was carried out.

Materials and Methods

Animals

PTX3 KO animals were generated at the Humanitas research institute as described in detail before [52]. Complete peripheral blood cell counts and microscopic examination of blood smears of PTX3 KO did not show statistically significant differences compared to WT animals. Microscopic examination of organs and tissues of young or adult mice (ten months old) did not reveal morphological abnormalities. Heterozygous females and males are normal and fertile and breeding yielded the predicted number of homozygous null mice at a mendelian frequency. However, PTX3 KO females exhibit a severe defect in fertility [52]. P-selectin KO mice were from the Jackson Laboratories and P-selectin/PTX3 KO mice were generated by crossing the two animal models. All mice were on a C57BL/6J background.

The investigation conforms to the European Commission Directive 2010/63/EU and was approved by the Ethical Committee (Progetto di Ricerca 2009/3 and Progetto di Ricerca 2012/02).

Bone marrow transplantation

Wild-type (WT) or PTX3 KO mice were lethally irradiated with a total dose of 900 cGy. Two hours later, mice were injected in the tail vein with 5×10^6 nucleated bone marrow (BM) cells obtained by flushing of the cavity of a freshly dissected femur from a WT or PTX3 KO donor. Recipient mice received gentalyn (0.4 mg/ml in drinking water) starting 10 days before irradiation and maintained thereafter [57]. At 8 weeks after BM transplantation, the FeCl3 injury model was carried out as described below.

$FeCl_3$ injury: experimental arterial thrombosis model

Experimental arterial thrombosis was induced as originally described in the work of Kurz and colleagues [199]. Briefly, mice (8-12 week old) were anesthetized with ketamine chlorydrate (75 mg/Kg) and medetomidine (1 mg/Kg; Virbic). The left carotid artery was dissected free and placed in the probe (model 0.7V, Transonic System) connected to transonic flow meter (Transonic T106). After blood flow stabilization (baseline flow constant for 7 min), filter paper imbibed with $FeCl_3$ (10-20%) was applied downstream of the probe to the top of the exposed carotid. After 3

minutes, the filter paper was removed, the carotid artery was washed with PBS, and the flow was recorded for 30 minutes. In a group of experiments, human recombinant PTX3 (hPTX3, 5 mg/kg per mouse [57, 282]) or PBS (as negative control) was injected iv. before the arterial thrombosis experiment.

Pulmonary thromboembolism

A disseminated thrombosis model was generated in mice (8-12 week old) by i.v. injection of a mixture of collagen (0.45 mg/Kg) and epinephrine (0.055 mg/Kg); animals were monitored for 10 minutes. Death within this time frame was deemed to be a direct consequence of microthrombi formation in lung capillaries due to collagen/epinephrine administration.

Platelet count, tail bleeding time and fibrinogen, PT and aPTT measurement

Platelet were counted optically from whole blood collected by orbital sinus bleeding into Unopette System reservoirs. Bleeding time was measured on tails of anesthetized mice, and immersed in saline solution at 37°C. After 3 minutes the last part of the tail, 3 mm from its end, was cut with a sharp scalpel blade, then immediately re-immersed in saline solution. Bleeding was followed visually, and time was determined as the interval (sec) from the tail transection to cessation of bleeding; 900 sec was considered the cut off time for the purpose of statistical analysis [283, 284]. Fibrinogen levels were measured as previously described [285] from plasma (PPP) obtained after centrifugation of blood [collected by cardiac venipuncture from anesthetized mice into 3.8% sodium citrate (1:10 vol:vol)] at 1000 g for 10 minutes. For prothrombin time (PT) test, PPP was mixed with Tissue Factor (TF) (containing phospholipid) at 37°C and an excess of calcium chloride (25 mM) was added to initiate coagulation. Time was determined as the interval (sec) between calcium addition and clot formation. For activated partial thromboplastin time (APTT) test, PPP was incubated at 37°C with phospholipid (cephalin) and a contact activator (e.g. Kaolin) was added followed by the calcium (all pre-warmed to 37°C). Addition of calcium initiates clotting and time was determined (sec) as the interval taken for a fibrin clot to form.

PTX3 plasma levels –ELISA assay

PTX3 plasma levels were measured with a sandwich ELISA using 2 anti-murine PTX3 mAb (2C3 and 6B11) [42]. The ELISA assay did not cross-react with the short pentraxins CRP and SAP.

P-selectin and integrin αIIbβIII expression on platelet surface

Platelet rich plasma (PRP), isolated following centrifugation at 100xg with no break of citrated blood, from PTX3 KO and WT mice was stimulated with collagen (10 μg/mL, Mascia Brunelli, Italy) and U46619 (10 μM, Cayman Chemical, USA), an analogous of thromboxane for 1 or 10 minutes, for P-selectin or integrin αIIβIII, respectively, and then stained with the anti-CD42c FITC and anti-CD62P PE or αIIβIII PE antibodies (Emfret, Germany). Samples were fixed with PFA 4% and the expression of the platelet activation markers was evaluated through flow cytometry (BD FACS Calibur).

Platelet-leukocyte aggregate analysis

Citrated blood from PTX3 KO and WT mice was stimulated with ADP (40 μM, Sigma-Aldrich, Italy) for 30 seconds or 1 minute and fixed with BD lysis buffer; samples were stained with the anti-CD45 PE (BD) and anti-CD42c FITC antibodies (Emfret, Germany) and analyze through flow cytometry (BD FACS Calibur).

Histology and immunofluorescence

Mouse carotid arteries and lungs (perfused with PBS) and adipose tissue were excised, fixed in 10% neutral formalin, processed and then embedded in paraffin. Section of 5 μm were stained with hematoxylin and eosin, or DAPI and fluorescent antibodies against PTX3 and fibrin and visualized with Axiovision software at 10x magnification. PTX3 protein expression in carotid arteries was analyzed as described [41, 85].

Platelet aggregation

Citrated blood was diluted with HEPES-Tyrode buffer (137 mM NaCl, 20 mM HEPES, 5.6 mM glucose, 0.35% bovine serum (BSA), 1 mM MgCl2, 2.7 mM KCl, 3.3 mM NaH2PO4) and centrifuged. Washed platelets, obtained by serial

centrifugations of PRP with the addition of PGI2 and apyrase, were adjusted to 250 x 10^3 platelets/ μL, and aggregated by Born turbidimetric technique in presence of collagen (0.5 or 1μg/mL), ADP (0.5 or 1μM) and fibrinogen (0.25 mg/mL). For some experiments PTX3, its C-terminal or N-terminal domain (1μg/mL) were incubated for 1 hour at RT with fibrinogen (IMMUNO AG, Italy – ratio 1:10) or overnight at 4°C with collagen (Mascia Brunelli, Italy – ratio 1:1). As controls, same conditions were used for samples without PTX3 and its domains. Samples were incubated in an acid solution [70] (Diluent B, Mascia Brunelli, Italy). To exclude unspecific binding to collagen, the ability of collagen preincubated with BSA (1μg/mL, same experimental conditions used for PTX3) to stimulate aggregation was tested and resulted similar to that of collagen without preincubation with BSA (data not shown).

Diet induced obesity model

PTX3 KO and WT mice at 12 weeks of age were switched from the standard diet (Chow diet, 12% of the calories from fat) to an high fat diet (HFD), as a model of diet-induced obesity. Some WT mice were fed to a standard fat diet (SFD) and compared to WT mice fed to HFD. Both HFD and SFD were given for 20 weeks.

HFD composition

• Protein	24 g%	20 kcal%
• Carbohydrate	41 g%	35 kcal%
• Fat	24 g%	45 kcal%
• **Total**	**4,13 kcal/g**	**100 kcal%**

SFD composition

• Protein	19,2 g%	20 kcal%
• Carbohydrate	67,3 g%	70 kcal%
• Fat	4,3 g%	10 kcal%
• **Total**	**3,85 kcal/g**	**100 kcal%**

The diet was administered 3 times a week and food intake was measured daily for 4 weeks during both the HFD and SFD treatment. Body weight was measured weekly.

Glucose (GTT) and insulin (ITT) tolerance test

The impairment of glucose metabolism was investigated with the GTT and ITT tests. For the GTT, mice were left fasting overnight and the day after basal glycaemia was measured, with a commercial kit for glycaemia measurement, from a drop of blood taken from mouse tail. Soon after, a solution of glucose (20% w/v in PBS) was injected in the peritoneum and the glycaemia checked after 15, 30, 60, 90 and 120 minutes from injection. For the ITT, mice were left fasting for 4 hours; then basal glycaemia was measured and a solution of insulin (0,1mU/µL) was injected in the peritoneum. As described for GTT, glycaemia was checked after 15, 30, 60, 90 and 120 minutes from injection.

Magnetic resonance for imaging (MRI)

MRI is a test that uses a magnetic field and pulses of radio wave energy to make pictures of organs and structures inside the body. The MRI was used to monitor fat accumulation in the visceral, subcutaneous and intrascapular depots after 10 and 20 weeks of HFD in WT and PTX3 KO mice. Mice were anesthetize with isoflurane during the MRI analysis. The identification of fat was allowed by the different amount of water of this tissue compared to muscles: fat depot appeared white while muscles black. A total of 16 pictures were taken from the visceral and scapular area; then the area of fat depot was measured in 3 pictures per mouse and the average calculated.

Real time quantitative polymerase chain reaction

0,5 – 1 ng of RNA was reverse transcripted from the thoracic aorta or 30 mg of adipose tissue. Two µL of cDNA were amplified by realtime quantitative PCR with 1X Syber green universal PCR mastermix (BioRad, Italy). The specificity of the Syber green fluorescence was tested as described [286]. Each sample was analyzed in duplicate using the CFX-Cycler (BioRad). The PCR amplification was related to a standard curve ranging from 10-11 mol/L to 10-14 mol/Land data were normalized for the housekeeping gene ribosomal protein L13a (RLP13a) [71].

Adipose tissue digestion and analysis of leukocyte infiltration

Epididymal and subcutaneous fat were isolated and cut into small pieces in a solution of collagenase I in BSA 5% and 5mM $CaCl_2$ and incubated for 40 minutes at 37°C. To isolate the stromovascular fraction, digested solution of fat was centrifuged, washed in PBS and filtered with a 70 µM cell strainers. Cells were count and stained with 1 µL of Fc block, to prevent unspecific binding for 30 minutes at 4°C. Later cells were washed and stained with 2 µL of CD45 PerCP Cy 5.5, 1 µL of CD11b BV421, 1 µL of Ly6G PE, 1 µL of Ly6C FITC, 1,5 µL of F4/80 PECy7. Cells were analyzed with the BD Aria Sorter.

Statistical analysis

Statistical analyses were performed with GraphPad Prism6 or with IBM-SPSS statistic. Data were analyzed by the Wilcoxon rank-sum test or by ANOVA with repeated measures for main effects of treatment time and genotype, followed by a Bonferroni post hoc analysis. Data are presented as mean ± SEM.

Results

PTX3 plays a protective role in arterial thrombosis

To unravel the role of PTX3 in the context of arterial thrombosis in experimental models, $FeCl_3$ induced carotid artery thrombosis (**Figure 7A**) was evaluated in PTX3 KO and WT animals. Of note, under basal conditions PTX3 KO and WT present a similar blood flow in the carotid artery (0.67±0.03 mL/min vs 0.60±0.04 mL/min respectively, mean ± SEM are reported); instead, application of $FeCl_3$ 10% resulted in a reduction of blood flow after 30 minutes of -65.2±8.8% for PTX3 KO and -20.2±7.2% for WT (mean ± SEM are reported, $p<0.01$; **Figure 8A**). Furthermore, analysis of the area under the curve of carotid blood flow supported the latter results as PTX3 KO mice presented a significantly decreased AUC compared to WT ($p<0.01$; **Figure 8B**) and these findings were also corroborated by histological analysis of injured carotid arteries which showed increased thrombi occlusion in PTX3 KO than WT vessels (**Figure 8C, 8D**). These data demonstrated that PTX3 plays a protective role during arterial thrombosis.

PTX3 deficiency in vascular cells but not in myeloid cells is associated with increased arterial thrombosis

To disentangle the contribution of bone marrow (BM) cells and of vascular cells in the increased arterial thrombosis observed in PTX3 KO mice, we performed the $FeCl_3$ arterial thrombosis experiment in irradiated PTX3 KO mice reconstituted with the BM of PTX3 KO or WT mice (PTX3 KO/BMT_PTX3 KO or PTX3 KO/BMT_WT) and in irradiated WT reconstituted with the BM of PTX3 KO or WT mice (WT/BMT_PTX3 KO or WT/BMT_WT) (**Figure 9A**). Following the application of $FeCl_3$ (10%), WT transplanted with BM of PTX3 KO behaved similarly in terms of arterial thrombosis to WT transplanted with BM of WT (reduction of blood flow after 30 minutes of -45.5±1.4% for WT/BM_WT and -53.4±9.8% for WT/BM_PTX3 KO; **Figure 10A**) with a similar AUC of blood flow during the 30 minutes after $FeCl_3$ application (**Figure 10B**). In contrast, PTX3 KO transplanted with BM of WT or with BM of PTX3 KO showed a similar reduction of carotid artery blood flow (reduction of blood flow after 30 minutes of -80.4±11.5% for PTX3 KO/BM_WT and -95.5±4.5% for PTX3 KO/BM_PTX3 KO; **Figure 10A**) and in the AUC of blood flow (**Figure 10B**) compared to WT mice transplanted with

both BM of PTX3 KO and WT ($p<0.05$). The differences between groups in carotid arterial thrombus formation were further confirmed by histological analysis (**Figures from 10C to 10F**). These data suggest a critical role of PTX3 originated from the vessel wall in the modulation of thrombus formation observed in PTX3 KO mice while limit the role of PTX3 stored and acutely released by neutrophils described in cardiovascular events [108].

In agreement with this, PTX3 plasma levels, after arterial thrombosis, were similar in WT mice transplanted with either WT or PTX3 KO bone marrow, while the protein was not detectable in PTX3 KO mice independently of being transplanted with WT or PTX3 KO bone marrow (**Figure 10G**).

PTX3 protective activity does not dependent on P-selectin modulation

We next addressed whether PTX3 protective role derived from the modulation of P-selectin; indeed, P-selectin is a key player of platelet-platelet, platelet-leukocyte and platelet-endothelium interaction during thrombosis [287] and it is targeted by PTX3 to dampen neutrophils recruitment [57]. Thus, increased P-selectin-dependent thrombotic response might represent a logical mechanism to explain the pro-thrombotic phenotype observed in PTX3 KO mice [70]. To address this issue, we generated P-selectin/PTX3 double KO mice (P-selectin/PTX3 DKO) and investigated carotid blood flow following arterial thrombosis in these animals compared to P-selectin KO mice.

Following the application of $FeCl_3$ (10%), P-selectin/PTX3 DKO showed increased arterial thrombosis compared to P-selectin KO mice, with a reduction of blood flow after 30 minutes of -32.4±7% for P-selectin KO and -90.5±11% for P-selectin/PTX3 DKO (mean ± SEM are reported, $p<0.01$; **Figure 11A**). The AUC of blood flow during the 30 minutes after $FeCl_3$ application was significantly higher for P-selectin KO compared to P-selectin/PTX3 DKO ($p<0.01$; **Figure 11B**), indicating a significant increased arterial thrombosis in DKO mice as confirmed by histological analysis (**Figures 11C-11D**). Of note, the lack of both proteins resulted in a thrombotic phenotype similar to that observed in PTX3 KO mice, while the only absence of P-selectin was not able to induce the formation of a thrombus, thus suggesting that the protection toward arterial thrombosis exerted by PTX3 might be

independent on P-selectin modulation. Given the partial resistance of P-selectin KO to $FeCl_3$ induced arterial thrombosis, we next investigated the effect of a more robust induction of arterial thrombosis in these mice (application of $FeCl_3$ 20%), to study whether PTX3 deficiency could affect thrombus formation and leukocyte recruitment in the context of P-selectin deficiency. In spite of larger thrombi observed in P-selectin/PTX3 DKO compared to P-selectin KO (**Figures from 12A to 12C**; $p<0.05$), leukocytes recruitment in the thrombus (**Figure 12D**) and the percentage of circulating platelet-leukocyte aggregates, after 30 minutes from $FeCl_3$ application (**Figure 12E**), were not significantly different between P-selectin KO and P-selectin/PTX3 DKO. The latter findings suggested also that the increased thrombus formation in DKO was not dependent on a different leukocyte recruitment during thrombosis. In line with this, ADP stimulation of whole blood from PTX3 KO and WT mice resulted in a similar percentage of platelet-leukocyte aggregates (**Figure 12F**). These observations limit the relevance of the interaction between PTX3 and P-selectin during arterial thrombosis and suggest that PTX3 produced by myeloid cells, including the protein stored in neutrophils, does not contribute to the protection toward arterial thrombosis.

PTX3 deficiency does not affect platelet activation and hemostatic properties

In line with the previous results showing a marginal role of PTX3 in hematopoietic cells, we confirmed that PTX3 deficiency had no effect on platelets aggregation (**Figures 13A-13B**) and function in terms of P-selectin expression and integrin αIIbβIII activation after stimulation with various agonists (**Figures 13C-13F**). This finding was corroborated, *in vivo,* by the observation of a similar mice survival following pulmonary thromboembolism induced by rapid intravenous administration of a mixture of collagen and epinephrine (50% for PTX3 KO and 55.5% for WT mice respectively, **Figure 14A-14B)**, thus limiting a direct effect of PTX3 deficiency on platelet function.

Furthermore, PTX3 KO and WT mice had similar number of circulating platelets (**Figure 15A**), comparable plasma fibrinogen levels (**Figure 15B**) and tail bleeding time (**Figure 15C**). In addition, similar prothrombin time (PT) and activated partial prothrombin time (APTT) were measured in the two groups of mice under basal

conditions (**Figure 15D-15E**). Finally, we excluded that the increased thrombosis observed in PTX3 KO mice was a consequence of an impaired expression of tissue factor (TF) by the vessel wall as aortas from PTX3 KO and WT presented a similar TF expression of mRNA level (**Figure 15F**).

PTX3 acts at the interface between the damaged vascular wall and the thrombus by dampening fibrinogen and collagen pro-thrombotic effects

Following arterial thrombosis, PTX3 localized mainly at the interface between the damaged endothelium and the thrombus **(Figure 16A**), and co-localized with fibrin (**Figure 16B**). Furthermore, based on the recent observation that PTX3 deficiency induces fibrin deposition after tissue injury [70], we investigated whether the interaction of PTX3 with fibrinogen [70] and/or with extracellular matrix components could explain the phenotype observed.

Therefore, we initially performed platelet aggregation with fibrinogen with or without the pre-incubation with PTX3 or its domains. Although platelet aggregation was significantly reduced by 18.72% ± 5.20% when fibrinogen was pre-incubated with PTX3 (mean ± SE are reported**,** $p<0.01$; **Figure 16C**), an effect dependent on the PTX3 N-terminal domain (- 32.50% ± 6.61%, mean ± SE are reported**,** $p<0.01$; **Figure 16C**), this reduction was not enough to explain the phenotype observed *in vivo*. We thus tested the ability of collagen pre-incubated with PTX3 to induce platelet aggregation. Of note, under this condition, a decreased platelet aggregation by 38.67% ± 3.17% compared to collagen alone was observed (mean ± SE are reported**,** $p<0.01$; **Figure 16D**). Interestingly, PTX3 tuning of collagen induced platelet aggregation was dependent on the C-terminal domain (-44.17% ± 5.53%, mean ± SE are reported**,** $p<0.01$; **Figure 16D**). Finally, we reported that the pre-incubation of either fibrinogen and collagen with PTX3 resulted in a synergic effect with a reduction by -35.83% ± 2.19% of platelet aggregation when fibrinogen and collagen were pre-incubated with PTX3 compared to fibrinogen and collagen alone (mean ± SE are reported**,** $p<0.001$; **Figure 16E**). Furthermore, the observation that N-terminal domain appears to be more selective for fibrinogen while PTX3 C-terminal domain appears to be more selective for collagen supported the hypothesis that PTX3 might dampen both fibrinogen and collagen effect, resulting in a

synergistic control of their pro-thrombotic activity. Indeed, when platelet aggregation was investigated in cells treated both with fibrinogen incubated with PTX3 N-terminal domain and with collagen pre-incubated with PTX3 C-terminal domain, a significant reduction of -46% ± 8.81% compared to collagen and fibrinogen alone was observed (mean ± SE are reported**,** $p<0.001$; **Figure 16E**), suggesting a synergistic effect of PTX3 *in vitro*.

Administration of recombinant human PTX3 protects from arterial thrombosis

Data collected so far suggested the possibility that the protective effect of PTX3 on platelet aggregation could be the result of a synergistic control of collagen and fibrinogen pro-thrombotic activity. To extend these findings *in vivo*, we tested whether human recombinant PTX3 (hPTX3) was able to revert the prothombotic phenotype observed in PTX3 KO mice. Mice were injected i.v. with human recombinant PTX3 (5 mg/kg) [57, 282] followed by $FeCl_3$ (10%) injury. While PTX3 KO mice injected with PBS showed a reduction in carotid artery blood flow of -60.8% ± 7.7%, PTX3 KO mice injected with hPTX3 presented a reduction of -11.8% ± 7.3% ($p<0.05$; **Figure 17A**); the AUC of blood flow during the 30 minutes after $FeCl_3$ application was significantly higher in PTX3 KO mice injected with hPTX3 compared to PTX3 KO mice injected with PBS ($p<0.01$; **Figure 17B**) and was further confirmed by histological analysis (**Figure 17C, 17D**). Similar results were observed when the effect of PTX3 injection was tested in wild type mice following $FeCl_3$ (20%) injury. All WT mice injected with PBS showed a reduction in carotid artery blood flow of -88.9% ± 7.4% compared to WT mice injected with hPTX3 which presented a reduction of -60.9% ± 14,8% (**Figure 17E**) and the AUC of blood flow during the 30 minutes after $FeCl_3$ application was significantly higher in WT mice injected with hPTX3 compared to WT mice injected with PBS ($p<0.05$; **Figure 17F**) as was thrombus formation (**Figure 17G-17H**).

PTX3 deficiency protects mice from diet induced obesity

During this PhD project we were also aimed at investigating the role of PTX3 in other immuno-inflammatory diseases, as the case of obesity and its related metabolic impairment. To validate the use of high fat diet (HFD, 45% of calories from fat) as a model of diet-induced obesity, we first compared the effect of this diet to a control diet (SFD, 10% of calories from fat) in WT animals. We observed that WT mice fed to HFD presented a significant increment of weight gain compared to those fed to SFD just after 4 weeks of diet ($p<0.01$; **Figure 18A**), as also demonstrated by the measurement of the area under the curve of weight gain versus time ($p<0.001$; **Figure 18B**); however, we excluded that this result was a consequence of a different palatability of the HFD as both groups presented a similar daily food intake (**Figure 18C**). WT mice fed to HFD also developed glucose intolerance compared to SFD mice as shown by a significant increased levels of plasma glucose during glucose tolerance test (**Figure 18D**), confirmed by the area under the curve of glucose plasma levels versus time ($p<0.05$; **Figure 18E**). We also confirmed that the prolongation of HFD resulted in a further increment of body weight ($p<0.001$; **Figure 19A**), elevation of basal glycaemia ($p<0.01$; **Figure 19B**) with a fall of insulin sensitivity (**Figure 19C**).

As we confirmed that HFD was a good model to investigate obesity and metabolic syndrome in mice, we fed WT and PTX3 KO mice with this diet for 20 weeks. Although at the start of HFD both groups had a similar body weight (**Figure 20A**), during time PTX3 KO mice gained less weight compared to WT (**Figure 20A**) and presented a significantly reduced weight gain compared to WT ($p<0.05$; **Figure 20B and 20C**), an observation independent on food intake (**Figure 20D**).

PTX3 deficiency does not impair glucose and insulin tolerance during 20 week-HFD

Given that obesity is the most important predisposing factor for glucose and insulin resistance we investigated whether the decreased weight gain due to PTX3 deficiency further affected glucose and insulin tolerance. Basal glycaemia, after an overnight fasting, was similar between groups at both 10 week (**Figure 21A**) and 20 weeks of HFD (**Figure 21B**), as well as glucose (**Figure 21C-21D**) and insulin

tolerance (**Figure 21E-21F**) assessed by a glucose (GTT) and insulin (ITT) tolerance test. These data excluded that PTX3 has a direct role on gluco- and insulin-metabolism.

PTX3 affects white but not brown adipose tissue deposition

In addition to weight, we performed a quali-quantitative analysis of adipose tissue deposition in the visceral (VAT), subcutaneous (SCAT) and intrascapular (usually the area of brown adipose tissue, BAT, accumulation in mice) fat depots through magnetic resonance for imaging (MRI). PTX3 KO mice presented a significant decreased accumulation of fat both in the visceral and subcutaneous adipose tissue at 10 weeks ($p<0.05$; **Figure 22A-22C**) and 20 weeks of HFD ($p<0.05$; **Figure 22B-22D**). However, intrascapular fat deposition was similar between WT and PTX3 KO mice at both 10 and 20 weeks of HFD (**Figure from 22E to 22G**). These results correlate the decreased weight gain in PTX3 KO mice with a decreased deposition of white adipose tissue (VAT and SCAT); however we excluded a different thermoregulation and energy expenditure in PTX3 KO mice since brown adipose tissue (BAT) depots were similar to those of WT.

PTX3 impairs the inflammatory response associated to visceral adipose tissue

Central obesity is a key feature of metabolic syndrome and it's the place where inflammation perpetuates; therefore, given that PTX3 is a key molecule of immune response, we have recently started investigating the immune-inflammatory response which takes place in white adipose tissue. Histological analysis showed that size of adipocytes was significantly smaller in visceral adipose tissue (VAT) of PTX3 KO compared to WT ($p<0.01$; **Figure 23A-23C**), while a similar size was observed in adipocytes from subcutaneous adipose tissue (SCAT) between WT and PTX3 KO mice (**Figure 23B-23D**). We also observed that VAT of PTX3 KO mice presented a decreased infiltration of immune cells (leukocytes, **Figure 24A**) and reduced expression of the pro-inflammatory cytokines MCP-1 and IL-6, while no difference was noticed in the expression of IL-10 ($p<0.05$; **Figure 24B**). These data suggested that the reduced expansion of white adipose tissue in PTX3 KO mice might be strictly associated to a limited immune-inflammatory response to HFD treatment.

Discussion

Aim of this PhD project was to investigate the role of the long pentraxin 3 (PTX3) in two common morbidities that affect particularly Western countries: arterial thrombosis, a critical complication of atherosclerotic plaque rupture (correlated with the clinical manifestation of myocardial infarction and stroke), obesity and its related metabolic complications, a worldwide epidemic with increasing socioeconomic cost.
PTX3 belongs to the pentraxin superfamily, soluble, multifunctional, pattern recognition proteins, and is an essential component of the humoral arm of innate immunity. More recently, it's role in cardiometabolic diseases has gained attention and PTX3 has emerged as a key acute phase protein associated to inflammation in cardiovascular disorders, including heart failure, atherosclerosis, acute coronary syndromes and peripheral vascular diseases [138, 288, 289]. Although PTX3 is a prognostic marker of acute myocardial infarction, [290] genetically determined high PTX3 levels do not influence the risk of AMI, suggesting that PTX3 concentration itself is unlikely to be even a modest causal factor for AMI [149]. However, PTX3 plasma levels were found to be both positively associated with predisposing factors of metabolic syndrome as BMI, insulin plasma levels, low HDL and high triglycerides, [119, 121] but also negatively correlated with gluco-stimulated insulin secretion. [122] On the other hand, data from animal models point to a protective function of the protein: PTX3 overexpression limits neointimal thickening after balloon injury of rat carotid artery [76], while PTX3 KO mice, following ischemia/reperfusion (I/R) injury, present a significantly larger infarcted area compared to WT mice [41]. PTX3 deficiency has been also associated with increased atherosclerosis, increased macrophage accumulation and inflammation in the atherosclerotic lesions [85], and, more recently, to the recruitment of anti-inflammatory macrophages, promotion of angiogenesis and tumor growth [117]. The observations coming from animal studies point to a protective effect of PTX3 potentially associated with the tuning of inflammation during cardiovascular diseases [288], however the increased levels observed in patients with cardiometabolic diseases indicate that PTX3 might be a bystander or represent an extreme attempt of the body to limit an excessive inflammatory response.

In this project, we demonstrated that PTX3 has multifunctional roles as it is involved in several inflammatory processes, on one side protecting from arterial thrombosis

but on the other promoting adipose tissue deposition and the inflammatory response associated to obesity.

In the first part of the project, we observed that PTX3 KO compared to wild type mice presented a significant increased carotid occlusion with a reduction of blood flow after $FeCl_3$ topic application on the carotid artery, an experimental model of arterial thrombosis. We demonstrated that PTX3 protective effects depend on the protein produced by vascular cells and not myeloid cells as only the deficiency of PTX3 in the vasculature, but not in myeloid cells, was associated to a pro-thrombotic phenotype, similar to that of PTX3 KO mice. Next, we excluded that this effect was related to P-selectin, a ligand of PTX3, which mediates the recruitment of leukocytes to the activated endothelium, and also the interactions between platelets and leukocytes. Indeed P-selectin/PTX3 double KO mice showed an increased carotid artery occlusion following arterial thrombosis compared to P-selectin KO mice. This observation coupled with those indicating that the protection toward arterial thrombosis is dependent on vascular produced PTX3, that the modulation of P-selectin activity depends on PTX3 produced by myeloid cells [57], that PTX3 plasma levels do not peak after arterial thrombosis, further limiting the contribution of PTX3 derived from myeloid cells [108], excludes the role of PTX3 in mediating P-selectin dependent leukocyte recruitment and platelet-leukocyte interactions as a protective mechanism during arterial thrombosis. Moreover, the survival rate following pulmonary thromboembolism (a platelet restricted thrombosis model) was similar in PTX3 KO and WT mice as it was platelet aggregation and function (in terms of expression of activation markers), further excluding that PTX3 affects platelet activation, and pointing toward an effect dependent on increased vascular thrombogenicity. The latter hypothesis was further sustained by the absence of main differences in WT and PTX3 KO mice hemostatic properties, including fibrinogen levels, tail bleeding, PT and APTT. Furthermore, although PTX3 was initially described to induce TF expression in endothelial cells and monocytes *in vitro* [61, 291], later studies failed to confirm this *in vivo* [70] and indeed we showed that TF expression in the aorta of PTX3 KO and WT mice was similar, arguing against a pro-thrombotic effect of PTX3.

PTX3 localizes at the interface between damaged endothelium and thrombus rather than within it, in agreement with the vascular origin of the protein involved in arteries homeostasis. Indeed PTX3, beyond to be produced and stored by myeloid cells [30, 57, 292], is synthesized by several type of stromal cells including fibroblasts [33], smooth muscle cells [33, 35], endothelial cells [42, 293] and is a component of tissue extracellular matrix (ECM) [63]. PTX3 interacts with other components of the ECM, including the viscoelastic HA-rich matrix of the cumulus oophorus complex that surrounds the preovulatory follicle [62, 63], and also plays a critical role during tissue repair following wound healing, a mechanism which is dependent on the acidic microenvironment which is generated following tissue injury [70]. These tissue-related functions of PTX3 appear to be independent of those associated with acute phase conditions, such as endotoxic shock, sepsis and other inflammatory and infectious states, but also from myocardial infarction [60], where PTX3 increases in few hours and is contributed by neutrophils following the interaction with activated platelets [108], limits neutrophils infiltration and ROS generation in the ischemic area [98], thus further supporting the hypothesis for a different role of PTX3 produced by myeloid compared to that derived from stromal cells.

Here we extend the activities played by vascular derived PTX3 which protect toward arterial thrombosis showing that this effect was dependent on the ability to interact with fibrinogen and collagen thus dampening their pro-thrombotic effects. Indeed, after application of $FeCl_3$, vascular wall loose its integrity leading to the exposure of inner layers and particularly components of extracellular matrix, as collagen which triggers platelet activation and aggregation, leading to the generation of fibrin clot [294]. Furthermore, as PTX3 is a component of ECM (probably derived from endothelial, smooth muscle cells and fibroblasts) [63], and similarly it is exposed during arterial thrombosis (and indeed it is found on the damaged endothelium), it may interact with collagen and fibrinogen limiting their pro-thrombotic effects. We indeed demonstrated that specific protein domains of PTX3 mimicked the activity of the full protein with the PTX3 N-terminal domain inhibiting fibrinogen-mediated platelet activation and the PTX3 C-terminal domain blocking collagen effects. More importantly, the two domains worked synergistically to dampen both fibrinogen and

collagen-induced platelet aggregation. We might speculate that these interactions might result from the profound homology between these pro-thrombotic molecules and highly conserved sequences of proteins belonging to the innate immune system: indeed, the first component of complement C1q and other related proteins as collectins and ficolins which are ligands of PTX3, resulting in the activation of complement system, possess respectively a collagen-like region and a fibrinogen like domain [11, 295, 296]. Furthermore, it has been shown that the different functions ascribed to PTX3 might originate from the high glycosilation variability among PTX3 isolated from different cellular sources: this suggests that the glycosylation pattern might change depending on cell type and inducing stimuli, thus modulating the crosstalk between PTX3 with different ligands in different conditions (as complement components and P-selectin) [297].

Although it is tempting to speculate that the interaction of PTX3 through its N- and C-terminal domain with fibrinogen and collagen respectively may dampen the generation of the pro-thrombotic fibrin from fibrinogen and the exposure of collagen during vascular injury, an effect favored by local acidification occurring during tissue injury [70], we cannot exclude the possibility that PTX3 might also influence additional pathways in the atherothrombotic response, as the fibrinolytic system; indeed, PTX3 through its N-terminal domain was observed to bind plasminogen and *in vitro*, fibrin gel degradation mediated by plasmin and triggered by uPA and tPA was potentiated in the presence of PTX3 [70].

Finally, the observation that the injection of recombinant PTX3 rescues the phenotype observed in PTX3 deficient mice and improves the outcome in wild type mice, supports the need of further studies aimed at addressing the pharmacological potential of PTX3 in the context of atherothrombosis.

More recently we have started investigating the role of PTX3 in metabolic complications associated to obesity; indeed, the modulation of immuno-inflammatory response during metabolic complications is gaining growing interest, leading scientists to coin the new word “metainflammation” to define the metabolically triggered inflammation [2].

Both metabolic syndrome and obesity are linked to an increased incidence of cardiovascular diseases [215, 298], particularly due to the chronic low grade

inflammation which characterizes these pathological conditions [299, 300] and great efforts have been done to identify novel targets to control the over activation of the inflammatory response as pharmacological treatments [301, 302]; however, further studies are needed to better understand the molecular mechanisms of this pathological immuno-inflammatory response.

Aim of the second part of this PhD project was to investigate how PTX3 affects the immuno-inflammatory response associated to obesity and adipose tissue, given that chronic inflammation particularly affects visceral adipose tissue [223, 303, 304], and PTX3 is a key molecule mediating innate immune and inflammatory responses. We first validated the use of high fat diet (HFD, consisting of 45% of calories from fat, a commonly used model of diet induced obesity) [277, 305] as a good model to study obesity and metabolic syndrome and following WT and PTX3 KO mice were fed with HFD for 20 weeks; indeed, after 16–20 weeks of HFD, mice will typically exhibit 20–30% increase in body weight when compared to chow-fed mice [279] and the full manifested picture of obesity develops with adipocyte hyperplasia, fat deposition in mesentery, increased fat mass, diabetes, and hypertension [281].

We reported that, although both groups had a similar body weight at the start of HDF, during time PTX3 KO mice gained significantly less weight compared to WT, an effect independent of food intake. We failed to observed difference in glucose and insulin tolerance, key features of metabolic impairment associated to obesity, suggesting that PTX3 deficiency has not a direct effect on gluco-metabolism. In agreement with the decreased body weight, PTX3 KO mice presented a significant reduced deposition of both visceral and subcutaneous white adipose tissue, while no difference was observed in the deposition of the brown adipose tissue, an essential regulator of energetic balance. Indeed, histological characterization of white adipose tissue showed that the size of adipocytes was significantly smaller in the visceral, but not in the subcutaneous adipose tissue of PTX3 KO mice compared to wild type. Adipocyte hypertrophy is deeply connected with adipose tissue inflammation caused by the production of pro-inflammatory cytokines (MCP-1, IL-6, INFγ) and the recruitment of pro-inflammatory immune cells, particularly macrophages, which are usually polarized toward an M1, pro-inflammatory phenotype compared to macrophages found in the lean adipose tissue which are of the M2, anti-inflammatory

phenotype [237, 306, 307]. As PTX3 has been shown to be present in adipose tissue and its gene expression increased during obesity [34, 119, 122], we hypothesized a role in modulating visceral adipose tissue inflammation thus leading to an impaired expansion of adipose tissue. Indeed, both in humans and mice visceral adipose tissue, PTX3 gene expression has been found to be directly related to TNFα expression in the same tissue [34, 119]. Furthermore, in humans, body mass index (BMI) is significantly correlated with circulating levels of pro-inflammatory cytokines, and among those, TNFα; therefore we might speculate that the increased plasma levels of PTX3, observed in association with cardiometabolic risk factors, are the mirror of those of TNFα. However, our data suggest that PTX3 during HFD is not just a bystander of the immune-inflammatory response associated to obesity, but plays an active role: indeed, we observed that the deficiency of PTX3 correlates with a decreased recruitment of leukocytes in the visceral adipose tissue, which is an event directly associated with the degree of inflammation and expansion of the tissue [303, 308]; furthermore, the evidence of a decreased inflammation of visceral adipose tissue of PTX3 KO mice came from the analysis of gene expression of pro-inflammatory cytokines (MCP-1 and IL-6) which was significantly decreased compared to WT. This observation seems to be in line to what reported in tumor context: PTX3 deficiency has been associated to cancerogenesis thanks to its ability to promote an M2 versus M1 macrophage polarization, which is detrimental for tumor growth [117]. Therefore, we might speculate that PTX3 deficiency, promoting the switch toward the M2 versus M1 subsets of macrophages, decreased the immuno-inflammatory response of visceral adipose tissue leading to a reduced accumulation of white adipose tissue and thus protecting PTX3 KO mice toward diet induced obesity. However, much work needs to be done to better characterize the mechanism behind the reduced expansion of visceral adipose tissue in PTX3 KO mice: identify the phenotype of immune cells infiltrating white adipose tissue, the source of PTX3 which in the context of visceral obesity plays a detrimental role, and how a decreased immuno-inflammatory response leads to reduced fat deposition. Furthermore we still have to provide a better metabolic phenotype of mice fed to HFD with the measurement of plasma triglycerides, cholesterol, insulin levels, to check the deposition of ectopic fat (as the case of the liver) and explain why, even though

visceral adiposity, the most important predisposing factor for insulin resistance, [309] is decreased in PTX3 KO mice, glucose and insulin sensitivity are similar to those of WT mice. As a key molecule of immune system, PTX3 might not directly affect metabolic profile during the early stages of HFD feeding, but modulate the immuno-inflammatory response which follows visceral adipose tissue deposition, probably favoring metabolic dysfunction. Therefore, a prolongation of the diet is likely to exacerbate a difference in the metabolic phenotype of PTX3 KO mice, thus leading to reveal an intimate connection between immuno-inflammatory response and metabolic dysfunctions.

Conclusions

Concluding, my PhD project has shown the multifunctional role of the long pentraxin 3 which plays a protective role in arterial thrombosis, while in a model of diet-induced obesity is associated with the promotion of inflammation and fat deposition in the visceral adipose tissue. These contrasting results are not surprising as PTX3 has been shown to be produced by a variety of cell types under pro- and anti-inflammatory stimulation and play multifunctional roles; furthermore, depending on the insult that triggers the inflammatory response, PTX3 effects might be affected: while $FeCl_3$-induced arterial thrombosis represents an acute inflammatory response, the HFD feeding exacerbates a chronic inflammation in which visceral adiposity significantly correlates with circulating levels of pro-inflammatory cytokines, as IL-6 and TNFα; we might speculate that, as PTX3 gene expression directly correlates with TNFα, it is likely that PTX3 overexpression worsen the resolution of inflammation during obesity. Finally, the highly variable glycosylation pattern, depending on the cell source, suggests that PTX3 may play different functions depending on the origin and the site of action. Therefore, it is tempting to propose further studies aimed at addressing a possible cell and/or tissue promotion or inhibition of PTX3 as a new pharmacological target for the treatment of cardiometabolic diseases.

Figures

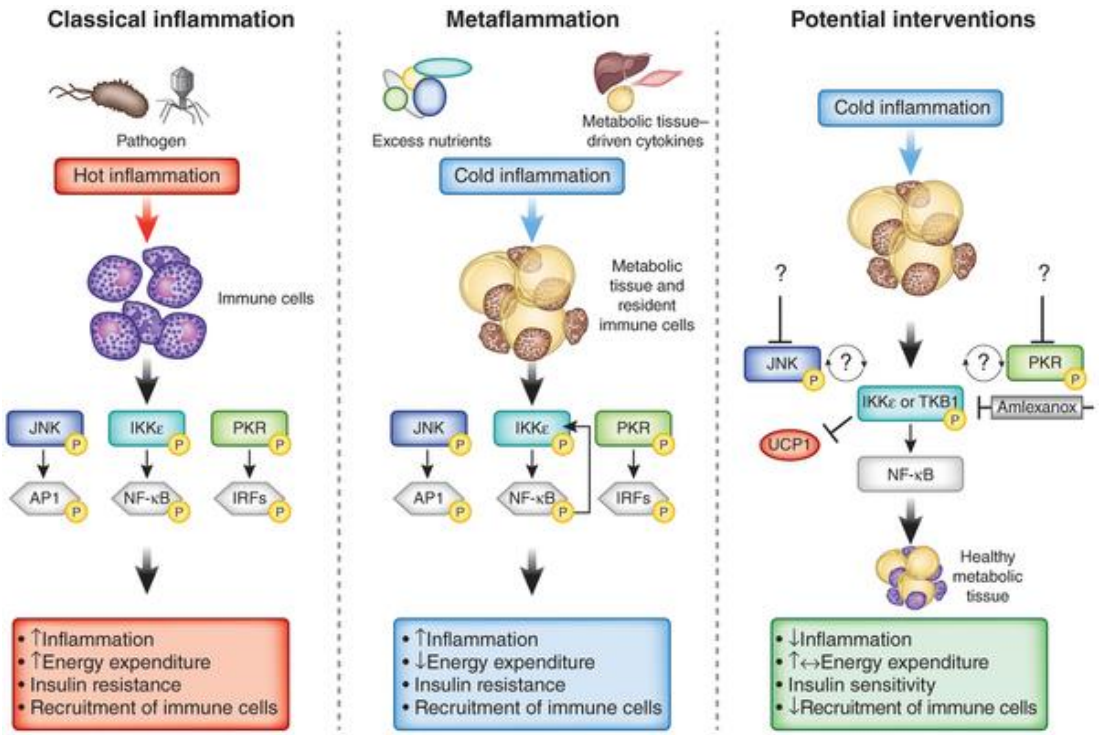

Figure 1. Signaling pathways involved in classical inflammation and metaflammation

Left, classical inflammation: pathogens acutely and robustly activate inflammatory kinases in immune cells causing a catabolic, 'hot' state of increased energy expenditure, and proinflammatory pathways are activated. This results in the recruitment of more immune cells via cytokines, causing acute insulin resistance (and enhanced glucose use through non–insulin-mediated pathways). Middle, metaflammation: metabolically induced, chronic, low-grade and 'cold' inflammation occurring in metabolic tissues that involves stromal and resident immune cells without an increase in basal energy expenditure. There is some overlap in the repertoire of inflammatory kinases and downstream events in both scenarios, except that insulin resistance persists in an anabolic state in metaflammation. Reilly et al. [310] now show that this paradox can be managed by a pharmacological intervention to suppress chronic inflammation, restore insulin sensitivity and increase energy expenditure by targeting IKKε and TBK1. IRFs, interferon-regulated factors [311].

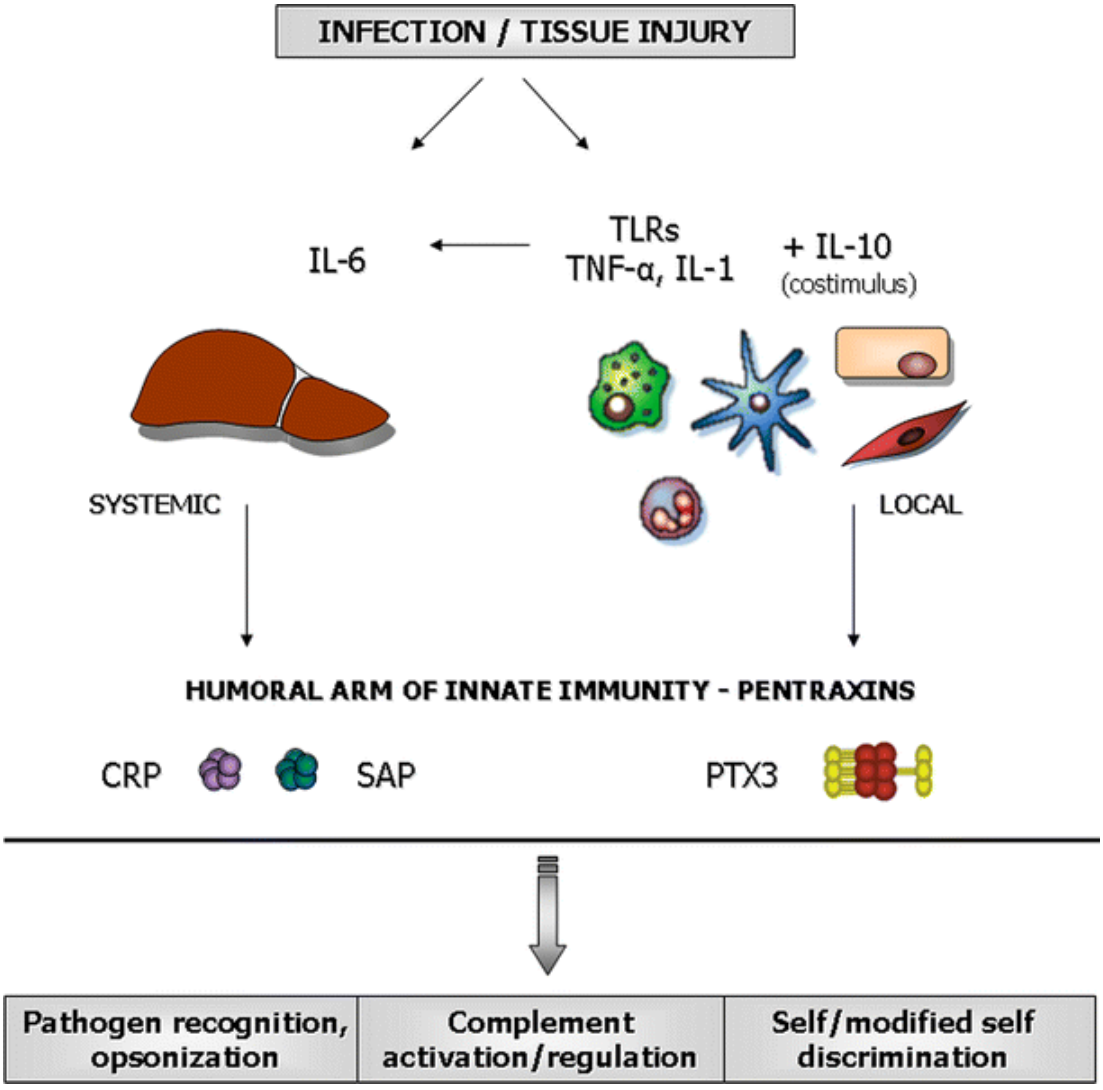

Figure 2. Overview of pentraxins in innate immunity

Pentraxins constitute a superfamily of multifunctional multimeric proteins that are phylogenetically conserved from arachnids to mammals. They are divided in short pentraxin (CRP and SAP), which are mainly produced by the liver in response to IL-6, and long pentraxins (PTX3), which are produced by a variety of cells after both pro- and anti-inflammatory stimulation. Together, they contribute to the humoral arm of innate immunity, promoting the opsonization, regulating complement activation and discriminating self from non-self components. (IL interleukin, TLR toll-like receptor, TNF tumour necrosis factor, CRP C-reactive protein, SAP serum amyloid P-component, PTX pentraxin) [312].

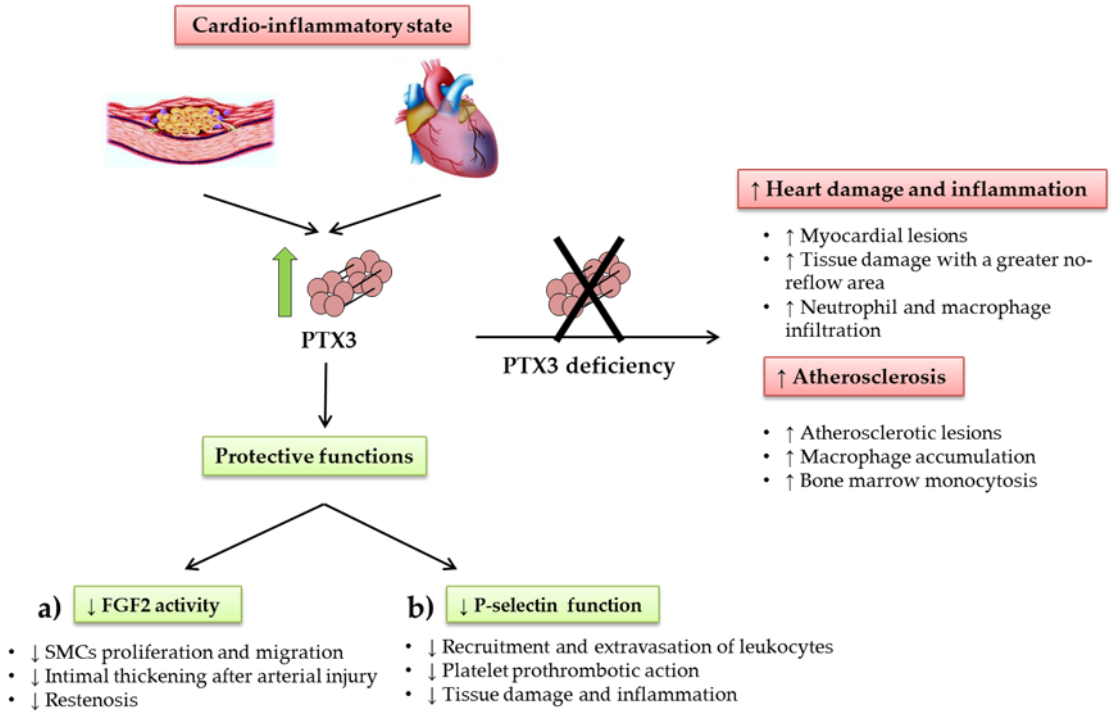

Figure 3. Effects of PTX3 in cardiovascular diseases

Increased PTX3 plasma levels are observed during myocardial infarction (MI) and atherosclerosis and the deficiency results in a marked heart damage after MI and a more inflamed atherosclerotic plaque. Functional PTX3 interacts with a) FGF2 and inhibits its activity, thus dampening SMCs proliferation and migration associated to restenosis, and b) P-selectin thus reducing the recruitment of leukocytes associated to tissue damage and inflammation [288].

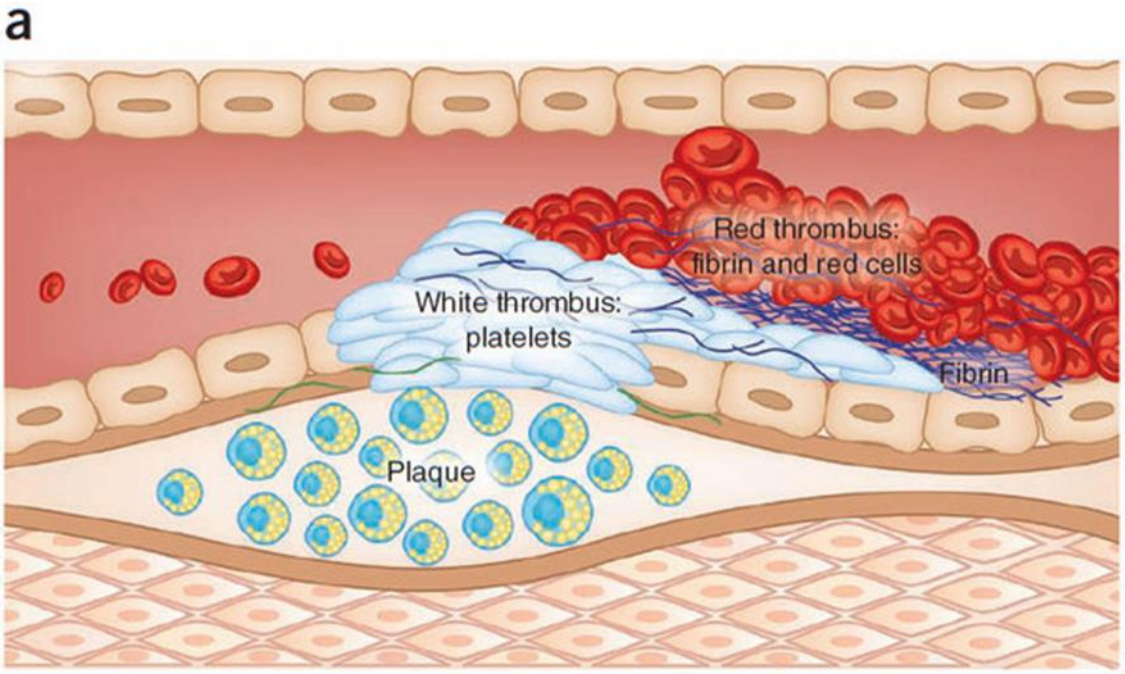

Figure 4. Occlusive arterial thrombi at sites of atherosclerosis plaque rupture.

A platelet-rich thrombus (white thrombus or platelet-rich mural thrombus) builds up on the surface of a disrupted atherosclerotic plaque, beginning in the intima and propagating into the intraluminal space, where it can induce major hemodynamic changes at the site of injury. A red thrombus, composed of red blood cells and fibrin, preferentially forms in the low flow recirculation zones on the downstream margin of the developing thrombus (adapted from [313]).

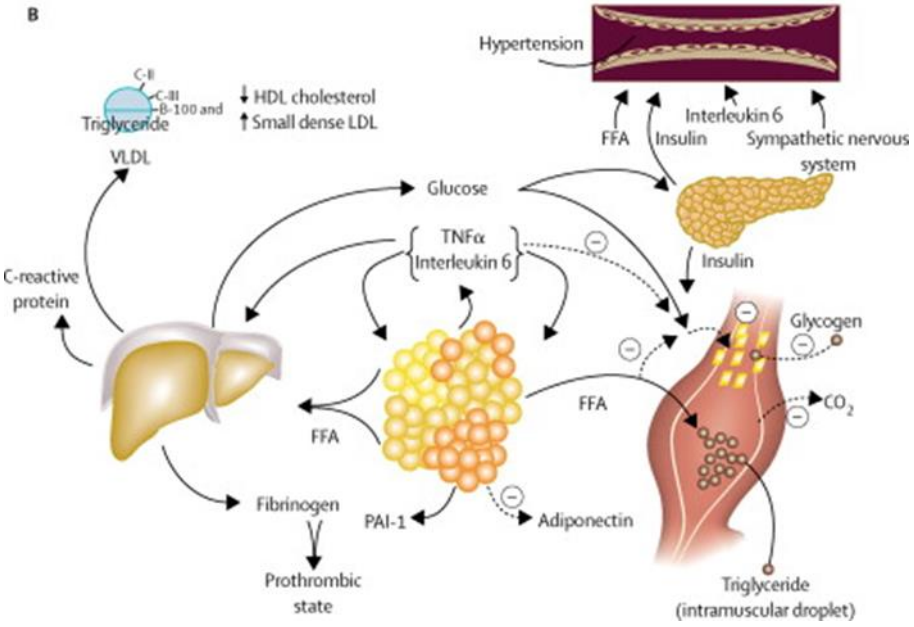

Figure 5. Pathophysiology of the metabolic syndrome (insulin resistance)

Superimposed and contributory to the insulin resistance produced by excessive FFA is the paracrine and endocrine effect of the pro-inflammatory state. Produced by a variety of cells in adipose tissue including adipocytes and monocyte-derived macrophages, the enhanced secretion of interleukin-6 (IL-6) and tumor necrosis factor alpha (TNF-α) among others results in more insulin resistance and lipolysis of adipose tissue triglyceride stores to circulating FFA. IL-6 and other cytokines also are increased in the circulation and may enhance hepatic glucose production, the production of VLDL by the liver and insulin resistance in muscle. Cytokines and FFA also increase the production of fibrinogen and plasminogen activator inhibitor-1 (PAI-1) by the liver that complements the overproduction of PAI-1 by adipose tissue. This results in a pro-thrombotic state. Reductions in the production of the anti-inflammatory and insulin sensitizing cytokine adiponectin are also associated with the metabolic syndrome and may contribute to the pathophysiology of the syndrome. PAI1=plasminogen activator inhibitor 1; FFA=free fatty acids; (adapted from [314]).

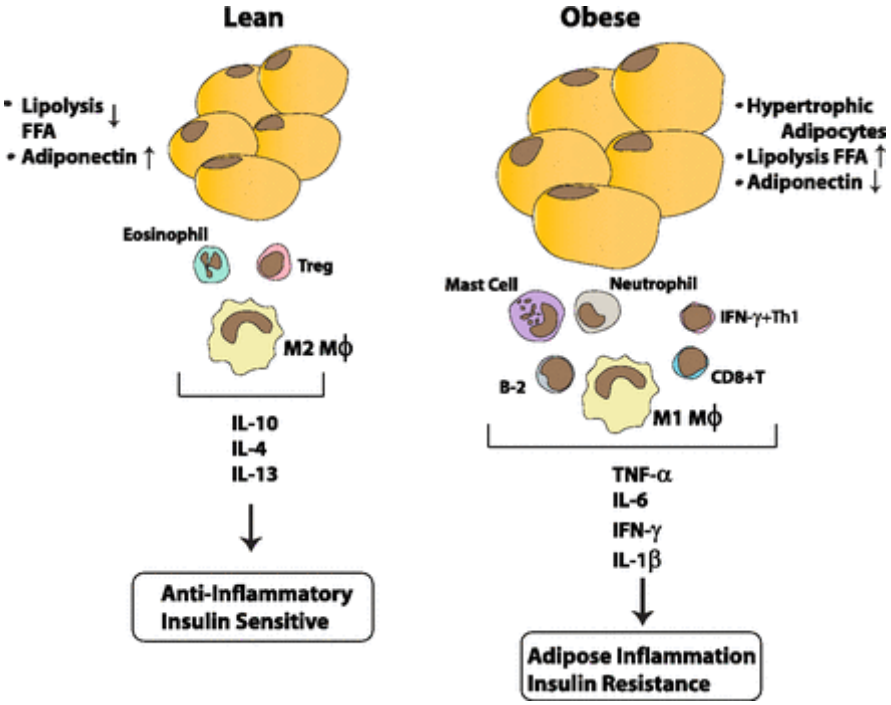

Figure 6. Obesity-associated adipose tissue inflammation

In the lean state, immune cells in adipose tissues (primarily resident M2-like macrophages together with T regulatory (Treg) cells and eosinophils) synthesize IL-10, IL-4, and IL-13 and help to maintain an anti-inflammatory environment that contributes to the insulin-sensitive state. Obesity drives a shift in the number and phenotype of immune cells. Monocytes are recruited from the blood into the obese adipose tissue, where they become M1 polarized and produce pro-inflammatory cytokines, including TNF-α, IL-1β, and IL-6, which contribute to insulin resistance. Other changes contributing to the pro-inflammatory state include decreased numbers of eosinophils and Tregs, and increased numbers of neutrophils, B cells, mast cells, and interferon γ–producing Th1 and CD8+ T cells. The pro-inflammatory cytokines and chemokines act in autocrine, paracrine, and endocrine manners to promote inflammation and insulin resistance in adipose and other target tissues [315].

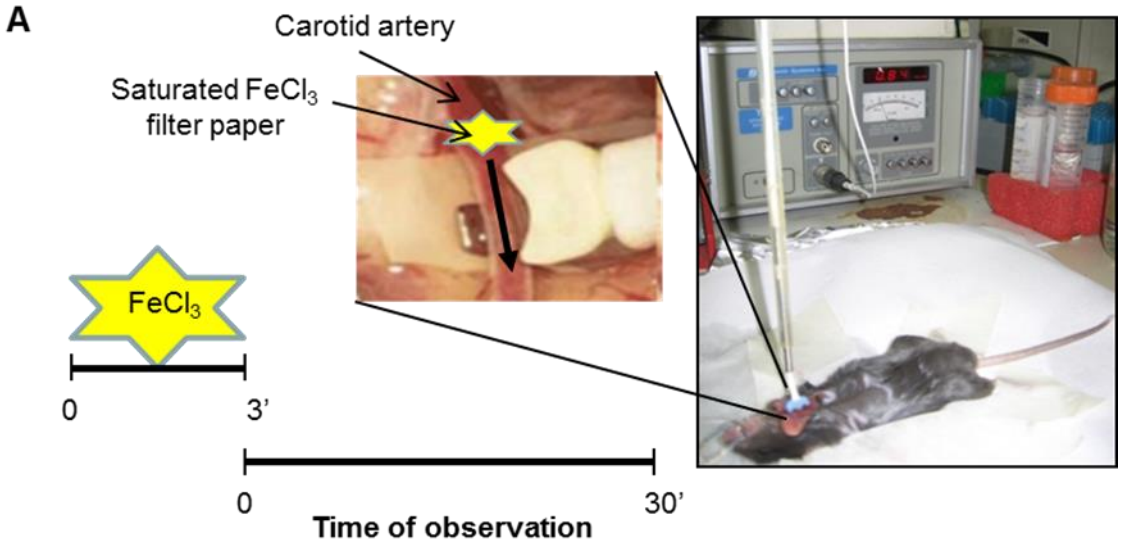

Figure 7. Experimental model of arterial thrombosis induced by FeCl3 10%

Panel A: representative pictures of $FeCl_3$ injury assay; a $FeCl_3$ saturated filter paper is applied on the exposed carotid artery for 3 minutes followed by blood flow measurement with an ultra-sonographic probe.

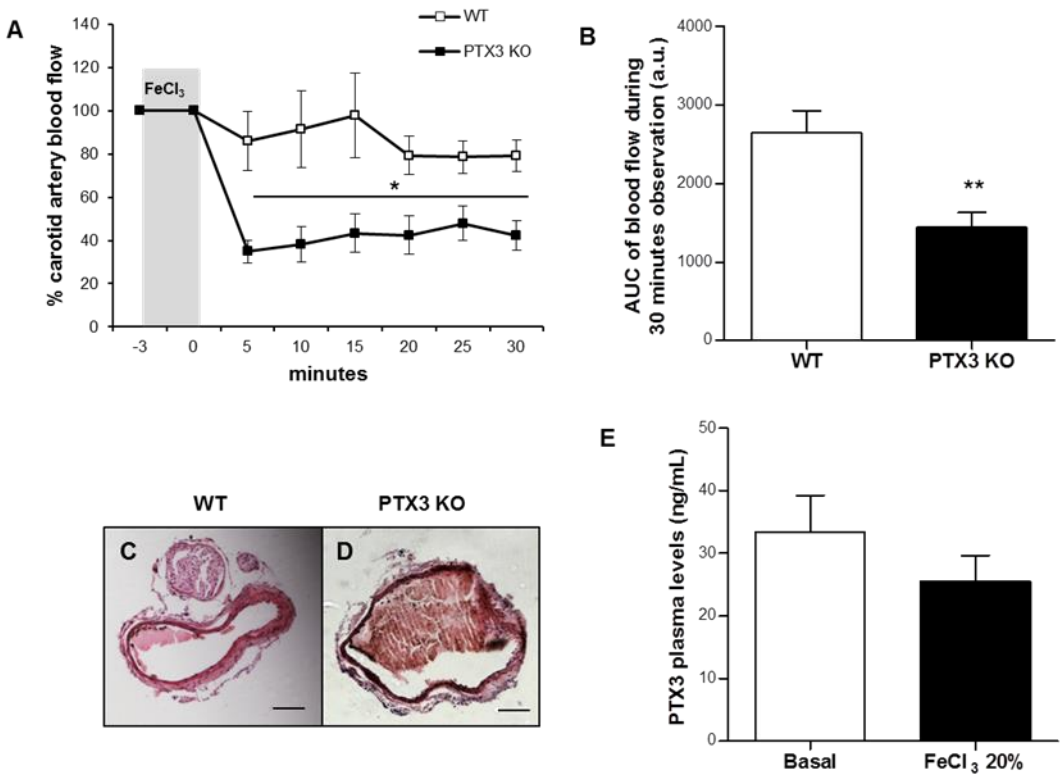

Figure 8. PTX3 KO mice show an enhanced thrombus formation in vivo after topic application of $FeCl_3$ 10%

Panel A: carotid artery blood flow in PTX3 KO and WT mice after topic application of $FeCl_3$ (10%); data, expressed as relative percentage to the value before injury, are mean ± SEM, PTX3 KO n=17, WT n=11, * $p<0.01$. **Panel B:** area under the curve (AUC) of carotid artery blood flow during 30 minutes of observation after topic application of $FeCl_3$ 10% to PTX3 KO and WT; data shown are mean ± SEM, * $p<0.01$. **Panel C, D:** representative hematoxylin and eosine (H/E) stained cross-sections of carotid arterial thrombi from PTX3 KO and WT mice, scale bar=100μm. **Panel E:** PTX3 plasma levels after 30 minutes $FeCl_3$ 20% treatment; data were obtained from plasma of WT mice with ELISA sandwich test and are mean ± SE, basic levels n=4, after $FeCl_3$ n=3.

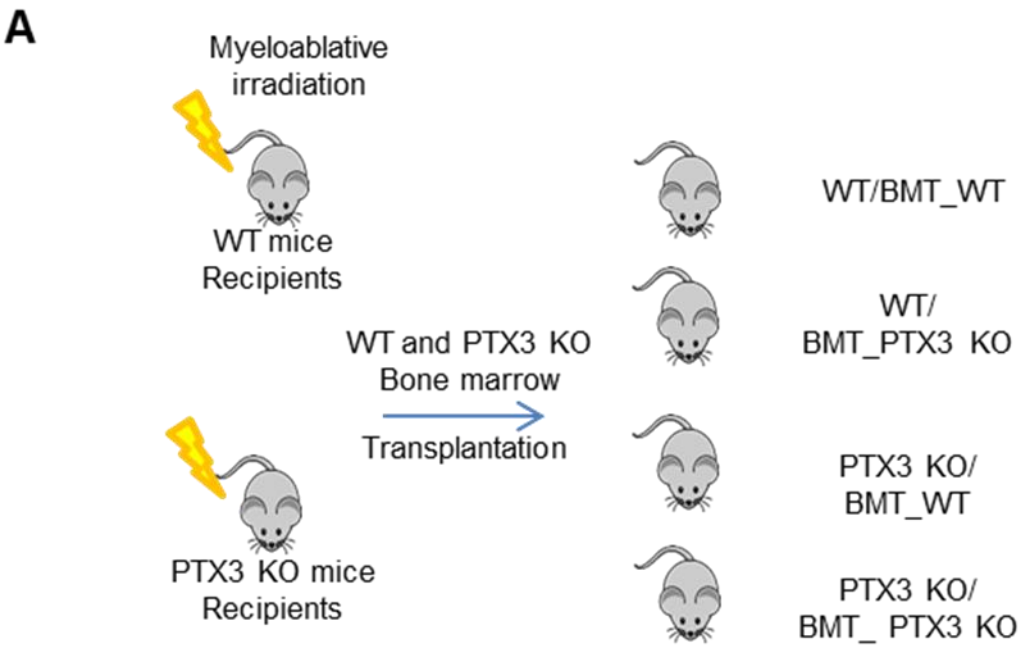

Figure 9. Bone marrow transplantation in WT and PTX3 KO mice

Panel A: Generation of WT and PTX3 KO bone marrow transplanted mice by myeloablative irradiation of WT and PTX3 KO recipient followed by transplantation of bone marrow isolated from WT and PTX3 KO mice.

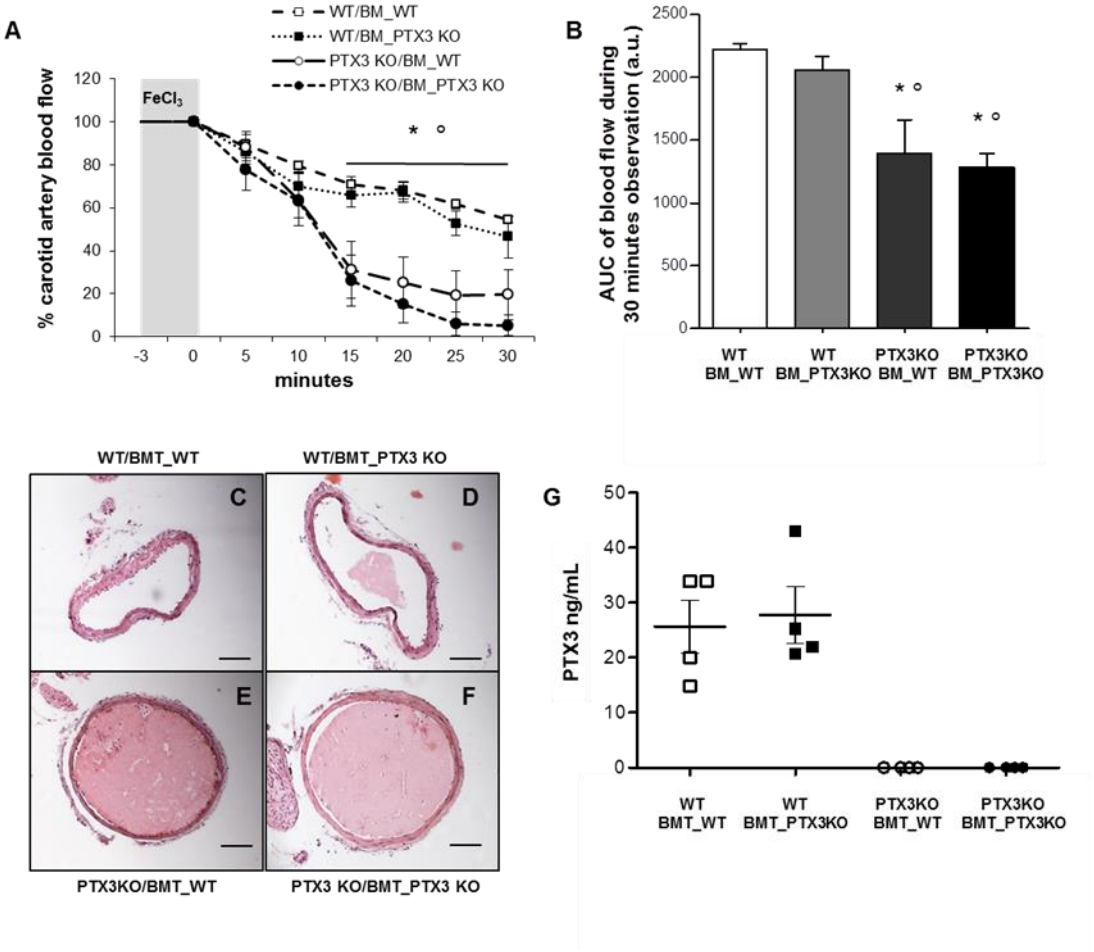
A
WT/BM_WT
WT/BM_PTX3 KO
PTX3 KO/BM_WT
PTX3 KO/BM_PTX3 KO
FeCl3
% carotid artery blood flow
minutes
B
AUC of blood flow during 30 minutes observation (a.u.)
WT BM_WT
WT BM_PTX3KO
PTX3KO BM_WT
PTX3KO BM_PTX3KO
WT/BMT_WT
WT/BMT_PTX3 KO
C
D
E
F
PTX3KO/BMT_WT
PTX3 KO/BMT_PTX3 KO
G
PTX3 ng/mL
WT BMT_WT
WT BMT_PTX3KO
PTX3KO BMT_WT
PTX3KO BMT_PTX3KO

Figure 10. PTX3 KO mice bone marrow transplanted with BM from WT and PTX3 KO show an enhanced thrombus formation in vivo compared to WT mice transplanted with BM from WT and PTX3 KO mice after topic application of FeCl3 10%

Panel A: carotid artery blood flow in BM transplanted (BMT) PTX3 KO and WT mice expressed as relative percentage to the value before injury; data shown are mean ± SEM, * $p<0.01$ WT/BMT_WT (n=4) vs PTX3 KO/BMT_WT (n=6) and PTX3 KO/BMT_KO (n=4), ° $p<0.05$ WT/BMT_PTX3 KO (n=6) vs PTX3 KO/BMT_KO (n=6). **Panel B**: area under the curve (AUC) of carotid artery blood flow during 30 minutes of observation after topic application of $FeCl_3$ 10%; data shown are mean ± SEM, * $p<0.05$ WT/BMT_WT vs PTX3 KO/BMT_WT and PTX3 KO/BMT_KO; ° $p<0.05$ WT/BMT_PTX3 KO vs PTX3 KO/BMT_WT and PTX3 KO/BMT_KO. **Panel C-F:** representative hematoxylin and eosine (H/E) stained cross-sections of carotid arterial thrombi from BMT mice, scale bar=100μm. **Panel G:** PTX3 plasma levels after 30 minutes $FeCl_3$ treatment (10%); data were obtained from plasma with ELISA sandwich test and are mean ± SEM.

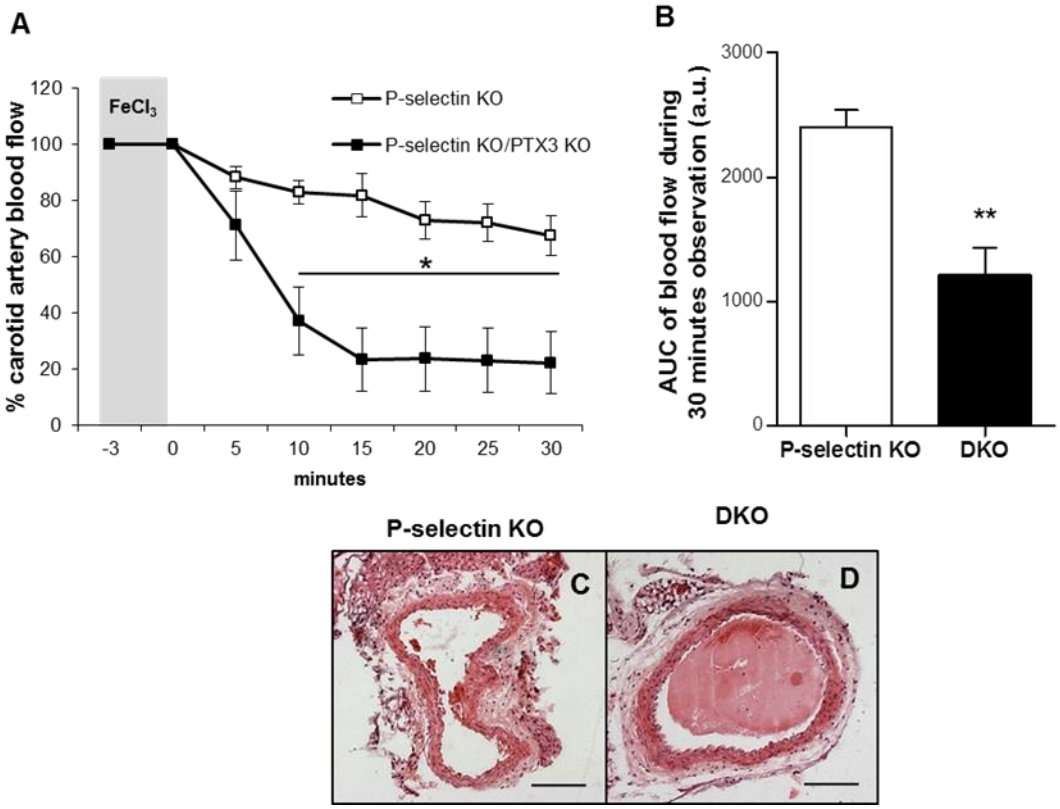

Figure 11. Protective effect of PTX3 goes beyond the interaction with P-selectin (I)

Panel A: carotid artery blood flow in P-selectin KO and P-selectin KO/PTX3 KO mice after topic application of $FeCl_3$ (10%); data, expressed as relative percentage to the value before injury, are mean ± SE, n=5/group, * $p<0.01$. **Panel B:** area under the curve (AUC) of carotid artery blood flow during 30 minutes of observation after topic application of $FeCl_3$ 10%; data shown are mean ± SEM, ** $p<0.01$. **Panel C-D:** representative hematoxylin and eosine (H/E) stained cross-sections of carotid arterial thrombi from P-selectin KO and P-selectin KO/PTX3 KO mice after $FeCl_3$ 10% treatment, scale bar=100μm.

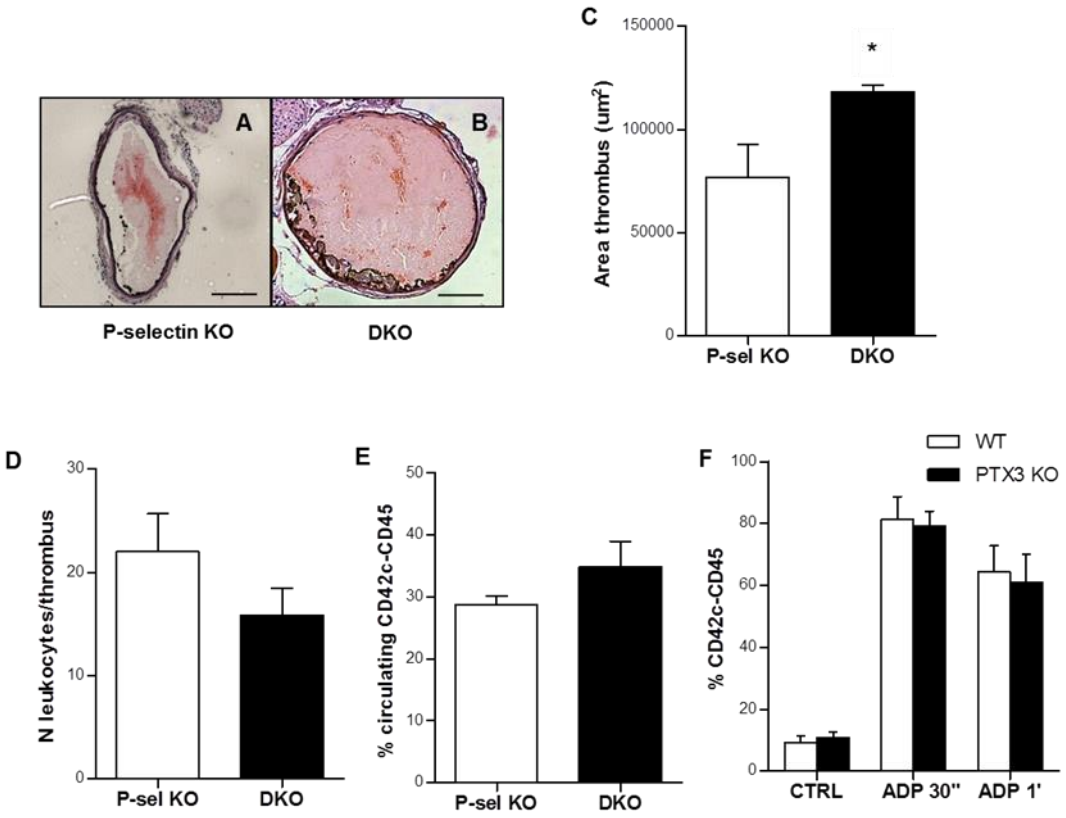

Figure 12. Protective effect of PTX3 goes beyond the interaction with P-selectin (II)

Panel A-B: representative hematoxylin and eosine (H/E) stained cross-sections of carotid arterial thrombi from P-selectin KO and P-selectin KO/PTX3 KO mice after $FeCl_3$ 20% treatment, scale bar=100μm. **Panel C:** measure of area thrombi after arterial thrombosis ($FeCl_3$ 20%) performed in P-selectin KO and PTX3 KO/P-selectin KO mice; data are mean ± SEM; n=4/group, * $p<0.05$. **Panel D:** number of leukocytes within thrombi from P-selectin KO and P-selectin KO/PTX3 KO after $FeCl_3$ 20% treatment; data shown are mean of leukocyte count from 4 sections taken along the length of carotid artery ± SEM, n=4/group. **Panel E:** percentage of platelet-leukocyte aggregates in whole blood from P-selectin KO and P-selectin KO/PTX3 KO after $FeCl_3$ 20% treatment; data shown are mean ± SEM, n=4/group. **Panel F:** Percentage of platelet-leukocyte aggregates after whole blood stimulation with adenosine diphosphate (ADP) for 30 second and 1 minute; samples were treated with fluorescence-conjugated anti-mouse monoclonal antibodies CD42c FITC and CD45 PE and analyzed using a flow cytometer; data shown are mean ± SEM, n=7/group.

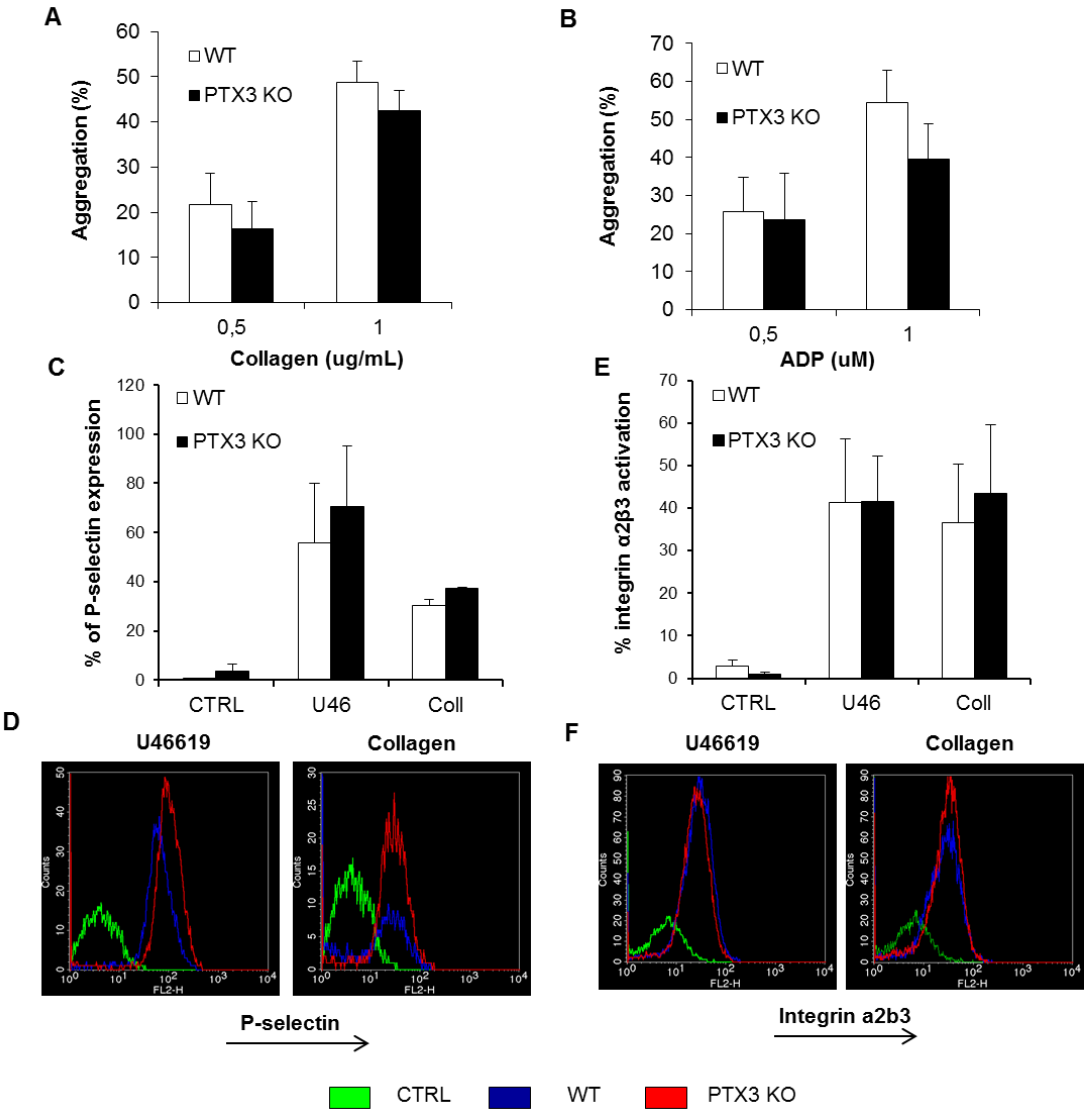
A
Aggregation (%)
WT
PTX3 KO
0,5
1
Collagen (ug/mL)
B
Aggregation (%)
WT
PTX3 KO
0,5
1
ADP (uM)
C
% of P-selectin expression
WT
PTX3 KO
CTRL
U46
Coll
E
% integrin α2β3 activation
WT
PTX3 KO
CTRL
U46
Coll
D
U46619
Collagen
Counts
FL2-H
P-selectin
F
U46619
Collagen
Counts
FL2-H
Integrin a2b3
CTRL
WT
PTX3 KO

Figure 13. PTX3 deficiency does not impair platelet activation (I)

Panel A-B: aggregation of platelet from WT and PTX3 KO mice induced by collagen (0.5 and 1 ug/mL) and ADP (0.5 and 1 uM). **Panel C-E:** expression of P-selectin and activation of integrin $\alpha_{IIb}\beta_{III}$ from PTX3 KO and WT PRP incubated with the analogous of thromboxane, U46619 (10 μM), or collagen (10 μg/mL); samples were treated with fluorescence-conjugated anti-mouse monoclonal antibodies CD42c FITC and CD62P PE, or CD42c FITC and integrin $\alpha_2\beta_3$ PE (active form). The expression of each surface antigen was analyzed using a flow cytometer. **Panel D-F:** representative pictures from cytofluorimetric analysis of P-selectin and integrin $\alpha_{IIb}\beta_{III}$ fluorescence intensity on platelet surface in basal condition or after stimulation with U46619 and collagen.

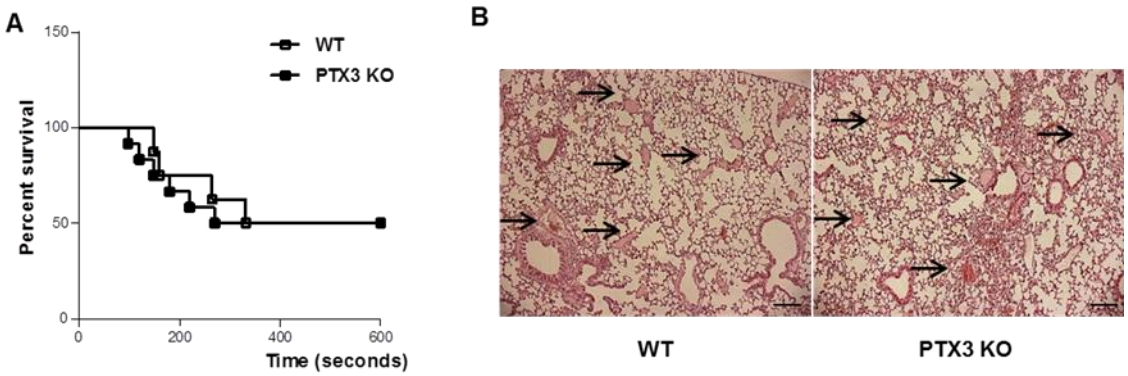

Figure 14. PTX3 deficiency does not impair platelet activation (II)

Panel A: survival curve after intravenous injection of collagen (11.5 μg) and epinephrine (1.4 μg) in PTX3 KO and WT mice (weight: 22-26 g); WT n=9, PTX3 KO n=12. **Panel B:** representative hematoxylin and eosine (H/E) stained cross-sections of lungs from mice. Arrows indicate thrombi. Scale bars= 100.

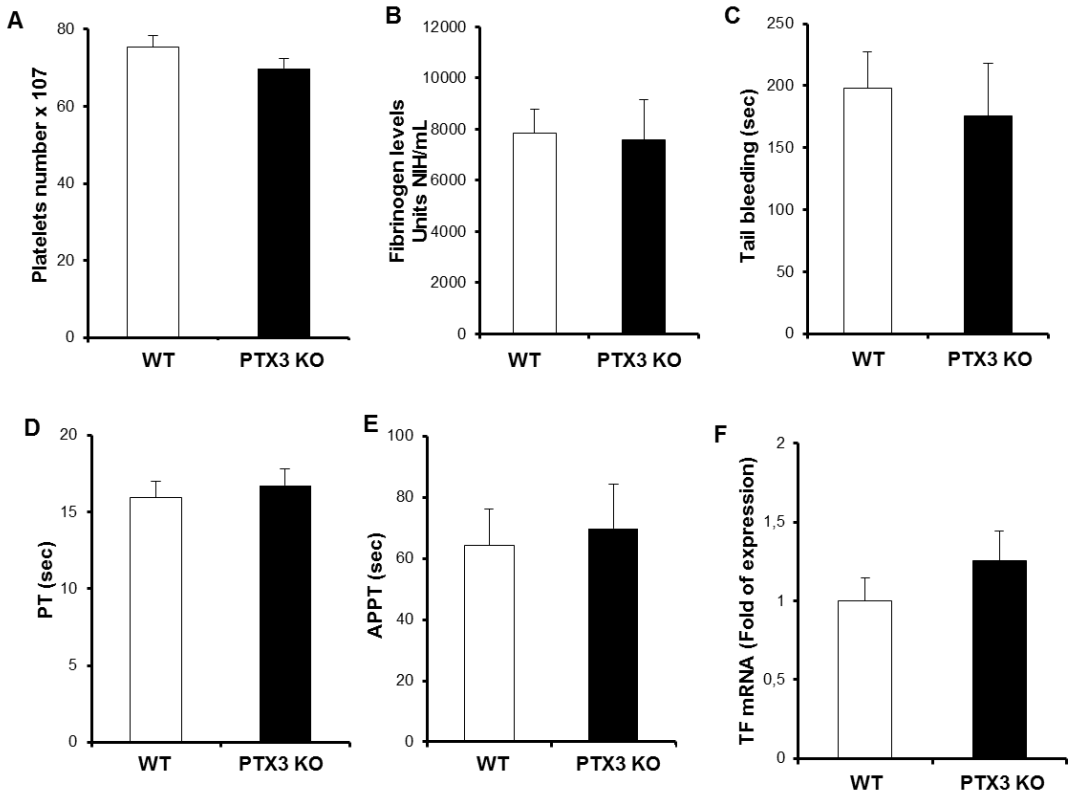

Figure 15. PTX3 deficiency does not impair platelet homeostasis and hemostatic properties

Panel A: platelet count in WT and PTX3 KO mice; data shown are mean ± SEM, n=13/group. **Panel B:** fibrinogen plasma levels detected with ELISA test, data are expressed as units NIH/mL and are a mean ± SEM, WT n=7, PTX3 KO n=6. **Panel C:** tail bleeding time, data are expressed as seconds of tail bleeding and are mean ± SEM, WT n=6, PTX3 KO n=4. **Panel D:** prothrombin time (PT) and **Panel E:** activated partial thromboplastin time (APTT) of WT and PTX3 KO mice; data shown are mean ± SEM, n=5/group. **Panel F:** mRNA expression of TF from PTX3 KO and WT aortas; data shown are mean ± SD, n=6/group.

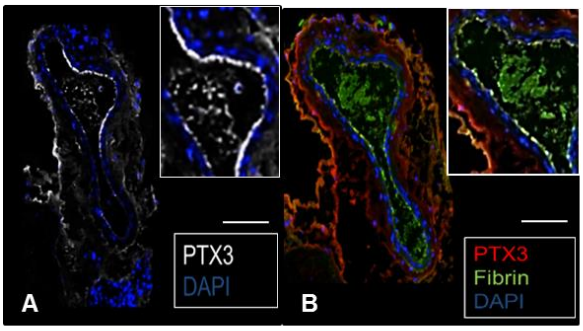
A
PTX3
DAPI
B
PTX3
Fibrin
DAPI

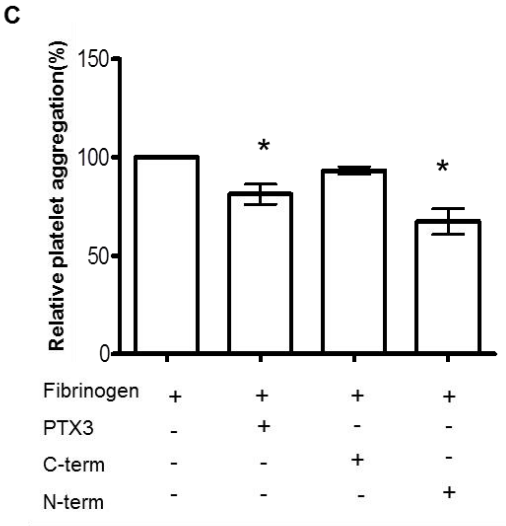
C
Relative platelet aggregation(%)
150
100
50
0
*
*
Fibrinogen + + + +
PTX3 - + - -
C-term - - + -
N-term - - - +

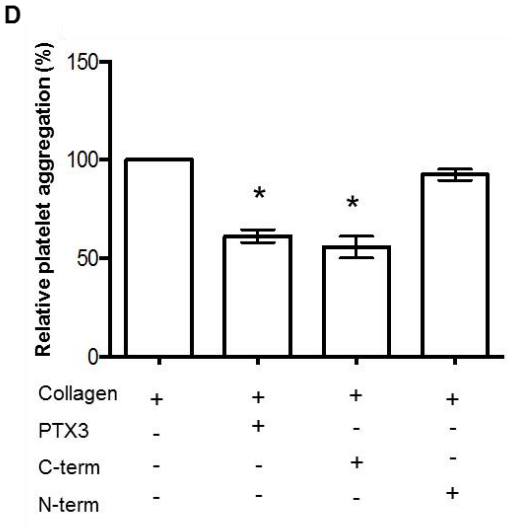
D
Relative platelet aggregation (%)
150
100
50
0
*
*
Collagen + + + +
PTX3 - + - -
C-term - - + -
N-term - - - +

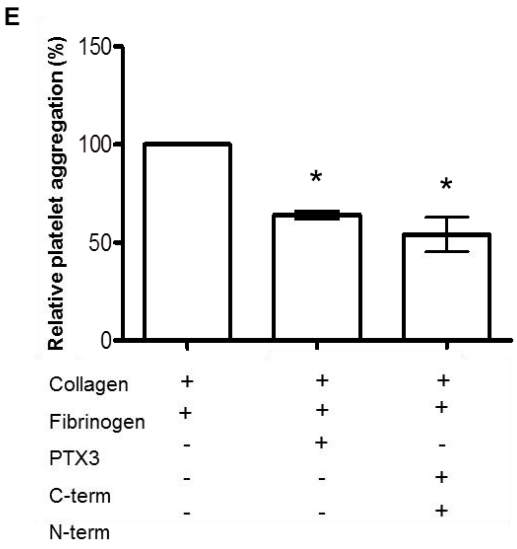
E
Relative platelet aggregation (%)
150
100
50
0
*
*
Collagen + + +
Fibrinogen + + +
PTX3 - + -
C-term - - +
N-term - - +

Figure 16. Protective effect of PTX3 is mediated through its interaction with collagen and fibrinogen

Panel A-B: immunohistochemistry analysis of PTX3 from thrombi from WT carotid artery after topic application of $FeCl_3$ (10%) scale bar=100μm. **Panel C:** platelet aggregation following stimulation with fibrinogen (0.25 mg/mL), fibrinogen pre-incubated with PTX3 (1μg/mL, 1 h RT), fibrinogen pre-incubated with PTX3 C-terminal domain (1μg/mL, 1 h RT) and fibrinogen pre-incubated with PTX3 N-terminal domain (1μg/mL, 1 h RT). Data shown are mean ± SEM; * $p<0.001$, n=3 and 4/group. **Panel D:** platelet aggregation following stimulation with collagen (1 μg/mL): collagen pre-incubated with PTX3 (1μg/mL, 18 h ON 4°C), collagen pre-incubated with PTX3 C-terminal domain (1μg/mL, 18 h ON 4°C) and collagen pre-incubated with PTX3 N-terminal domain (1μg/mL, 18 h ON 4°C). Data shown are mean ± SEM; * $p<0.001$, n=4/group. **Panel E:** platelet aggregation following stimulation with collagen (1μg/mL, 18 h ON 4°C) and fibrinogen (0.25 mg/mL), collagen pre-incubated with PTX3 (1μg/mL, 18 h ON 4°C) and fibrinogen pre-incubated with PTX3 (1μg/mL, 1 h RT), collagen pre-incubated with PTX3 C-terminal domain (1μg/mL, 18 h ON 4°C) and fibrinogen pre-incubated with PTX3 N-terminal domain (1μg/mL, 1 h RT). Data shown are mean ± SE; * $p<0.001$, n=3 and 4/group.

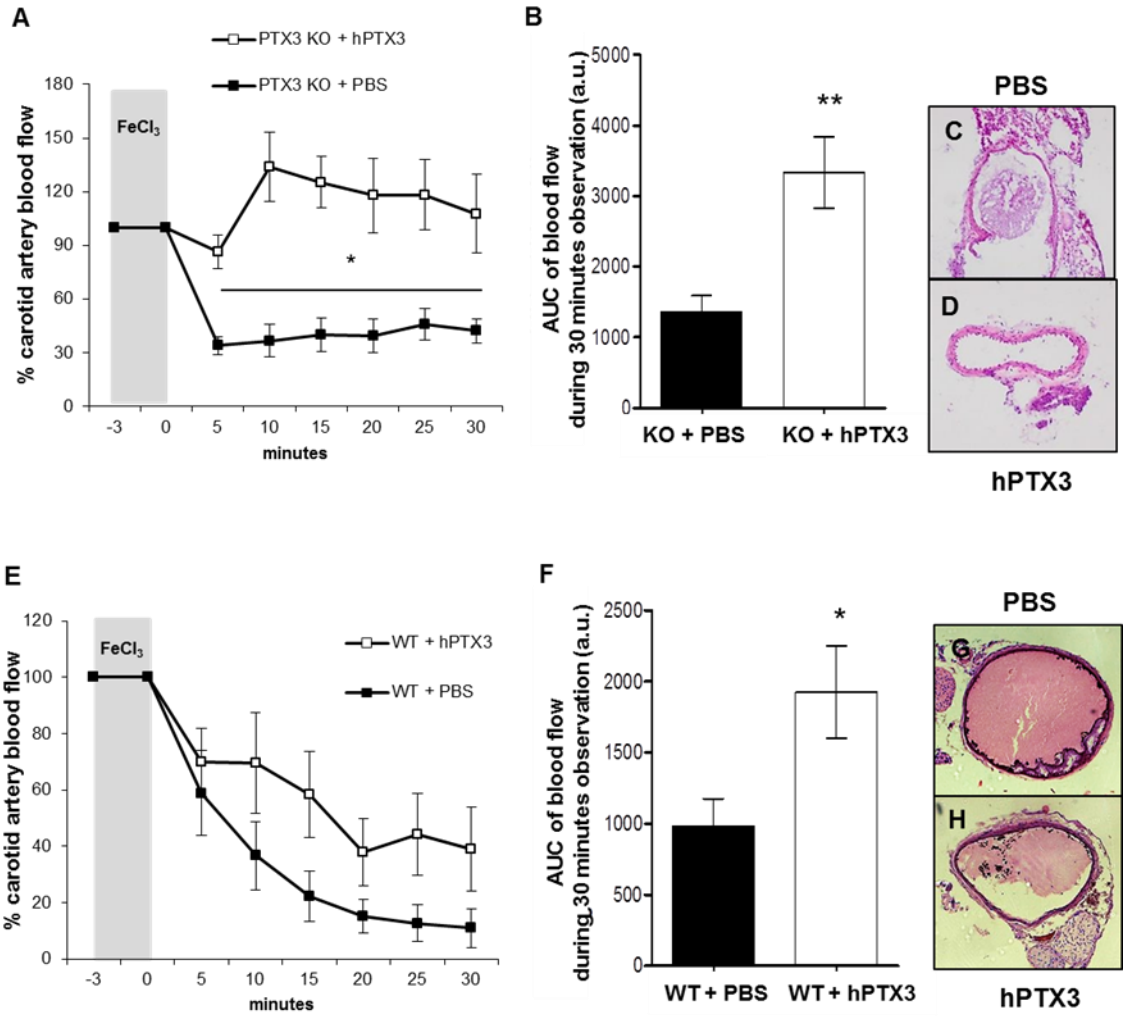
A
PTX3 KO + hPTX3
PTX3 KO + PBS
FeCl3
% carotid artery blood flow
minutes
*
B
AUC of blood flow during 30 minutes observation (a.u.)
**
KO + PBS
KO + hPTX3
PBS
C
D
hPTX3
E
WT + hPTX3
WT + PBS
FeCl3
% carotid artery blood flow
minutes
F
AUC of blood flow during 30 minutes observation (a.u.)
*
WT + PBS
WT + hPTX3
PBS
G
H
hPTX3

Figure 17. Administration of human recombinant PTX3 (5mg/kg) strongly prevented the arterial thrombus formation induced by $FeCl_3$, both in PTX3 KO and in WT mice

Panel A: carotid artery blood flow in PTX3 KO mice injected with PBS or hPTX3 after topic application of $FeCl_3$ (10%); data, expressed as relative percentage to the value before injury, are mean ± SEM; PTX3 KO+PBS n=6, PTX3 KO+hPTX3 n=4, * $p<0.05$. **Panel B:** area under the curve (AUC) of carotid artery blood flow during 30 minutes of observation after topic application of $FeCl_3$ 10% to PTX3 KO mice injected with PBS or hPTX3; data shown are mean ± SEM; * $p<0.01$. **Panel C and D:** representative hematoxylin and eosine (H/E) stained cross-sections of carotid arterial thrombi from PTX3 KO injected with PBS or hPTX3, scale bar=100μm. **Panel E:** carotid artery blood flow in WT mice injected with PBS or hPTX3 after topic application of $FeCl_3$ (20%); data, expressed as relative percentage to the value before injury, are mean ± SEM; WT+PBS n=8, WT+hPTX3 n=8. **Panel F:** area under the curve (AUC) of carotid artery blood flow during 30 minutes of observation after topic application of $FeCl_3$ 20% to WT mice injected with PBS or hPTX3; data shown are mean ± SEM, * $p<0.05$. **Panel G and H:** representative hematoxylin and eosine (H/E) stained cross-sections of carotid arterial thrombi from WT injected with PBS or hPTX3, scale bar=100μm.

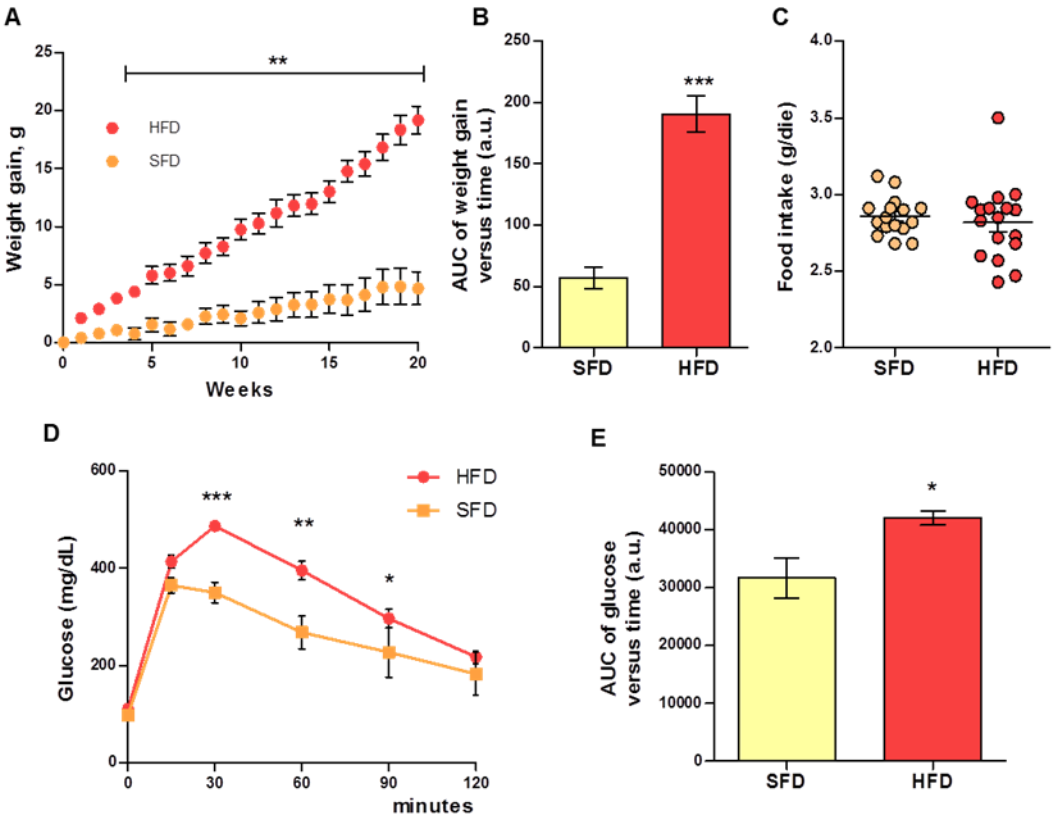

Figure 18. High fat diet (HFD) promotes the development of obesity and its related metabolic impairments (I)

Panel A: weight gain (g) of wild type mice fed with the HFD or standard fat diet (SFD for 20 weeks); data are presented as mean of weight gain per week ± SEM; ** $p<0.01$, n=10/group. **Panel B:** area under the curve of weight gain versus time (a.u.) of wild type fed with HFD and SFD for 20 weeks; data are presented as mean of AUC/mouse ± SEM; ** $p<0.001$, n=10/group. **Panel C:** food intake (g) of wild type fed with HFD and SFD; data are mean of the average of food intake/day monitored for two weeks ± SEM; n=10/group. **Panel D:** glucose tolerance test performed after 10 weeks of diet in wild type fed with HFD and SFD; data are presented as mean of glucose concentration/mouse checked before glucose injection (2 mg/g) and after 15, 30, 60, 90 and 120 minutes ± SEM; *** $p<0.001$, ** $p<0.01$, * $p<0.05$; n=10/group. **Panel E:** area under the curve of glucose concentrations during GTT performed in wild type fed with HFD and SFD; data are presented as mean of AUC/mouse ± SEM; ** $p<0.05$, n=10/group.

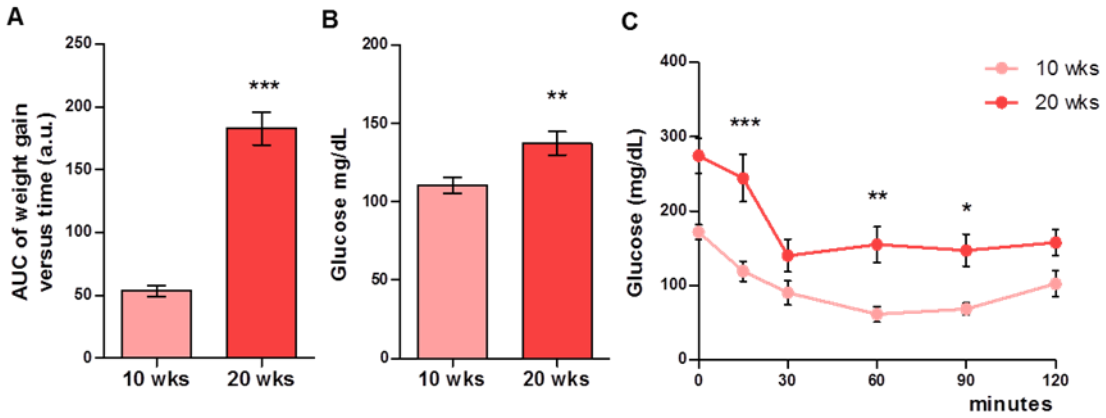

Figure 19. High fat diet (HFD) promotes the development of obesity and its related metabolic impairments (II)

Panel A: area under the curve of weight gain versus time (a.u.) of wild type fed with HFD for 10 or 20 weeks; data are presented as mean of AUC/mouse ± SEM; ** $p<0.001$, n=5/group. **Panel B:** basal glycaemia after an overnight fasting in wild type fed with HFD for 10 or 20 weeks; data are presented as mean of basal glycaemia/mouse ± SEM; ** $p<0.01$, n=5/group. **Panel C:** insulin tolerance test performed in wild type mice fed with HFD for 10 and 20 weeks; data are presented as mean of glucose concentration/mouse checked before insulin injection (0,1mU/µL) and after 15, 30, 60, 90 and 120 minutes ± SEM; *** $p<0.001$, ** $p<0.01$, * $p<0.05$; n=5/group.

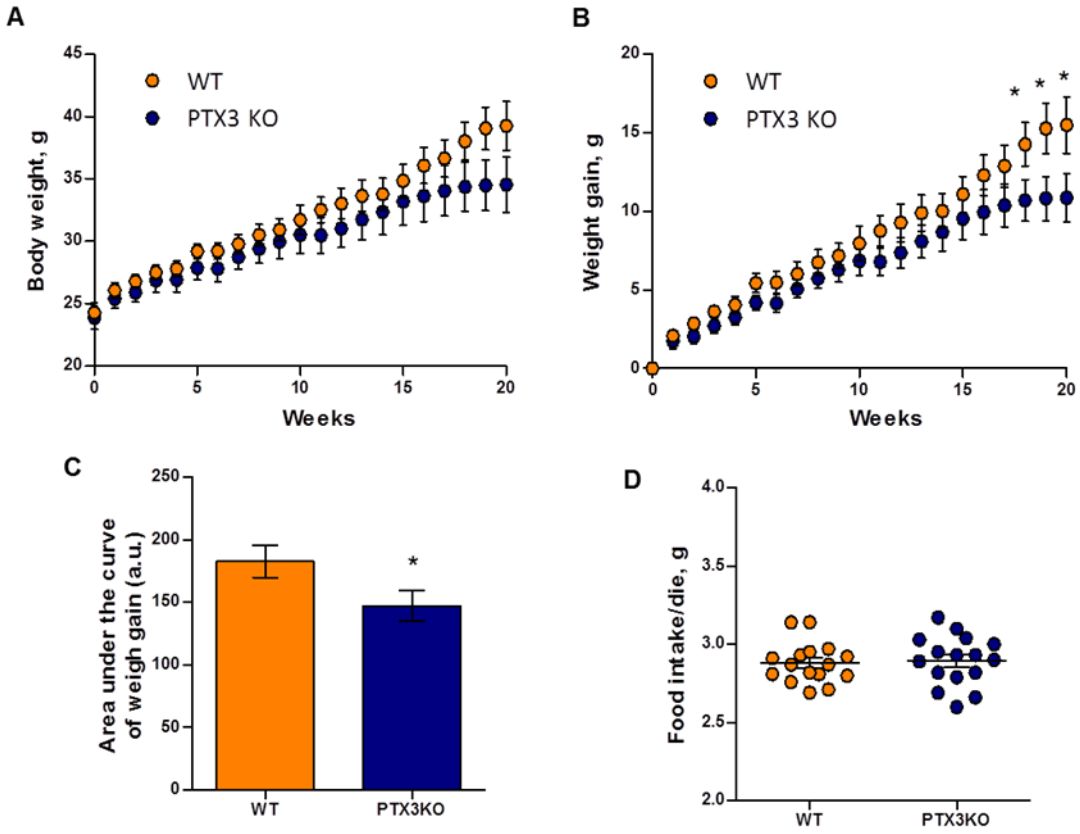

Figure 20. PTX3 deficiency protects from diet-induced obesity

Panel A: body weight (g) of WT and PTX3 KO mice fed with HFD for 20 weeks; data are presented as mean of body weight; n=10/group. **Panel B:** weight gain (g) of WT and PTX3 KO mice fed with the HFD for 20 weeks; data are presented as mean of weight gain per week ± SEM; * $p<0.05$, n=10/group. **Panel C:** area under the curve of weight gain versus time (a.u.) of WT and PTX3 KO fed with HFD for 20 weeks; data are presented as mean of AUC/mouse ± SEM; * $p<0.05$, n=10/group. **Panel D:** food intake (g) of WT and PTX3 KO mice fed with HFD; data are mean of the average of food intake/day monitored for two weeks ± SEM; n=10/group.

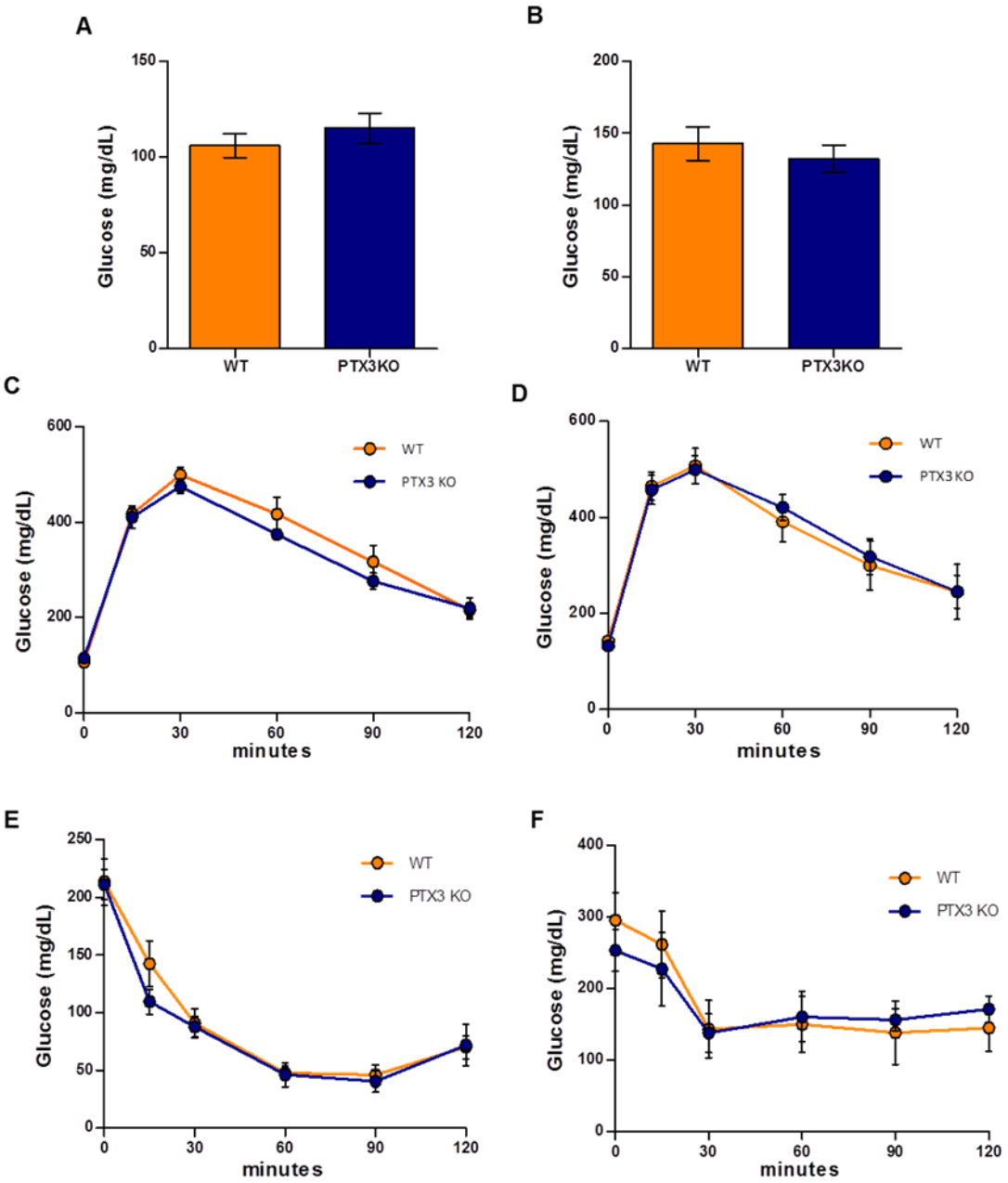
A
Glucose (mg/dL)
150
100
50
0
WT
PTX3KO
B
Glucose (mg/dL)
200
150
100
50
0
WT
PTX3KO
C
Glucose (mg/dL)
600
400
200
0
0
30
60
90
120
minutes
WT
PTX3 KO
D
Glucose (mg/dL)
600
400
200
0
0
30
60
90
120
minutes
WT
PTX3 KO
E
Glucose (mg/dL)
250
200
150
100
50
0
0
30
60
90
120
minutes
WT
PTX3 KO
F
Glucose (mg/dL)
400
300
200
100
0
0
30
60
90
120
minutes
WT
PTX3 KO

Figure 21. PTX3 deficiency does not impair glucose and insulin tolerance

Panel A: basal glycaemia after an overnight fasting in WT and PTX3 KO mice fed with HFD for 10 weeks; data are presented as mean of basal glycaemia/mouse ± SEM; n=10/group. **Panel B:** basal glycaemia after an overnight fasting in WT and PTX3 KO mice fed with HFD for 10 weeks; data are presented as mean of basal glycaemia/mouse ± SEM; n=10/group. **Panel C:** glucose tolerance test performed after 10 weeks of diet in WT and PTX3 KO fed with HFD; data are presented as mean of glucose concentration/mouse checked before glucose injection (2 mg/g) and after 15, 30, 60, 90 and 120 minutes ± SEM; n=10/group. **Panel D:** glucose tolerance test performed after 20 weeks of diet in WT and PTX3 KO fed with HFD; data are presented as mean of glucose concentration/mouse checked before glucose injection (2 mg/g) and after 15, 30, 60, 90 and 120 minutes ± SEM; n=10/group. **Panel E:** insulin tolerance test performed at 10 weeks in WT e PTX3 KO mice fed with HFD; data are presented as mean of glucose concentration/mouse checked before insulin injection (0,1mU/µL) and after 15, 30, 60, 90 and 120 minutes ± SEM; n=10/group. **Panel F:** insulin tolerance test performed at 20 weeks in WT e PTX3 KO mice fed with HFD; data are presented as mean of glucose concentration/mouse checked before insulin injection (0,1mU/µL) and after 15, 30, 60, 90 and 120 minutes ± SEM; n=10/group.

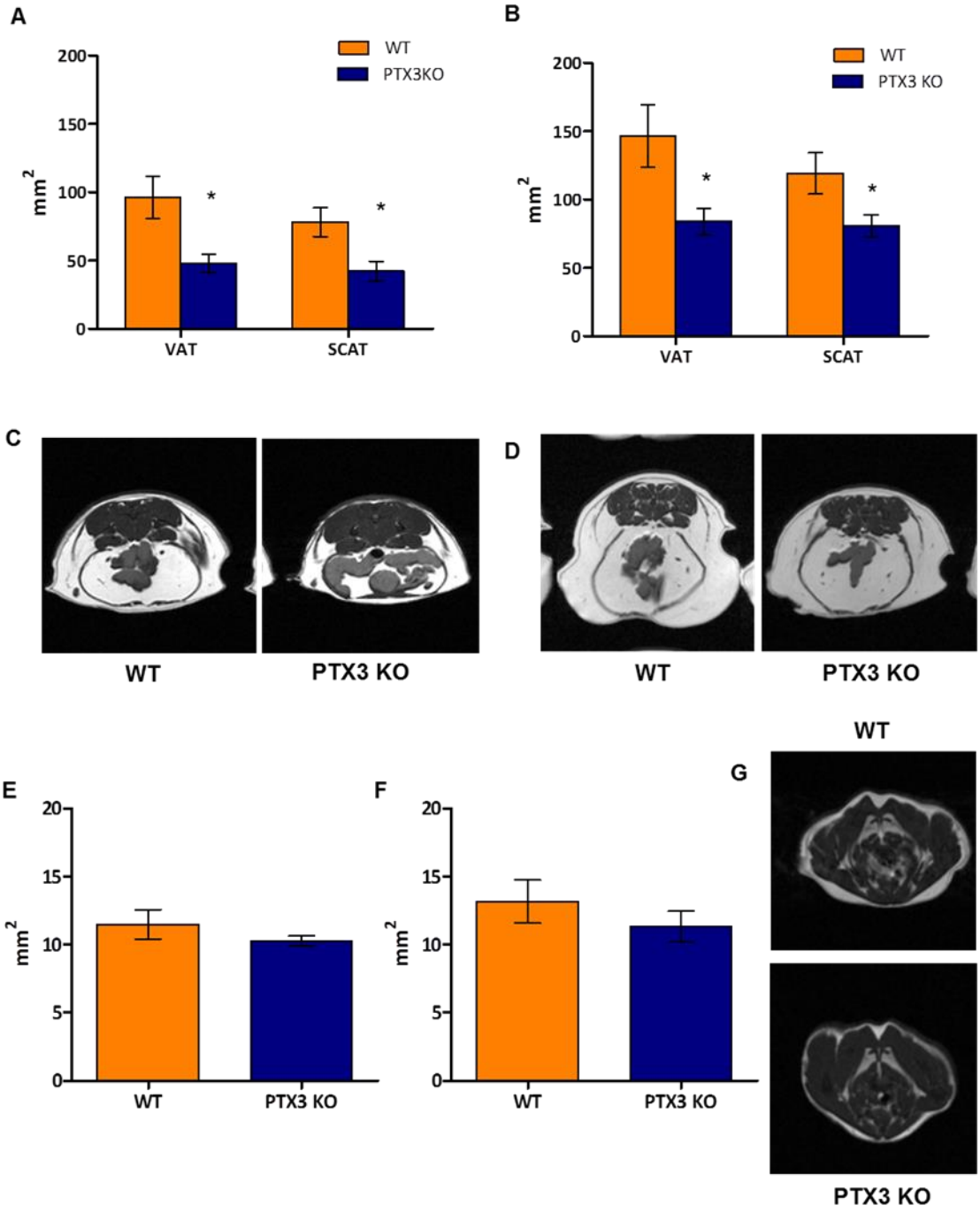
A
WT
PTX3KO
200
150
100
50
0
mm2
*
*
VAT
SCAT
B
WT
PTX3 KO
200
150
100
50
0
mm2
*
*
VAT
SCAT
C
WT
PTX3 KO
D
WT
PTX3 KO
E
20
15
10
5
0
mm2
WT
PTX3 KO
F
20
15
10
5
0
mm2
WT
PTX3 KO
G
WT
PTX3 KO

Figure 22. PTX3 deficiency leads to a decreased accumulation of white but not brown adipose tissue

Panel A: area of visceral (VAT) and subcutaneous (SCAT) adipose tissue of WT and PTX3 KO mice fed with HFD for 10 weeks obtained through magnetic resonance for imaging (MRI); data are presented as mean of 3 sections/mouse ± SEM; $p<0.05$, n=5/group. **Panel B:** area of visceral (VAT) and subcutaneous (SCAT) adipose tissue of WT and PTX3 KO mice fed with HFD for 20 weeks obtained through MRI; data are presented as mean of 3 sections/mouse ± SEM; $p<0.05$, n=7/group. **Panel C:** representative transversal pictures of mouse abdomen from MRI software at 10 weeks of HFD. **Panel D:** representative transversal pictures of mouse abdomen from MRI software at 20 weeks of HFD. **Panel E:** area of brown adipose tissue (BAT) of WT and PTX3 KO mice fed with HFD for 10 weeks obtained through MRI; data are presented as mean of 3 sections/mouse ± SEM; $p<0.05$, n=5/group. **Panel F:** area of brown adipose tissue (BAT) of WT and PTX3 KO mice fed with HFD for 20 weeks obtained through MRI; data are presented as mean of 3 sections/mouse ± SEM; $p<0.05$, n=5/group. **Panel G:** representative transversal pictures of mouse cervical region from MRI software at 20 weeks of HFD.

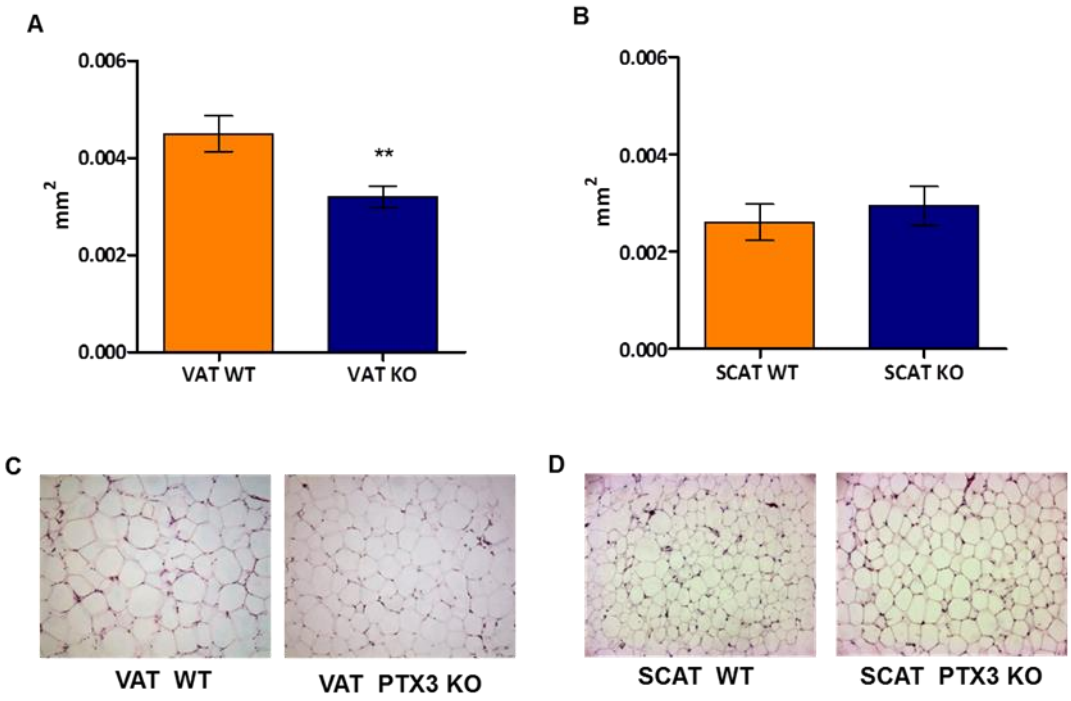

Figure 23. PTX3 deficiency is associated with a decreased area of adipocytes in the visceral but not in the subcutaneous adipose tissue

Panel A: area of adipocytes from visceral adipose tissue (VAT) of WT and PTX3 KO mice after 20 weeks of diet; data are presented as mean of adipocyte area/VAT section of mouse ± SEM; $p<0.01$; n=10/group. **Panel B:** area of adipocytes from subcutaneous adipose tissue (SCAT) of WT and PTX3 KO mice after 20 weeks of diet; data are presented as mean of adipocyte area/SCAT section of mouse ± SEM; $p<0.01$; n=10/group. **Panel C:** representative hematoxylin and eosine (H/E) stained cross-sections of VAT from WT and PTX3 KO mice at 20 weeks of diet. **Panel D:** representative hematoxylin and eosine (H/E) stained cross-sections of SCAT from WT and PTX3 KO mice at 20 weeks of diet.

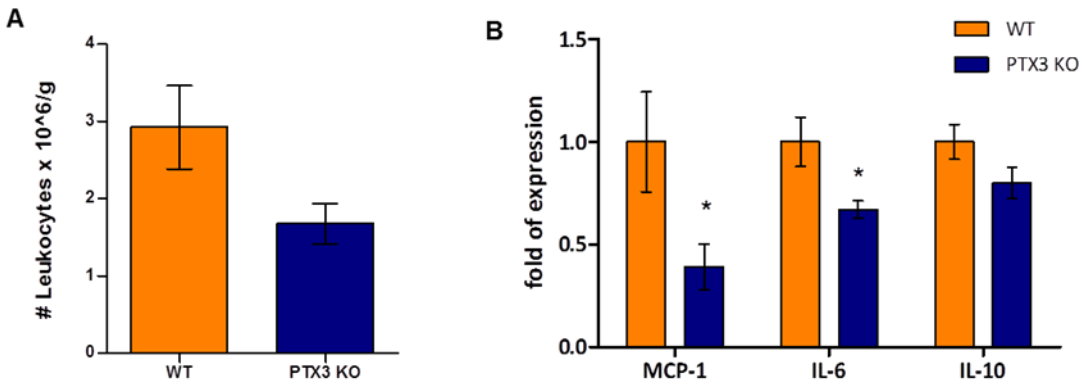

Figure 24. PTX3 deficiency is associated with a decreased inflammation of visceral adipose tissue

Panel A: leukocyte infiltrated in VAT of WT and PTX3 KO mice; data are presented as mean of counted leukocytes/g of VAT ± SEM; p=0.08; n=5/group. **Panel B:** expression of cytokines in VAT of WT and PTX3 KO mice; data are presented as fold of expression compared to WT and corrected on RLP gene; $p<0.05$, n=10.

References

1. Larsen, G.L. and P.M. Henson, *Mediators of inflammation.* Annu Rev Immunol, 1983. **1**: p. 335-59.
2. Hotamisligil, G.S., *Inflammation and metabolic disorders.* Nature, 2006. **444**(7121): p. 860-7.
3. Norata, G.D., et al., *The Cellular and Molecular Basis of Translational Immunometabolism.* Immunity, 2015. **43**(3): p. 421-34.
4. Szalai, A.J., et al., *C-reactive protein: structural biology and host defense function.* Clin Chem Lab Med, 1999. **37**(3): p. 265-70.
5. Pepys, M.B. and G.M. Hirschfield, *C-reactive protein: a critical update.* J Clin Invest, 2003. **111**(12): p. 1805-12.
6. Hirschfield, G.M. and M.B. Pepys, *C-reactive protein and cardiovascular disease: new insights from an old molecule.* QJM, 2003. **96**(11): p. 793-807.
7. Mantovani, A., et al., *Pentraxins in innate immunity: from C-reactive protein to the long pentraxin PTX3.* J Clin Immunol, 2008. **28**(1): p. 1-13.
8. Garlanda, C., et al., *Pentraxins at the crossroads between innate immunity, inflammation, matrix deposition, and female fertility.* Annu Rev Immunol, 2005. **23**: p. 337-66.
9. Bottazzi, B., et al., *Pentraxins as a key component of innate immunity.* Curr Opin Immunol, 2006. **18**(1): p. 10-5.
10. Rubio, N., et al., *Structure, expression, and evolution of guinea pig serum amyloid P component and C-reactive protein.* J Biochem, 1993. **113**(3): p. 277-84.
11. Bottazzi, B., et al., *An integrated view of humoral innate immunity: pentraxins as a paradigm.* Annu Rev Immunol, 2010. **28**: p. 157-83.
12. Szalai, A.J., *The antimicrobial activity of C-reactive protein.* Microbes Infect, 2002. **4**(2): p. 201-5.
13. Roumenina, L.T., et al., *Interaction of C1q with IgG1, C-reactive protein and pentraxin 3: mutational studies using recombinant globular head modules of human C1q A, B, and C chains.* Biochemistry, 2006. **45**(13): p. 4093-104.
14. Chang, M.K., et al., *C-reactive protein binds to both oxidized LDL and apoptotic cells through recognition of a common ligand: Phosphorylcholine of oxidized phospholipids.* Proc Natl Acad Sci U S A, 2002. **99**(20): p. 13043-8.
15. Hingorani, A.D., et al., *C-reactive protein and coronary heart disease: predictive test or therapeutic target?* Clin Chem, 2009. **55**(2): p. 239-55.
16. Botto, M., et al., *Amyloid deposition is delayed in mice with targeted deletion of the serum amyloid P component gene.* Nat Med, 1997. **3**(8): p. 855-9.
17. Reid, M.S. and C.P. Blobel, *Apexin, an acrosomal pentaxin.* J Biol Chem, 1994. **269**(51): p. 32615-20.
18. Noland, T.D., et al., *The sperm acrosomal matrix contains a novel member of the pentaxin family of calcium-dependent binding proteins.* J Biol Chem, 1994. **269**(51): p. 32607-14.
19. Omeis, I.A., Y.C. Hsu, and M.S. Perin, *Mouse and human neuronal pentraxin 1 (NPTX1): conservation, genomic structure, and chromosomal localization.* Genomics, 1996. **36**(3): p. 543-5.
20. Schlimgen, A.K., et al., *Neuronal pentraxin, a secreted protein with homology to acute phase proteins of the immune system.* Neuron, 1995. **14**(3): p. 519-26.
21. Hsu, Y.C. and M.S. Perin, *Human neuronal pentraxin II (NPTX2): conservation, genomic structure, and chromosomal localization.* Genomics, 1995. **28**(2): p. 220-7.
22. Tsui, C.C., et al., *Narp, a novel member of the pentraxin family, promotes neurite outgrowth and is dynamically regulated by neuronal activity.* J Neurosci, 1996. **16**(8): p. 2463-78.

23. Dodds, D.C., et al., *Neuronal pentraxin receptor, a novel putative integral membrane pentraxin that interacts with neuronal pentraxin 1 and 2 and taipoxin-associated calcium-binding protein 49.* J Biol Chem, 1997. **272**(34): p. 21488-94.
24. Kirkpatrick, L.L., et al., *Biochemical interactions of the neuronal pentraxins. Neuronal pentraxin (NP) receptor binds to taipoxin and taipoxin-associated calcium-binding protein 49 via NP1 and NP2.* J Biol Chem, 2000. **275**(23): p. 17786-92.
25. Inforzato, A., et al., *Structural characterization of PTX3 disulfide bond network and its multimeric status in cumulus matrix organization.* J Biol Chem, 2008. **283**(15): p. 10147-61.
26. Inforzato, A., et al., *The long pentraxin PTX3 at the crossroads between innate immunity and tissue remodelling.* Tissue Antigens, 2011. **77**(4): p. 271-82.
27. Breviario, F., et al., *Interleukin-1-inducible genes in endothelial cells. Cloning of a new gene related to C-reactive protein and serum amyloid P component.* J Biol Chem, 1992. **267**(31): p. 22190-7.
28. Lee, G.W., T.H. Lee, and J. Vilcek, *TSG-14, a tumor necrosis factor- and IL-1-inducible protein, is a novel member of the pentaxin family of acute phase proteins.* J Immunol, 1993. **150**(5): p. 1804-12.
29. Introna, M., et al., *Cloning of mouse ptx3, a new member of the pentraxin gene family expressed at extrahepatic sites.* Blood, 1996. **87**(5): p. 1862-72.
30. Doni, A., et al., *Production of the soluble pattern recognition receptor PTX3 by myeloid, but not plasmacytoid, dendritic cells.* Eur J Immunol, 2003. **33**(10): p. 2886-93.
31. Alles, V.V., et al., *Inducible expression of PTX3, a new member of the pentraxin family, in human mononuclear phagocytes.* Blood, 1994. **84**(10): p. 3483-93.
32. Polentarutti, N., et al., *Inducible expression of the long pentraxin PTX3 in the central nervous system.* J Neuroimmunol, 2000. **106**(1-2): p. 87-94.
33. Goodman, A.R., et al., *Differential regulation of TSG-14 expression in murine fibroblasts and peritoneal macrophages.* J Leukoc Biol, 2000. **67**(3): p. 387-95.
34. Abderrahim-Ferkoune, A., et al., *Characterization of the long pentraxin PTX3 as a TNFalpha-induced secreted protein of adipose cells.* J Lipid Res, 2003. **44**(5): p. 994-1000.
35. Klouche, M., et al., *Modified atherogenic lipoproteins induce expression of pentraxin-3 by human vascular smooth muscle cells.* Atherosclerosis, 2004. **175**(2): p. 221-8.
36. Vouret-Craviari, V., et al., *Expression of a long pentraxin, PTX3, by monocytes exposed to the mycobacterial cell wall component lipoarabinomannan.* Infect Immun, 1997. **65**(4): p. 1345-50.
37. Bottazzi, B., et al., *The long pentraxin PTX3 as a prototypic humoral pattern recognition receptor: interplay with cellular innate immunity.* Immunol Rev, 2009. **227**(1): p. 9-18.
38. Presta, M., et al., *Role of the soluble pattern recognition receptor PTX3 in vascular biology.* J Cell Mol Med, 2007. **11**(4): p. 723-38.
39. Doni, A., et al., *Regulation of PTX3, a key component of humoral innate immunity in human dendritic cells: stimulation by IL-10 and inhibition by IFN-gamma.* J Leukoc Biol, 2006. **79**(4): p. 797-802.
40. Maina, V., et al., *Coregulation in human leukocytes of the long pentraxin PTX3 and TSG-6.* J Leukoc Biol, 2009. **86**(1): p. 123-32.
41. Salio, M., et al., *Cardioprotective function of the long pentraxin PTX3 in acute myocardial infarction.* Circulation, 2008. **117**(8): p. 1055-64.

42. Norata, G.D., et al., *Long pentraxin 3, a key component of innate immunity, is modulated by high-density lipoproteins in endothelial cells.* Arterioscler Thromb Vasc Biol, 2008. **28**(5): p. 925-31.
43. Doni, A., et al., *Cell-specific regulation of PTX3 by glucocorticoid hormones in hematopoietic and nonhematopoietic cells.* J Biol Chem, 2008. **283**(44): p. 29983-92.
44. Jaillon, S., et al., *Endogenous PTX3 translocates at the membrane of late apoptotic human neutrophils and is involved in their engulfment by macrophages.* Cell Death Differ, 2009. **16**(3): p. 465-74.
45. Jaillon, S., et al., *The humoral pattern recognition receptor PTX3 is stored in neutrophil granules and localizes in extracellular traps.* J Exp Med, 2007. **204**(4): p. 793-804.
46. Brinkmann, V., et al., *Neutrophil extracellular traps kill bacteria.* Science, 2004. **303**(5663): p. 1532-5.
47. Fuchs, T.A., et al., *Novel cell death program leads to neutrophil extracellular traps.* J Cell Biol, 2007. **176**(2): p. 231-41.
48. Bottazzi, B., et al., *The long pentraxin PTX3 as a link among innate immunity, inflammation, and female fertility.* J Leukoc Biol, 2006. **79**(5): p. 909-12.
49. Bottazzi, B., et al., *Multimer formation and ligand recognition by the long pentraxin PTX3. Similarities and differences with the short pentraxins C-reactive protein and serum amyloid P component.* J Biol Chem, 1997. **272**(52): p. 32817-23.
50. Nauta, A.J., et al., *Biochemical and functional characterization of the interaction between pentraxin 3 and C1q.* Eur J Immunol, 2003. **33**(2): p. 465-73.
51. Inforzato, A., et al., *Pentraxins in humoral innate immunity.* Adv Exp Med Biol, 2012. **946**: p. 1-20.
52. Garlanda, C., et al., *Non-redundant role of the long pentraxin PTX3 in anti-fungal innate immune response.* Nature, 2002. **420**(6912): p. 182-6.
53. Diniz, S.N., et al., *PTX3 function as an opsonin for the dectin-1-dependent internalization of zymosan by macrophages.* J Leukoc Biol, 2004. **75**(4): p. 649-56.
54. Jeannin, P., et al., *Complexity and complementarity of outer membrane protein A recognition by cellular and humoral innate immunity receptors.* Immunity, 2005. **22**(5): p. 551-60.
55. Dias, A.A., et al., *TSG-14 transgenic mice have improved survival to endotoxemia and to CLP-induced sepsis.* J Leukoc Biol, 2001. **69**(6): p. 928-36.
56. Ravizza, T., et al., *Dynamic induction of the long pentraxin PTX3 in the CNS after limbic seizures: evidence for a protective role in seizure-induced neurodegeneration.* Neuroscience, 2001. **105**(1): p. 43-53.
57. Deban, L., et al., *Regulation of leukocyte recruitment by the long pentraxin PTX3.* Nat Immunol, 2010. **11**(4): p. 328-34.
58. Han, B., et al., *Protective effects of long pentraxin PTX3 on lung injury in a severe acute respiratory syndrome model in mice.* Lab Invest, 2012. **92**(9): p. 1285-96.
59. Muller, B., et al., *Circulating levels of the long pentraxin PTX3 correlate with severity of infection in critically ill patients.* Crit Care Med, 2001. **29**(7): p. 1404-7.
60. Peri, G., et al., *PTX3, A prototypical long pentraxin, is an early indicator of acute myocardial infarction in humans.* Circulation, 2000. **102**(6): p. 636-41.
61. Napoleone, E., et al., *Long pentraxin PTX3 upregulates tissue factor expression in human endothelial cells: a novel link between vascular inflammation and clotting activation.* Arterioscler Thromb Vasc Biol, 2002. **22**(5): p. 782-7.
62. Varani, S., et al., *Knockout of pentraxin 3, a downstream target of growth differentiation factor-9, causes female subfertility.* Mol Endocrinol, 2002. **16**(6): p. 1154-67.

63. Salustri, A., et al., *PTX3 plays a key role in the organization of the cumulus oophorus extracellular matrix and in in vivo fertilization.* Development, 2004. **131**(7): p. 1577-86.
64. Zhuo, L. and K. Kimata, *Cumulus oophorus extracellular matrix: its construction and regulation.* Cell Struct Funct, 2001. **26**(4): p. 189-96.
65. Fulop, C., et al., *Impaired cumulus mucification and female sterility in tumor necrosis factor-induced protein-6 deficient mice.* Development, 2003. **130**(10): p. 2253-61.
66. Day, A.J. and G.D. Prestwich, *Hyaluronan-binding proteins: tying up the giant.* J Biol Chem, 2002. **277**(7): p. 4585-8.
67. Tammi, M.I., A.J. Day, and E.A. Turley, *Hyaluronan and homeostasis: a balancing act.* J Biol Chem, 2002. **277**(7): p. 4581-4.
68. Wisniewski, H.G. and J. Vilcek, *Cytokine-induced gene expression at the crossroads of innate immunity, inflammation and fertility: TSG-6 and PTX3/TSG-14.* Cytokine Growth Factor Rev, 2004. **15**(2-3): p. 129-46.
69. Milner, C.M. and A.J. Day, *TSG-6: a multifunctional protein associated with inflammation.* J Cell Sci, 2003. **116**(Pt 10): p. 1863-73.
70. Doni, A., et al., *An acidic microenvironment sets the humoral pattern recognition molecule PTX3 in a tissue repair mode.* J Exp Med, 2015. **212**(6): p. 905-25.
71. Norata, G.D., C. Garlanda, and A.L. Catapano, *The long pentraxin PTX3: a modulator of the immunoinflammatory response in atherosclerosis and cardiovascular diseases.* Trends Cardiovasc Med, 2010. **20**(2): p. 35-40.
72. Klint, P. and L. Claesson-Welsh, *Signal transduction by fibroblast growth factor receptors.* Front Biosci, 1999. **4**: p. D165-77.
73. Rusnati, M., et al., *Selective recognition of fibroblast growth factor-2 by the long pentraxin PTX3 inhibits angiogenesis.* Blood, 2004. **104**(1): p. 92-9.
74. Camozzi, M., et al., *Identification of an antiangiogenic FGF2-binding site in the N terminus of the soluble pattern recognition receptor PTX3.* J Biol Chem, 2006. **281**(32): p. 22605-13.
75. Margheri, F., et al., *Modulation of the angiogenic phenotype of normal and systemic sclerosis endothelial cells by gain-loss of function of pentraxin 3 and matrix metalloproteinase 12.* Arthritis Rheum, 2010. **62**(8): p. 2488-98.
76. Camozzi, M., et al., *Pentraxin 3 inhibits fibroblast growth factor 2-dependent activation of smooth muscle cells in vitro and neointima formation in vivo.* Arterioscler Thromb Vasc Biol, 2005. **25**(9): p. 1837-42.
77. Koyama, H. and M.A. Reidy, *Expression of extracellular matrix proteins accompanies lesion growth in a model of intimal reinjury.* Circ Res, 1998. **82**(9): p. 988-95.
78. Jackson, C.L. and M.A. Reidy, *Basic fibroblast growth factor: its role in the control of smooth muscle cell migration.* Am J Pathol, 1993. **143**(4): p. 1024-31.
79. Fox, J.C. and J.R. Shanley, *Antisense inhibition of basic fibroblast growth factor induces apoptosis in vascular smooth muscle cells.* J Biol Chem, 1996. **271**(21): p. 12578-84.
80. Miyamoto, T., et al., *Autocrine FGF signaling is required for vascular smooth muscle cell survival in vitro.* J Cell Physiol, 1998. **177**(1): p. 58-67.
81. Segev, A., et al., *Inhibition of vascular smooth muscle cell proliferation by a novel fibroblast growth factor receptor antagonist.* Cardiovasc Res, 2002. **53**(1): p. 232-41.
82. Agrotis, A., et al., *Proliferation of neointimal smooth muscle cells after arterial injury. Dependence on interactions between fibroblast growth factor receptor-2 and fibroblast growth factor-9.* J Biol Chem, 2004. **279**(40): p. 42221-9.

83. Leali, D., et al., *Long pentraxin 3/tumor necrosis factor-stimulated gene-6 interaction: a biological rheostat for fibroblast growth factor 2-mediated angiogenesis.* Arterioscler Thromb Vasc Biol, 2012. **32**(3): p. 696-703.
84. Deban, L., et al., *Pentraxins: multifunctional proteins at the interface of innate immunity and inflammation.* Biofactors, 2009. **35**(2): p. 138-45.
85. Norata, G.D., et al., *Deficiency of the long pentraxin PTX3 promotes vascular inflammation and atherosclerosis.* Circulation, 2009. **120**(8): p. 699-708.
86. Rolph, M.S., et al., *Production of the long pentraxin PTX3 in advanced atherosclerotic plaques.* Arterioscler Thromb Vasc Biol, 2002. **22**(5): p. e10-4.
87. Tipping, P.G. and W.W. Hancock, *Production of tumor necrosis factor and interleukin-1 by macrophages from human atheromatous plaques.* Am J Pathol, 1993. **142**(6): p. 1721-8.
88. Galea, J., et al., *Interleukin-1 beta in coronary arteries of patients with ischemic heart disease.* Arterioscler Thromb Vasc Biol, 1996. **16**(8): p. 1000-6.
89. Frostegard, J., et al., *Cytokine expression in advanced human atherosclerotic plaques: dominance of pro-inflammatory (Th1) and macrophage-stimulating cytokines.* Atherosclerosis, 1999. **145**(1): p. 33-43.
90. Savchenko, A., et al., *Expression of pentraxin 3 (PTX3) in human atherosclerotic lesions.* J Pathol, 2008. **215**(1): p. 48-55.
91. Matsuura, Y., et al., *Different distribution of pentraxin 3 and C-reactive protein in coronary atherosclerotic plaques.* J Atheroscler Thromb, 2012. **19**(9): p. 837-45.
92. Ammirati, E., et al., *Effector Memory T cells Are Associated With Atherosclerosis in Humans and Animal Models.* J Am Heart Assoc, 2012. **1**(1): p. 27-41.
93. Norata, G.D., et al., *Effect of Tie-2 conditional deletion of BDNF on atherosclerosis in the ApoE null mutant mouse.* Biochim Biophys Acta, 2012. **1822**(6): p. 927-35.
94. Norata, G.D., et al., *Anti-inflammatory and anti-atherogenic effects of cathechin, caffeic acid and trans-resveratrol in apolipoprotein E deficient mice.* Atherosclerosis, 2007. **191**(2): p. 265-71.
95. Mallat, Z. and A. Tedgui, *HDL, PTX3, and vascular protection.* Arterioscler Thromb Vasc Biol, 2008. **28**(5): p. 809-11.
96. Latini, R., et al., *Prognostic significance of the long pentraxin PTX3 in acute myocardial infarction.* Circulation, 2004. **110**(16): p. 2349-54.
97. Zhu, H., et al., *Long pentraxin PTX3 attenuates ischemia reperfusion injury in a cardiac transplantation model.* Transpl Int, 2014. **27**(1): p. 87-95.
98. Shimizu, T., et al., *Cardio-protective effects of pentraxin 3 produced from bone marrow-derived cells against ischemia/reperfusion injury.* J Mol Cell Cardiol, 2015.
99. Rodriguez-Grande, B., et al., *The acute-phase protein PTX3 is an essential mediator of glial scar formation and resolution of brain edema after ischemic injury.* J Cereb Blood Flow Metab, 2014. **34**(3): p. 480-8.
100. Souza, D.G., et al., *Increased mortality and inflammation in tumor necrosis factor-stimulated gene-14 transgenic mice after ischemia and reperfusion injury.* Am J Pathol, 2002. **160**(5): p. 1755-65.
101. Souza, D.G., et al., *The long pentraxin PTX3 is crucial for tissue inflammation after intestinal ischemia and reperfusion in mice.* Am J Pathol, 2009. **174**(4): p. 1309-18.
102. Chen, J., et al., *Endothelial pentraxin 3 contributes to murine ischemic acute kidney injury.* Kidney Int, 2012. **82**(11): p. 1195-207.
103. Lech, M., et al., *Endogenous and exogenous pentraxin-3 limits postischemic acute and chronic kidney injury.* Kidney Int, 2013. **83**(4): p. 647-61.
104. Vestweber, D. and J.E. Blanks, *Mechanisms that regulate the function of the selectins and their ligands.* Physiol Rev, 1999. **79**(1): p. 181-213.

105. McEver, R.P., *Selectins: lectins that initiate cell adhesion under flow.* Curr Opin Cell Biol, 2002. **14**(5): p. 581-6.
106. Ley, K., et al., *Getting to the site of inflammation: the leukocyte adhesion cascade updated.* Nat Rev Immunol, 2007. **7**(9): p. 678-89.
107. Buffon, A., et al., *Widespread coronary inflammation in unstable angina.* N Engl J Med, 2002. **347**(1): p. 5-12.
108. Maugeri, N., et al., *Early and transient release of leukocyte pentraxin 3 during acute myocardial infarction.* J Immunol, 2011. **187**(2): p. 970-9.
109. Sardana, G., et al., *Proteomic analysis of conditioned media from the PC3, LNCaP, and 22Rv1 prostate cancer cell lines: discovery and validation of candidate prostate cancer biomarkers.* J Proteome Res, 2008. **7**(8): p. 3329-38.
110. Diamandis, E.P., et al., *Pentraxin-3 is a novel biomarker of lung carcinoma.* Clin Cancer Res, 2011. **17**(8): p. 2395-9.
111. Willeke, F., et al., *Overexpression of a member of the pentraxin family (PTX3) in human soft tissue liposarcoma.* Eur J Cancer, 2006. **42**(15): p. 2639-46.
112. Kondo, S., et al., *Clinical impact of pentraxin family expression on prognosis of pancreatic carcinoma.* Br J Cancer, 2013. **109**(3): p. 739-46.
113. Ronca, R., et al., *Long pentraxin-3 as an epithelial-stromal fibroblast growth factor-targeting inhibitor in prostate cancer.* J Pathol, 2013. **230**(2): p. 228-38.
114. Acevedo, V.D., M. Ittmann, and D.M. Spencer, *Paths of FGFR-driven tumorigenesis.* Cell Cycle, 2009. **8**(4): p. 580-8.
115. Rhodes, D.R., et al., *ONCOMINE: a cancer microarray database and integrated data-mining platform.* Neoplasia, 2004. **6**(1): p. 1-6.
116. Hsiao, Y.W., et al., *CCAAT/enhancer binding protein delta in macrophages contributes to immunosuppression and inhibits phagocytosis in nasopharyngeal carcinoma.* Sci Signal, 2013. **6**(284): p. ra59.
117. Bonavita, E., et al., *PTX3 is an extrinsic oncosuppressor regulating complement-dependent inflammation in cancer.* Cell, 2015. **160**(4): p. 700-14.
118. Cousin, B., et al., *A role for preadipocytes as macrophage-like cells.* FASEB J, 1999. **13**(2): p. 305-12.
119. Alberti, L., et al., *Expression of long pentraxin PTX3 in human adipose tissue and its relation with cardiovascular risk factors.* Atherosclerosis, 2009. **202**(2): p. 455-60.
120. Miyaki, A., et al., *Is pentraxin 3 involved in obesity-induced decrease in arterial distensibility?* J Atheroscler Thromb, 2010. **17**(3): p. 278-84.
121. Zanetti, M., et al., *Circulating pentraxin 3 levels are higher in metabolic syndrome with subclinical atherosclerosis: evidence for association with atherogenic lipid profile.* Clin Exp Med, 2009. **9**(3): p. 243-8.
122. Osorio-Conles, O., et al., *Plasma PTX3 protein levels inversely correlate with insulin secretion and obesity, whereas visceral adipose tissue PTX3 gene expression is increased in obesity.* Am J Physiol Endocrinol Metab, 2011. **301**(6): p. E1254-61.
123. Barazzoni, R., et al., *Obesity and high waist circumference are associated with low circulating pentraxin-3 in acute coronary syndrome.* Cardiovasc Diabetol, 2013. **12**: p. 167.
124. Miyamoto, T., et al., *Inverse relationship between the inflammatory marker pentraxin-3, fat body mass, and abdominal obesity in end-stage renal disease.* Clin J Am Soc Nephrol, 2011. **6**(12): p. 2785-91.
125. Ogawa, T., et al., *Reciprocal contribution of pentraxin 3 and C-reactive protein to obesity and metabolic syndrome.* Obesity (Silver Spring), 2010. **18**(9): p. 1871-4.
126. Yamasaki, K., et al., *Determination of physiological plasma pentraxin 3 (PTX3) levels in healthy populations.* Clin Chem Lab Med, 2009. **47**(4): p. 471-7.

127. Boden, W.E., *High-density lipoprotein cholesterol as an independent risk factor in cardiovascular disease: assessing the data from Framingham to the Veterans Affairs High--Density Lipoprotein Intervention Trial.* Am J Cardiol, 2000. **86**(12A): p. 19L-22L.
128. Hong, Y., et al., *Metabolic syndrome, its preeminent clusters, incident coronary heart disease and all-cause mortality--results of prospective analysis for the Atherosclerosis Risk in Communities study.* J Intern Med, 2007. **262**(1): p. 113-22.
129. Wallenfeldt, K., J. Hulthe, and B. Fagerberg, *The metabolic syndrome in middle-aged men according to different definitions and related changes in carotid artery intima-media thickness (IMT) during 3 years of follow-up.* J Intern Med, 2005. **258**(1): p. 28-37.
130. van Rossum, A.P., et al., *Abundance of the long pentraxin PTX3 at sites of leukocytoclastic lesions in patients with small-vessel vasculitis.* Arthritis Rheum, 2006. **54**(3): p. 986-91.
131. Fazzini, F., et al., *PTX3 in small-vessel vasculitides: an independent indicator of disease activity produced at sites of inflammation.* Arthritis Rheum, 2001. **44**(12): p. 2841-50.
132. Redman, C.W., G.P. Sacks, and I.L. Sargent, *Preeclampsia: an excessive maternal inflammatory response to pregnancy.* Am J Obstet Gynecol, 1999. **180**(2 Pt 1): p. 499-506.
133. Cetin, I., et al., *Elevated maternal levels of the long pentraxin 3 (PTX3) in preeclampsia and intrauterine growth restriction.* Am J Obstet Gynecol, 2006. **194**(5): p. 1347-53.
134. Rovere-Querini, P., et al., *Plasma and tissue expression of the long pentraxin 3 during normal pregnancy and preeclampsia.* Obstet Gynecol, 2006. **108**(1): p. 148-55.
135. Benyo, D.F., et al., *Expression of inflammatory cytokines in placentas from women with preeclampsia.* J Clin Endocrinol Metab, 2001. **86**(6): p. 2505-12.
136. Rinehart, B.K., et al., *Expression of the placental cytokines tumor necrosis factor alpha, interleukin 1beta, and interleukin 10 is increased in preeclampsia.* Am J Obstet Gynecol, 1999. **181**(4): p. 915-20.
137. Knoflach, M., et al., *Pentraxin-3 as a marker of advanced atherosclerosis results from the Bruneck, ARMY and ARFY Studies.* PLoS One, 2012. **7**(2): p. e31474.
138. Jenny, N.S., et al., *Associations of pentraxin 3 with cardiovascular disease and all-cause death: the Cardiovascular Health Study.* Arterioscler Thromb Vasc Biol, 2009. **29**(4): p. 594-9.
139. Ustundag, M., et al., *Comparative diagnostic accuracy of serum levels of neutrophil activating peptide-2 and pentraxin-3 versus troponin-I in acute coronary syndrome.* Anadolu Kardiyol Derg, 2011. **11**(7): p. 588-94.
140. Inoue, K., et al., *Establishment of a high sensitivity plasma assay for human pentraxin3 as a marker for unstable angina pectoris.* Arterioscler Thromb Vasc Biol, 2007. **27**(1): p. 161-7.
141. Kotooka, N., et al., *Pentraxin3 is a novel marker for stent-induced inflammation and neointimal thickening.* Atherosclerosis, 2008. **197**(1): p. 368-74.
142. Latini, R., et al., *Pentraxin-3 in chronic heart failure: the CORONA and GISSI-HF trials.* Eur J Heart Fail, 2012. **14**(9): p. 992-9.
143. Kotooka, N., et al., *Prognostic value of pentraxin 3 in patients with chronic heart failure.* Int J Cardiol, 2008. **130**(1): p. 19-22.

144. Matsubara, J., et al., *Pentraxin 3 is a new inflammatory marker correlated with left ventricular diastolic dysfunction and heart failure with normal ejection fraction.* J Am Coll Cardiol, 2011. **57**(7): p. 861-9.
145. Olesen, R., et al., *DC-SIGN (CD209), pentraxin 3 and vitamin D receptor gene variants associate with pulmonary tuberculosis risk in West Africans.* Genes Immun, 2007. **8**(6): p. 456-67.
146. Chiarini, M., et al., *PTX3 genetic variations affect the risk of Pseudomonas aeruginosa airway colonization in cystic fibrosis patients.* Genes Immun, 2010. **11**(8): p. 665-70.
147. May, L., et al., *Genetic variation in pentraxin (PTX) 3 gene associates with PTX3 production and fertility in women.* Biol Reprod, 2010. **82**(2): p. 299-304.
148. Diamond, J.M., et al., *Variation in PTX3 is associated with primary graft dysfunction after lung transplantation.* Am J Respir Crit Care Med, 2012. **186**(6): p. 546-52.
149. Barbati, E., et al., *Influence of pentraxin 3 (PTX3) genetic variants on myocardial infarction risk and PTX3 plasma levels.* PLoS One, 2012. **7**(12): p. e53030.
150. Cunha, C., et al., *Genetic PTX3 deficiency and aspergillosis in stem-cell transplantation.* N Engl J Med, 2014. **370**(5): p. 421-32.
151. Carmo, R.F., et al., *Genetic variation in PTX3 and plasma levels associated with hepatocellular carcinoma in patients with HCV.* J Viral Hepat, 2015.
152. Viles-Gonzalez, J.F., V. Fuster, and J.J. Badimon, *Atherothrombosis: a widespread disease with unpredictable and life-threatening consequences.* Eur Heart J, 2004. **25**(14): p. 1197-207.
153. Behrendt, D. and P. Ganz, *Endothelial function. From vascular biology to clinical applications.* Am J Cardiol, 2002. **90**(10C): p. 40L-48L.
154. Weiss, N., et al., *Endothelial dysfunction and atherothrombosis in mild hyperhomocysteinemia.* Vasc Med, 2002. **7**(3): p. 227-39.
155. Stary, H.C., et al., *A definition of initial, fatty streak, and intermediate lesions of atherosclerosis. A report from the Committee on Vascular Lesions of the Council on Arteriosclerosis, American Heart Association.* Arterioscler Thromb, 1994. **14**(5): p. 840-56.
156. Glagov, S., et al., *Compensatory enlargement of human atherosclerotic coronary arteries.* N Engl J Med, 1987. **316**(22): p. 1371-5.
157. Kikano, G.E. and M.T. Brown, *Antiplatelet therapy for atherothrombotic disease: an update for the primary care physician.* Mayo Clin Proc, 2007. **82**(5): p. 583-93.
158. Varga-Szabo, D., I. Pleines, and B. Nieswandt, *Cell adhesion mechanisms in platelets.* Arterioscler Thromb Vasc Biol, 2008. **28**(3): p. 403-12.
159. Thijs, T., et al., *Platelet physiology and antiplatelet agents.* Clin Chem Lab Med, 2010. **48 Suppl 1**: p. S3-13.
160. Spronk, H.M., D. van der Voort, and H. Ten Cate, *Blood coagulation and the risk of atherothrombosis: a complex relationship.* Thromb J, 2004. **2**(1): p. 12.
161. Gruner, S., et al., *Multiple integrin-ligand interactions synergize in shear-resistant platelet adhesion at sites of arterial injury in vivo.* Blood, 2003. **102**(12): p. 4021-7.
162. Adams, R.L. and R.J. Bird, *Review article: Coagulation cascade and therapeutics update: relevance to nephrology. Part 1: Overview of coagulation, thrombophilias and history of anticoagulants.* Nephrology (Carlton), 2009. **14**(5): p. 462-70.
163. Lievens, D. and P. von Hundelshausen, *Platelets in atherosclerosis.* Thromb Haemost, 2011. **106**(5): p. 827-38.
164. Semple, J.W. and J. Freedman, *Platelets and innate immunity.* Cell Mol Life Sci, 2010. **67**(4): p. 499-511.

165. Diacovo, T.G., et al., *Neutrophil rolling, arrest, and transmigration across activated, surface-adherent platelets via sequential action of P-selectin and the beta 2-integrin CD11b/CD18.* Blood, 1996. **88**(1): p. 146-57.
166. Kuijper, P.H., et al., *Platelet-dependent primary hemostasis promotes selectin- and integrin-mediated neutrophil adhesion to damaged endothelium under flow conditions.* Blood, 1996. **87**(8): p. 3271-81.
167. Dole, V.S., et al., *Activated platelets induce Weibel-Palade-body secretion and leukocyte rolling in vivo: role of P-selectin.* Blood, 2005. **106**(7): p. 2334-9.
168. Huo, Y., et al., *Circulating activated platelets exacerbate atherosclerosis in mice deficient in apolipoprotein E.* Nat Med, 2003. **9**(1): p. 61-7.
169. Mayadas, T.N., et al., *Leukocyte rolling and extravasation are severely compromised in P selectin-deficient mice.* Cell, 1993. **74**(3): p. 541-54.
170. Yang, J., et al., *Targeted gene disruption demonstrates that P-selectin glycoprotein ligand 1 (PSGL-1) is required for P-selectin-mediated but not E-selectin-mediated neutrophil rolling and migration.* J Exp Med, 1999. **190**(12): p. 1769-82.
171. Maugeri, N., et al., *Leukocyte and platelet activation in patients with giant cell arteritis and polymyalgia rheumatica: a clue to thromboembolic risks?* Autoimmunity, 2009. **42**(4): p. 386-8.
172. Manfredi, A.A., P. Rovere-Querini, and N. Maugeri, *Dangerous connections: neutrophils and the phagocytic clearance of activated platelets.* Curr Opin Hematol, 2010. **17**(1): p. 3-8.
173. Michelson, A.D., *Antiplatelet therapies for the treatment of cardiovascular disease.* Nat Rev Drug Discov, 2010. **9**(2): p. 154-69.
174. Maugeri, N., et al., *Translational mini-review series on immunology of vascular disease: mechanisms of vascular inflammation and remodelling in systemic vasculitis.* Clin Exp Immunol, 2009. **156**(3): p. 395-404.
175. Linden, M.D., et al., *Indices of platelet activation and the stability of coronary artery disease.* J Thromb Haemost, 2007. **5**(4): p. 761-5.
176. Furman, M.I., et al., *Circulating monocyte-platelet aggregates are an early marker of acute myocardial infarction.* J Am Coll Cardiol, 2001. **38**(4): p. 1002-6.
177. Michelson, A.D., et al., *Circulating monocyte-platelet aggregates are a more sensitive marker of in vivo platelet activation than platelet surface P-selectin: studies in baboons, human coronary intervention, and human acute myocardial infarction.* Circulation, 2001. **104**(13): p. 1533-7.
178. van Gils, J.M., J.J. Zwaginga, and P.L. Hordijk, *Molecular and functional interactions among monocytes, platelets, and endothelial cells and their relevance for cardiovascular diseases.* J Leukoc Biol, 2009. **85**(2): p. 195-204.
179. Yokoyama, S., et al., *Platelet P-selectin plays an important role in arterial thrombogenesis by forming large stable platelet-leukocyte aggregates.* J Am Coll Cardiol, 2005. **45**(8): p. 1280-6.
180. Larsen, E., et al., *PADGEM protein: a receptor that mediates the interaction of activated platelets with neutrophils and monocytes.* Cell, 1989. **59**(2): p. 305-12.
181. Ramos, C.L., et al., *Direct demonstration of P-selectin- and VCAM-1-dependent mononuclear cell rolling in early atherosclerotic lesions of apolipoprotein E-deficient mice.* Circ Res, 1999. **84**(11): p. 1237-44.
182. Woollard, K.J. and J. Chin-Dusting, *P-selectin antagonism in inflammatory disease.* Curr Pharm Des, 2010. **16**(37): p. 4113-8.
183. Yurchenco, P.D., *Basement membranes: cell scaffoldings and signaling platforms.* Cold Spring Harb Perspect Biol, 2011. **3**(2).

184. Wagenseil, J.E. and R.P. Mecham, *Vascular extracellular matrix and arterial mechanics.* Physiol Rev, 2009. **89**(3): p. 957-89.
185. Bergmeier, W. and R.O. Hynes, *Extracellular matrix proteins in hemostasis and thrombosis.* Cold Spring Harb Perspect Biol, 2012. **4**(2).
186. Hechler, B., et al., *Arterial thrombosis: relevance of a model with two levels of severity assessed by histologic, ultrastructural and functional characterization.* J Thromb Haemost, 2010. **8**(1): p. 173-84.
187. Kehrel, B., et al., *Glycoprotein VI is a major collagen receptor for platelet activation: it recognizes the platelet-activating quaternary structure of collagen, whereas CD36, glycoprotein IIb/IIIa, and von Willebrand factor do not.* Blood, 1998. **91**(2): p. 491-9.
188. Knight, C.G., et al., *The collagen-binding A-domains of integrins alpha(1)beta(1) and alpha(2)beta(1) recognize the same specific amino acid sequence, GFOGER, in native (triple-helical) collagens.* J Biol Chem, 2000. **275**(1): p. 35-40.
189. Knight, C.G., et al., *Identification in collagen type I of an integrin alpha2 beta1-binding site containing an essential GER sequence.* J Biol Chem, 1998. **273**(50): p. 33287-94.
190. Nieswandt, B. and S.P. Watson, *Platelet-collagen interaction: is GPVI the central receptor?* Blood, 2003. **102**(2): p. 449-61.
191. Offermanns, S., *Activation of platelet function through G protein-coupled receptors.* Circ Res, 2006. **99**(12): p. 1293-304.
192. Hynes, R.O., *Integrins: bidirectional, allosteric signaling machines.* Cell, 2002. **110**(6): p. 673-87.
193. Shattil, S.J., H. Kashiwagi, and N. Pampori, *Integrin signaling: the platelet paradigm.* Blood, 1998. **91**(8): p. 2645-57.
194. Savage, B., F. Almus-Jacobs, and Z.M. Ruggeri, *Specific synergy of multiple substrate-receptor interactions in platelet thrombus formation under flow.* Cell, 1998. **94**(5): p. 657-66.
195. Nieswandt, B., et al., *Glycoprotein VI but not alpha2beta1 integrin is essential for platelet interaction with collagen.* EMBO J, 2001. **20**(9): p. 2120-30.
196. Day, S.M., et al., *Murine thrombosis models.* Thromb Haemost, 2004. **92**(3): p. 486-94.
197. Nieswandt, B., et al., *Platelets in atherothrombosis: lessons from mouse models.* J Thromb Haemost, 2005. **3**(8): p. 1725-36.
198. Denis, C., et al., *A mouse model of severe von Willebrand disease: defects in hemostasis and thrombosis.* Proc Natl Acad Sci U S A, 1998. **95**(16): p. 9524-9.
199. Kurz, K.D., B.W. Main, and G.E. Sandusky, *Rat model of arterial thrombosis induced by ferric chloride.* Thromb Res, 1990. **60**(4): p. 269-80.
200. Matsuno, H., et al., *Photochemically induced thrombosis model in rat femoral artery and evaluation of effects of heparin and tissue-type plasminogen activator with use of this model.* J Pharmacol Methods, 1991. **25**(4): p. 303-17.
201. Westrick, R.J., M.E. Winn, and D.T. Eitzman, *Murine models of vascular thrombosis (Eitzman series).* Arterioscler Thromb Vasc Biol, 2007. **27**(10): p. 2079-93.
202. Lindner, V., R.A. Majack, and M.A. Reidy, *Basic fibroblast growth factor stimulates endothelial regrowth and proliferation in denuded arteries.* J Clin Invest, 1990. **85**(6): p. 2004-8.
203. Farrehi, P.M., et al., *Regulation of arterial thrombolysis by plasminogen activator inhibitor-1 in mice.* Circulation, 1998. **97**(10): p. 1002-8.

204. Konstantinides, S., et al., *Distinct antithrombotic consequences of platelet glycoprotein Ibalpha and VI deficiency in a mouse model of arterial thrombosis.* J Thromb Haemost, 2006. **4**(9): p. 2014-21.
205. Massberg, S., et al., *A crucial role of glycoprotein VI for platelet recruitment to the injured arterial wall in vivo.* J Exp Med, 2003. **197**(1): p. 41-9.
206. Eckly, A., et al., *Mechanisms underlying FeCl3-induced arterial thrombosis.* J Thromb Haemost, 2011. **9**(4): p. 779-89.
207. Barr, J.D., et al., *Red blood cells mediate the onset of thrombosis in the ferric chloride murine model.* Blood, 2013. **121**(18): p. 3733-41.
208. Ciciliano, J.C., et al., *Resolving the multifaceted mechanisms of the ferric chloride thrombosis model using an interdisciplinary microfluidic approach.* Blood, 2015. **126**(6): p. 817-24.
209. Kikuchi, S., et al., *Photochemically induced endothelial injury in the mouse as a screening model for inhibitors of vascular intimal thickening.* Arterioscler Thromb Vasc Biol, 1998. **18**(7): p. 1069-78.
210. Saniabadi, A.R., et al., *Vessel wall injury and arterial thrombosis induced by a photochemical reaction.* Thromb Haemost, 1995. **73**(5): p. 868-72.
211. Falati, S., et al., *Real-time in vivo imaging of platelets, tissue factor and fibrin during arterial thrombus formation in the mouse.* Nat Med, 2002. **8**(10): p. 1175-81.
212. Konishi, H., et al., *Platelets activated by collagen through immunoreceptor tyrosine-based activation motif play pivotal role in initiation and generation of neointimal hyperplasia after vascular injury.* Circulation, 2002. **105**(8): p. 912-6.
213. Massberg, S., et al., *A critical role of platelet adhesion in the initiation of atherosclerotic lesion formation.* J Exp Med, 2002. **196**(7): p. 887-96.
214. Gruner, S., et al., *Anti-glycoprotein VI treatment severely compromises hemostasis in mice with reduced alpha2beta1 levels or concomitant aspirin therapy.* Circulation, 2004. **110**(18): p. 2946-51.
215. Galassi, A., K. Reynolds, and J. He, *Metabolic syndrome and risk of cardiovascular disease: a meta-analysis.* Am J Med, 2006. **119**(10): p. 812-9.
216. Lorenzo, C., et al., *The metabolic syndrome as predictor of type 2 diabetes: the San Antonio heart study.* Diabetes Care, 2003. **26**(11): p. 3153-9.
217. Wahba, I.M. and R.H. Mak, *Obesity and obesity-initiated metabolic syndrome: mechanistic links to chronic kidney disease.* Clin J Am Soc Nephrol, 2007. **2**(3): p. 550-62.
218. Esposito, K., et al., *Metabolic syndrome and risk of cancer: a systematic review and meta-analysis.* Diabetes Care, 2012. **35**(11): p. 2402-11.
219. Naik, D., et al., *Chronic obstructive pulmonary disease and the metabolic syndrome: Consequences of a dual threat.* Indian J Endocrinol Metab, 2014. **18**(5): p. 608-16.
220. National Cholesterol Education Program Expert Panel on Detection, E. and A. Treatment of High Blood Cholesterol in, *Third Report of the National Cholesterol Education Program (NCEP) Expert Panel on Detection, Evaluation, and Treatment of High Blood Cholesterol in Adults (Adult Treatment Panel III) final report.* Circulation, 2002. **106**(25): p. 3143-421.
221. Shulman, G.I., *Cellular mechanisms of insulin resistance.* J Clin Invest, 2000. **106**(2): p. 171-6.
222. Bagby, S.P., *Obesity-initiated metabolic syndrome and the kidney: a recipe for chronic kidney disease?* J Am Soc Nephrol, 2004. **15**(11): p. 2775-91.
223. Wisse, B.E., *The inflammatory syndrome: the role of adipose tissue cytokines in metabolic disorders linked to obesity.* J Am Soc Nephrol, 2004. **15**(11): p. 2792-800.

224. Gregor, M.F. and G.S. Hotamisligil, *Inflammatory mechanisms in obesity.* Annu Rev Immunol, 2011. **29**: p. 415-45.
225. Hotamisligil, G.S., N.S. Shargill, and B.M. Spiegelman, *Adipose expression of tumor necrosis factor-alpha: direct role in obesity-linked insulin resistance.* Science, 1993. **259**(5091): p. 87-91.
226. Pickup, J.C., et al., *NIDDM as a disease of the innate immune system: association of acute-phase reactants and interleukin-6 with metabolic syndrome X.* Diabetologia, 1997. **40**(11): p. 1286-92.
227. Yudkin, J.S., et al., *C-reactive protein in healthy subjects: associations with obesity, insulin resistance, and endothelial dysfunction: a potential role for cytokines originating from adipose tissue?* Arterioscler Thromb Vasc Biol, 1999. **19**(4): p. 972-8.
228. Vozarova, B., et al., *High white blood cell count is associated with a worsening of insulin sensitivity and predicts the development of type 2 diabetes.* Diabetes, 2002. **51**(2): p. 455-61.
229. Phillips, C.M. and I.J. Perry, *Does inflammation determine metabolic health status in obese and nonobese adults?* J Clin Endocrinol Metab, 2013. **98**(10): p. E1610-9.
230. Chawla, A., K.D. Nguyen, and Y.P. Goh, *Macrophage-mediated inflammation in metabolic disease.* Nat Rev Immunol, 2011. **11**(11): p. 738-49.
231. Shoelson, S.E., J. Lee, and A.B. Goldfine, *Inflammation and insulin resistance.* J Clin Invest, 2006. **116**(7): p. 1793-801.
232. Ouchi, N., et al., *Adipokines in inflammation and metabolic disease.* Nat Rev Immunol, 2011. **11**(2): p. 85-97.
233. Weisberg, S.P., et al., *Obesity is associated with macrophage accumulation in adipose tissue.* J Clin Invest, 2003. **112**(12): p. 1796-808.
234. O'Rourke, R.W., et al., *Hypoxia-induced inflammatory cytokine secretion in human adipose tissue stromovascular cells.* Diabetologia, 2011. **54**(6): p. 1480-90.
235. Skurk, T., et al., *Relationship between adipocyte size and adipokine expression and secretion.* J Clin Endocrinol Metab, 2007. **92**(3): p. 1023-33.
236. Gordon, S. and P.R. Taylor, *Monocyte and macrophage heterogeneity.* Nat Rev Immunol, 2005. **5**(12): p. 953-64.
237. Lumeng, C.N., J.L. Bodzin, and A.R. Saltiel, *Obesity induces a phenotypic switch in adipose tissue macrophage polarization.* J Clin Invest, 2007. **117**(1): p. 175-84.
238. Cancello, R., et al., *Reduction of macrophage infiltration and chemoattractant gene expression changes in white adipose tissue of morbidly obese subjects after surgery-induced weight loss.* Diabetes, 2005. **54**(8): p. 2277-86.
239. Bruun, J.M., et al., *Diet and exercise reduce low-grade inflammation and macrophage infiltration in adipose tissue but not in skeletal muscle in severely obese subjects.* Am J Physiol Endocrinol Metab, 2006. **290**(5): p. E961-7.
240. Talukdar, S., et al., *Neutrophils mediate insulin resistance in mice fed a high-fat diet through secreted elastase.* Nat Med, 2012. **18**(9): p. 1407-12.
241. Liu, J., et al., *Genetic deficiency and pharmacological stabilization of mast cells reduce diet-induced obesity and diabetes in mice.* Nat Med, 2009. **15**(8): p. 940-5.
242. Ohmura, K., et al., *Natural killer T cells are involved in adipose tissues inflammation and glucose intolerance in diet-induced obese mice.* Arterioscler Thromb Vasc Biol, 2010. **30**(2): p. 193-9.
243. Feuerer, M., et al., *Lean, but not obese, fat is enriched for a unique population of regulatory T cells that affect metabolic parameters.* Nat Med, 2009. **15**(8): p. 930-9.
244. Nishimura, S., et al., *CD8+ effector T cells contribute to macrophage recruitment and adipose tissue inflammation in obesity.* Nat Med, 2009. **15**(8): p. 914-20.

245. Winer, S., et al., *Normalization of obesity-associated insulin resistance through immunotherapy.* Nat Med, 2009. **15**(8): p. 921-9.
246. Koster, A., et al., *Body fat distribution and inflammation among obese older adults with and without metabolic syndrome.* Obesity (Silver Spring), 2010. **18**(12): p. 2354-61.
247. Tchernof, A. and J.P. Despres, *Pathophysiology of human visceral obesity: an update.* Physiol Rev, 2013. **93**(1): p. 359-404.
248. Serfaty, L. and M. Lemoine, *Definition and natural history of metabolic steatosis: clinical aspects of NAFLD, NASH and cirrhosis.* Diabetes Metab, 2008. **34**(6 Pt 2): p. 634-7.
249. Cai, D., et al., *Local and systemic insulin resistance resulting from hepatic activation of IKK-beta and NF-kappaB.* Nat Med, 2005. **11**(2): p. 183-90.
250. Huang, W., et al., *Depletion of liver Kupffer cells prevents the development of diet-induced hepatic steatosis and insulin resistance.* Diabetes, 2010. **59**(2): p. 347-57.
251. Pickup, J.C. and M.A. Crook, *Is type II diabetes mellitus a disease of the innate immune system?* Diabetologia, 1998. **41**(10): p. 1241-8.
252. Nguyen, M.T., et al., *A subpopulation of macrophages infiltrates hypertrophic adipose tissue and is activated by free fatty acids via Toll-like receptors 2 and 4 and JNK-dependent pathways.* J Biol Chem, 2007. **282**(48): p. 35279-92.
253. Fink, L.N., et al., *Expression of anti-inflammatory macrophage genes within skeletal muscle correlates with insulin sensitivity in human obesity and type 2 diabetes.* Diabetologia, 2013. **56**(7): p. 1623-8.
254. Sell, H., et al., *Monocyte chemotactic protein-1 is a potential player in the negative cross-talk between adipose tissue and skeletal muscle.* Endocrinology, 2006. **147**(5): p. 2458-67.
255. del Aguila, L.F., K.P. Claffey, and J.P. Kirwan, *TNF-alpha impairs insulin signaling and insulin stimulation of glucose uptake in C2C12 muscle cells.* Am J Physiol, 1999. **276**(5 Pt 1): p. E849-55.
256. Plomgaard, P., et al., *Tumor necrosis factor-alpha induces skeletal muscle insulin resistance in healthy human subjects via inhibition of Akt substrate 160 phosphorylation.* Diabetes, 2005. **54**(10): p. 2939-45.
257. Donath, M.Y., *Inflammation as a sensor of metabolic stress in obesity and type 2 diabetes.* Endocrinology, 2011. **152**(11): p. 4005-6.
258. Maedler, K., et al., *Glucose-induced beta cell production of IL-1beta contributes to glucotoxicity in human pancreatic islets.* J Clin Invest, 2002. **110**(6): p. 851-60.
259. Woods, S.C., *The control of food intake: behavioral versus molecular perspectives.* Cell Metab, 2009. **9**(6): p. 489-98.
260. Zhang, F., et al., *Crystal structure of the obese protein leptin-E100.* Nature, 1997. **387**(6629): p. 206-9.
261. Brennan, A.M. and W.D. Gouvier, *Are we honestly studying malingering? A profile and comparison of simulated and suspected malingerers.* Appl Neuropsychol, 2006. **13**(1): p. 1-11.
262. Pan, H., J. Guo, and Z. Su, *Advances in understanding the interrelations between leptin resistance and obesity.* Physiol Behav, 2014. **130**: p. 157-69.
263. Bray, G.A. and D.A. York, *Hypothalamic and genetic obesity in experimental animals: an autonomic and endocrine hypothesis.* Physiol Rev, 1979. **59**(3): p. 719-809.
264. Campfield, L.A., et al., *Recombinant mouse OB protein: evidence for a peripheral signal linking adiposity and central neural networks.* Science, 1995. **269**(5223): p. 546-9.

265. Coleman, D.L., *Obese and diabetes: two mutant genes causing diabetes-obesity syndromes in mice.* Diabetologia, 1978. **14**(3): p. 141-8.
266. Friedman, J.M., *Leptin, leptin receptors, and the control of body weight.* Nutr Rev, 1998. **56**(2 Pt 2): p. s38-46; discussion s54-75.
267. Halaas, J.L., et al., *Weight-reducing effects of the plasma protein encoded by the obese gene.* Science, 1995. **269**(5223): p. 543-6.
268. Pelleymounter, M.A., et al., *Effects of the obese gene product on body weight regulation in ob/ob mice.* Science, 1995. **269**(5223): p. 540-3.
269. Chua, S.C., Jr., et al., *Phenotypes of mouse diabetes and rat fatty due to mutations in the OB (leptin) receptor.* Science, 1996. **271**(5251): p. 994-6.
270. Lu, D., et al., *Agouti protein is an antagonist of the melanocyte-stimulating-hormone receptor.* Nature, 1994. **371**(6500): p. 799-802.
271. Millar, S.E., et al., *Expression and transgenic studies of the mouse agouti gene provide insight into the mechanisms by which mammalian coat color patterns are generated.* Development, 1995. **121**(10): p. 3223-32.
272. Matsunaga, N., et al., *In situ localization of agouti signal protein in murine skin using immunohistochemistry with an ASP-specific antibody.* Biochem Biophys Res Commun, 2000. **270**(1): p. 176-82.
273. Michaud, E.J., et al., *The embryonic lethality of homozygous lethal yellow mice (Ay/Ay) is associated with the disruption of a novel RNA-binding protein.* Genes Dev, 1993. **7**(7A): p. 1203-13.
274. Michaud, E.J., et al., *A molecular model for the genetic and phenotypic characteristics of the mouse lethal yellow (Ay) mutation.* Proc Natl Acad Sci U S A, 1994. **91**(7): p. 2562-6.
275. Bultman, S.J., E.J. Michaud, and R.P. Woychik, *Molecular characterization of the mouse agouti locus.* Cell, 1992. **71**(7): p. 1195-204.
276. Huszar, D., et al., *Targeted disruption of the melanocortin-4 receptor results in obesity in mice.* Cell, 1997. **88**(1): p. 131-41.
277. Nilsson, C., et al., *Laboratory animals as surrogate models of human obesity.* Acta Pharmacol Sin, 2012. **33**(2): p. 173-81.
278. Collins, S., et al., *Genetic vulnerability to diet-induced obesity in the C57BL/6J mouse: physiological and molecular characteristics.* Physiol Behav, 2004. **81**(2): p. 243-8.
279. Speakman, J., et al., *Animal models of obesity.* Obes Rev, 2007. **8 Suppl 1**: p. 55-61.
280. Sato, A., et al., *Antiobesity effect of eicosapentaenoic acid in high-fat/high-sucrose diet-induced obesity: importance of hepatic lipogenesis.* Diabetes, 2010. **59**(10): p. 2495-504.
281. Inui, A., *Obesity--a chronic health problem in cloned mice?* Trends Pharmacol Sci, 2003. **24**(2): p. 77-80.
282. Lech, M., et al., *Endogenous and exogenous pentraxin-3 limits postischemic acute and chronic kidney injury.* Kidney Int. **83**(4): p. 647-61.
283. Murad, J.P., et al., *A novel antibody targeting the ligand binding domain of the thromboxane A(2) receptor exhibits antithrombotic properties in vivo.* Biochem Biophys Res Commun. **421**(3): p. 456-61.
284. Murad, J.P., et al., *Characterization of the in vivo antiplatelet activity of the antihypertensive agent losartan.* J Cardiovasc Pharmacol Ther. **17**(3): p. 308-14.
285. Tatsumi, K., et al., *Regulation of coagulation factors during liver regeneration in mice: mechanism of factor VIII elevation in plasma.* Thromb Res. **128**(1): p. 54-61.

286. Norata, G.D., et al., *Oxidised-HDL3 induces the expression of PAI-1 in human endothelial cells. Role of p38MAPK activation and mRNA stabilization.* Br J Haematol, 2004. **127**(1): p. 97-104.
287. Gawaz, M., H. Langer, and A.E. May, *Platelets in inflammation and atherogenesis.* J Clin Invest, 2005. **115**(12): p. 3378-84.
288. Bonacina, F., et al., *Long pentraxin 3: experimental and clinical relevance in cardiovascular diseases.* Mediators Inflamm, 2013. **2013**: p. 725102.
289. Soeki, T., et al., *Elevated concentrations of pentraxin 3 are associated with coronary plaque vulnerability.* J Cardiol, 2011. **58**(2): p. 151-7.
290. Latini, R., et al., *Prognostic significance of the long pentraxin PTX3 in acute myocardial infarction.* Circulation, 2004. **110**(16): p. 2349-54.
291. Napoleone, E., et al., *The long pentraxin PTX3 up-regulates tissue factor in activated monocytes: another link between inflammation and clotting activation.* J Leukoc Biol, 2004. **76**(1): p. 203-9.
292. Jaillon, S., et al., *The humoral pattern recognition receptor PTX3 is stored in neutrophil granules and localizes in extracellular traps.* J Exp Med, 2007. **204**(4): p. 793-804.
293. Breviario, F., et al., *Interleukin-1-inducible genes in endothelial cells. Cloning of a new gene related to C-reactive protein and serum amyloid P component.* J Biol Chem, 1992. **267**(31): p. 22190-7.
294. Eckly, A., et al., *Mechanisms underlying FeCl3-induced arterial thrombosis.* J Thromb Haemost. **9**(4): p. 779-89.
295. Ma, Y.J., et al., *Ficolin-1-PTX3 complex formation promotes clearance of altered self-cells and modulates IL-8 production.* J Immunol, 2013. **191**(3): p. 1324-33.
296. Groeneveld, T.W., et al., *Interactions of the extracellular matrix proteoglycans decorin and biglycan with C1q and collectins.* J Immunol, 2005. **175**(7): p. 4715-23.
297. Inforzato, A., et al., *The "sweet" side of a long pentraxin: how glycosylation affects PTX3 functions in innate immunity and inflammation.* Front Immunol, 2012. **3**: p. 407.
298. Mottillo, S., et al., *The metabolic syndrome and cardiovascular risk a systematic review and meta-analysis.* J Am Coll Cardiol, 2010. **56**(14): p. 1113-32.
299. Xia, X.R., N.A. Monteiro-Riviere, and J.E. Riviere, *Intrinsic biological property of colloidal fullerene nanoparticles (nC60): lack of lethality after high dose exposure to human epidermal and bacterial cells.* Toxicol Lett, 2010. **197**(2): p. 128-34.
300. Lumeng, C.N. and A.R. Saltiel, *Inflammatory links between obesity and metabolic disease.* J Clin Invest, 2011. **121**(6): p. 2111-7.
301. Sironi, L., et al., *Activation of NF-kB and ERK1/2 after permanent focal ischemia is abolished by simvastatin treatment.* Neurobiol Dis, 2006. **22**(2): p. 445-51.
302. Esser, N., N. Paquot, and A.J. Scheen, *Anti-inflammatory agents to treat or prevent type 2 diabetes, metabolic syndrome and cardiovascular disease.* Expert Opin Investig Drugs, 2015. **24**(3): p. 283-307.
303. Xu, H., et al., *Chronic inflammation in fat plays a crucial role in the development of obesity-related insulin resistance.* J Clin Invest, 2003. **112**(12): p. 1821-30.
304. Tilg, H. and A.R. Moschen, *Adipocytokines: mediators linking adipose tissue, inflammation and immunity.* Nat Rev Immunol, 2006. **6**(10): p. 772-83.
305. Wang, C.Y. and J.K. Liao, *A mouse model of diet-induced obesity and insulin resistance.* Methods Mol Biol, 2012. **821**: p. 421-33.
306. Suganami, T. and Y. Ogawa, *Adipose tissue macrophages: their role in adipose tissue remodeling.* J Leukoc Biol, 2010. **88**(1): p. 33-9.

307. Surmi, B.K. and A.H. Hasty, *Macrophage infiltration into adipose tissue: initiation, propagation and remodeling.* Future Lipidol, 2008. **3**(5): p. 545-556.
308. Bernstein, B.B. and S.B. Weisberg, *Southern California's marine monitoring system ten years after the National Research Council evaluation.* Environ Monit Assess, 2003. **81**(1-3): p. 3-14.
309. Bergman, R.N., et al., *Why visceral fat is bad: mechanisms of the metabolic syndrome.* Obesity (Silver Spring), 2006. **14 Suppl 1**: p. 16S-19S.
310. Reilly, S.M., et al., *An inhibitor of the protein kinases TBK1 and IKK-varepsilon improves obesity-related metabolic dysfunctions in mice.* Nat Med, 2013. **19**(3): p. 313-21.
311. Calay, E.S. and G.S. Hotamisligil, *Turning off the inflammatory, but not the metabolic, flames.* Nat Med, 2013. **19**(3): p. 265-7.
312. Deban, L., et al., *Pentraxins in innate immunity: lessons from PTX3.* Cell Tissue Res, 2011. **343**(1): p. 237-49.
313. Jackson, S.P., *Arterial thrombosis--insidious, unpredictable and deadly.* Nat Med, 2011. **17**(11): p. 1423-36.
314. Eckel, R.H., S.M. Grundy, and P.Z. Zimmet, *The metabolic syndrome.* Lancet, 2005. **365**(9468): p. 1415-28.
315. Samad, F. and W. Ruf, *Inflammation, obesity, and thrombosis.* Blood, 2013. **122**(20): p. 3415-22.

Ringrazio i professori Catapano e Norata per la fiducia, la stima, le opportunità e l’esempio professionale che hanno rappresentato.

Ringrazio le persone vicine, conosciute e incontrate in questi anni; l’affetto, i consigli, il conforto di ognuna di loro hanno guidato la mia crescita professionale e umana.